Models for Firewall Creation in Massless Scalar Field Theory

BY

Lingjun Zhou

A Thesis submitted to
the Faculty of Graduate Studies
in Partial Fulfillment of the Requirements for the Degree of

DOCTOR OF PHILOSOPHY

Department of Physics and Astronomy
University of Manitoba
Winnipeg, Manitoba

Abstract

We study the topic of quantum entanglement in the extreme spacetime background of a black hole. It was suggested by Almheiri et al (AMPS) that, unlike what is commonly believed, the event horizon of a black hole past Page time is very disruptive and violent. This disruption at the event horizon manifests itself as the so-called 'firewall', which incinerates any infalling object. As a result, quantum entanglement across the event horizon is also broken, and this saves us from the information loss conundrum.

AMPS did not propose a mechanism for such 'firewall', and many have been speculating how to realize such a singular structure.

In this thesis, following Brown and Louko, we study further the mechanism of singular energy density in the context of Minkowski spacetime. We generalize their one dimensional model to three dimensions. We study two spherically symmetric generalizations of Brown and Louko's model. The first is the creation of a null energy pulse with a time-dependent boundary condition at the space origin, and the second is the creation of an outgoing and an ingoing energy pulse by a time dependent boundary condition at a finite radius $r = a$. Both models generate singular energy pulses which at first sight seem to be strong enough to break quantum correlations. However, a singular energy pulse is not enough evidence to show that quantum correlation is broken[1]. A divergent response of an Unruh-DeWitt detector is needed. Our calculation shows that the three dimensional spherically symmetric model with a time-dependent boundary condition at the origin can be singular enough to destroy the quantum correlations. A similar calculation shows that the spherically symmetric model with a time-dependent boundary condition at finite radius $r = a$ is not singular enough, because the Unruh-DeWitt detector response does not diverge.

Our contributions to this topic consist of two models; 3+1 D pointlike source creation and 3+1 D shell creation. In both cases we extended Brown and Louko's 1+1 D model and studied properties of the energy density and response function.

[1]Besides having a divergent energy density, we also want a divergent Unruh-DeWitt detector response.

Dedication

For my wife, Jayne

Acknowledgements

This work would not exist without the help, patience, encouragement, dedication and delightful conversations from the following list of people and organizations.

I want to first thank my co-supervisors and collaborators Dr. Margaret Carrington (Meg) and Dr. Gabor Kunstatter, without whose help I would have been lost in details. Meg's dedication and mathematical skills helped me tremendously in walking through many difficult situations, and Gabor's great intuition has proven to be so important when it comes to pick a topic and see past the irrelevant details. They both are also dedicated "nitpickers" when it comes to grammatical mistakes I made as the result of either rushing through writing or being unobservant.

I would like to thank Dr. Jorma Louko from the University of Nottingham, whose first attempt on building a "firewall" model with operator extension inspired this thesis. Many of the key developments in the research would not be possible without his extraordinary analysis skills.

I would also like to thank my parents, who are living on the other side of the Pacific. My dad has always been an extraordinary mentor that is interested in science despite being in school only up to grade five. My mom has as usual been a good "audience" when I was studying at home, who still occasionally thinks chicken has three legs.

I give a special thanks to my wife Jayne, who has been so amazingly supportive from day one and happy with me taking up physics. Her patience and understanding have been the most significant reasons I can finish this thesis.

It is so lucky to have the small department of physics and its hospitable crew at the University of Winnipeg, where I met Mike Lang, Taraneh Andalib, Brad Cownden, Jonathan Ziprick, Fady Shaker, Mitul Patel, and many others as my peers.

This cozy environment would not be available without the following list of people: Dr. Dwight Vincent who gave me the lab instructor position when I was financially tight, Dr. Murray Alexander who has always been a great conversationalist to talk about life and stress, Andrea Wiebe who is great at helping me printing papers off the department printer.

I also thank the University of Manitoba and NSERC for funding.

Table of Contents

List of Figures

Chapter 1

Overview

According to general relativity, black holes are regions of spacetime with extreme curvatures from which nothing can escape. Black holes are 'black' in the sense that even light cannot escape. Theories of black holes test the limits of general relativity, which is one of the foundations of modern physics. The theoretical prediction of black holes was first made by Schwarzschild in 1915, and the first direct experimental observation of gravitational waves from black holes was in 2015 by Laser Interferometer Gravitational-Wave Observatory (LIGO) [1].

Classical black hole theories immediately reveal the limits of general relativity by introducing singularities. This means general relativity must breakdown in some physical circumstances, such as the center of black holes. In order to overcome the limits of general relativity, we hope to combine quantum theory with general relativity. A significant result of this semi-classical approach is that Hawking discovered black holes do actually radiate what we now call Hawking radiation. Black holes are not entirely black. But this semi-classical approach does not help when it comes to the singularity, where a better theory is needed.

So now we have two theories that are very successful in their own realms: general relativity and quantum theory, but give confusing results when combined. Situations like this often hint at incompleteness in the theories, we can understand it by recalling the discovery of blackbody radiation. Physicists of the day were unable to derive the Planck distribution from classical statistics, because one needs concepts from quantum mechanics for such distribution. Similarly, it is believed that quantum field theory in curved spacetime (a combination of quantum field theory and general relativity) may not be a good description of black holes, and that a complete theory of quantum gravity is required.

Our study focuses on the proposal that general relativity needs drastic modification and a singular structure (such as a 'firewall') around a black hole's horizon[1] is needed. We show

[1] can be naively understood as the black hole's boundary

in the following chapters that, at least in the flat spacetime of 1+1 and 3+1 dimensions, our simple models cannot create a singular structure such as a 'firewall'. That being said, it could also be plausible that a more exotic mechanism is needed in this situation.

There is one main issue facing anyone studying the theory of black holes: we do not fully understand how black holes evolve. A lot of issues come from this and we will lightly touch those issues in the following text.

We look at Einstein's equation [2]

$$G_{\mu\nu} = 8\pi G T_{\mu\nu} \,, \tag{1.0.1}$$

where the left hand side (LHS) is Einstein's tensor $G_{\mu\nu}$ constructed from the metric and the right hand side (RHS) is stress-energy tensor of whatever matter fields there are. G is Newton's constant.

In classical physics, we often solve for the vacuum solutions (where $T_{\mu\nu} = 0$) of Einstein's equation. We want to note two important features of black holes.

(1) One is the so-called Schwarzschild metric, where an unphysical singularity appears at the coordinate origin. The existence of a singularity usually hints at a breakdown of the theory near the Planck scale, so we expect some changes once we quantize it. It is therefore not quite clear how much of the Schwarzschild metric is physically accurate.

(2) Another is the so-called no-hair theorem, which states that we can always form the exactly same black hole regardless of the initial state. A chair and a book, if thrown into a black hole, end up as the same black hole, as long as their overall properties (such as total mass, angular momentum, charge) are the same. Information[2] about the chair/book is assumed to stay in the black hole. The incompleteness of classical theory shows up in that we do not have full information about the object that was thrown into the black hole. We need a theory of the black hole interior.

Two or more systems in a joint pure state are entangled if the joint pure state is not a product state [3] (for a mixed state this statement does not hold, and we still do not have a universal measurement of entanglement). If system 'a' is in state $|a\rangle$, system 'b' is in $|b\rangle$, they are entangled as long as the joint state is not $|a\rangle|b\rangle := |a\rangle \otimes |b\rangle$. Throughout this thesis, we often use the term 'information' to describe the quantum entanglement encoded in an object's atomic states.

Assuming a system has density matrix ρ (depending on the system is independent or part of a bigger system, its density matrix is either full or reduced), its Von Neumann entropy is defined as

$$S_{VN}(\rho) = -\operatorname{Tr}[\rho \ln \rho] \,, \tag{1.0.2}$$

[2]We define *'information'* in the following page.

where we have set $k_B = 1$. Throughout the thesis, we use Von Neumann entropy as the definition of entanglement entropy. The term *entanglement entropy* refers to Von Neumann entropy of *reduced* density matrix of a subsystem. We can associate Hawking-Bekenstein entropy with Von Neumann entropy, see [4, 5], but the connection is not well-understood. In this thesis, Hawking-Bekenstein entropy is understood as the maximum entropy a black hole can have and is always no smaller than its entanglement entropy [6].

The term 'entropy' initially came from thermodynamics where it is defined by the first and second law of thermodynamics

$$dE = TdS + pdV + \cdots \tag{1.0.3}$$

or

$$dS = \frac{đQ}{T} \,. \tag{1.0.4}$$

Then Gibbs related thermodynamics entropy to Gibbs entropy

$$S = -\sum_i p_i \ln p_i \tag{1.0.5}$$

using statistical mechanics, where p_i is the probability of state 'i'. A special form of Gibbs entropy occurs when all the probabilities p_i are identical, which gives rise to Boltzmann entropy

$$S = \ln W \,. \tag{1.0.6}$$

W is the number of all possible states in the system. A natural generalization to quantum systems leads us to von Neumann entropy as defined as eq.(1.0.2).

We consider a system 'a' described by density matrix ρ_a and has Hilbert space of dimension $d_{\mathcal{H}_a}$. According to reference [5], the *information* of such system is defined as the deviation of the system's von Neumann entropy from its maximum. We can derive this maximum by considering a state where the density matrix is maximally mixed, thus ρ_a has only identical diagonal elements. We know from definition that a density matrix should satisfy $\mathrm{Tr}\,\rho_a = 1$. Therefore, for a Hilbert space of dimension $d_{\mathcal{H}_a}$, the diagonal elements are all $1/d_{\mathcal{H}_a}$ and there are a total number of $d_{\mathcal{H}_a}$ of them. This gives rise to a maximum von Neumann entropy of $\ln d_{\mathcal{H}_a}$. Therefore, the information is given by the following expression

$$I = \ln d_{\mathcal{H}_a} - S_{VN}(\rho_a) \,, \tag{1.0.7}$$

where zero entropy means maximum information.

For an *isolated* black hole, it is believed that the joint system of black hole and its radiation is described by a pure state ρ_{rh} on a Hilbert space $\mathcal{H}_{rh}$, where the radiation subsystem belongs to Hilbert space $\mathcal{H}_r$ and is in mixed state $\rho_r = \mathrm{Tr}_h[\rho_{rh}]$, with the black

hole subsystem belongs to Hilbert space $\mathcal{H}_h$ and is in mixed state $\rho_h = \mathrm{Tr}_r[\rho_{rh}]$. The dimension of $\mathcal{H}_{rh}$ satisfies $d_{\mathcal{H}_{rh}} = d_{\mathcal{H}_r} \times d_{\mathcal{H}_h}$. The von Neumann or entanglement entropy of either subsystem is $S_r = -\mathrm{Tr}[\rho_r \ln \rho_r] = S_h = -\mathrm{Tr}[\rho_h \ln \rho_h]$. As the black hole continues to radiate, the black hole subsystem becomes smaller and smaller until it is completely evaporated. In order to preserve the unitarity of the entire system, at the end stage (when the black hole is gone) the radiation should be in a pure state.

The information loss conundrum is the question of when and how does the mixed state of the radiation subsystem (predicted by the semi-classical Hawking calculation) turn into a pure final state as the black hole evaporates.

The big problem with Hawking's discovery of black hole radiation [7, 8] is that the radiation is precisely thermal for the entire lifetime of the black hole, which leaves no mechanism for the radiation to evolve into a pure state (if the black hole is completely evaporated).

A potential problem arises.

If Hawking radiation continues and evaporates the entire black hole, we end up with only thermal radiation that has no information. This is even true if we throw a pure state into the black hole. So the overall process is a system evolving from pure to maximally mixed state, which does not make sense according to quantum unitary evolution.

As the black hole evaporates, three natural possibilities appear [9, 10, 11].

1. *There could be some kind of remnant, so that the joint system of radiation and remnant is pure.*

   Physically, the remnant should not be too small, otherwise a huge amount of information is stored in a ridiculously small amount of mass[3].

2. *The information gets out in some form, so that the final burst, or radiation, is not purely thermal.*

   The information could also gradually come out because we do not expect Hawking radiation to hold until the end. But no mechanism is known.

3. *There is a third possibility where information is indeed lost/destroyed.*

   W. Unruh and R. Wald have been avidly supporting this solution for a number of years [12].

We want to mention that many theories were proposed for the black hole remnant and how information can get out, including gradual information retrieve through late radiation [13], Planck size remnant theory [14], fuzzball theory [8], etc., to explain black hole's ability to swallow information.

[3]This violates the so-called Bekenstein bound which says there is an upper limit on how much entropy a unit mass can have.

In this thesis, we discuss a fourth possibility, the author takes the firewall argument seriously (the AMPS[4] [15, 16] argument), which states that a high energy barrier should exist near the horizon of a black hole to destroy quantum entanglement, although the mechanism is not known. This high energy barrier, a. k. a. firewall, is also a 3-dimensional null surface. We investigate the divergence properties of the energy pulse and particle detector response from a time-dependent scalar field theory in Minkowski space. We generalize Brown and Louko's work on firewall model [17] to 3+1 dimensions. We find out that a particular generalization where a time-dependent boundary condition is at the spatial origin produces a strong divergence [18], while a second generalization with time-dependent boundary condition at a finite radius does not provide a strong enough divergence to model the firewall [19].

In chapter II, we give a brief overview of the mathematical tools needed. In chapter III, we review black hole thermodynamics and introduce the firewall proposal. In chapter IV, we introduce a 1+1 dimensional model [17] of firewall creation and discuss how the energy pulse annihilates information/quantum entanglement. In chapter V, we discuss a 3+1 dimensional generalization of the 1+1 dimensional model, where the firewall is induced by a pointlike source. Then in chapter VI, we discuss another 3+1 dimensional generalization of the 1+1 dimensional model, where the firewall is induced by the creation of a spherical shell at finite radius. Chapter VII concludes with a discussion of our goals and results.

We use units where $\hbar = k_B = c = 1$ throughout the thesis. Time and length have the same unit $[T]$, and frequency, temperature, energy have the same unit $[T^{-1}]$. We also choose the mostly-minus metric with signature $diag(1, -1, -1, -1)$, and convention $R^{\mu}_{\nu\rho\sigma}V^{\nu} = [\nabla_{\sigma}, \nabla_{\rho}]V^{\mu}$, $R^{\alpha}_{\beta\gamma\delta} = \partial_{[\gamma}\Gamma^{\alpha}_{\delta]\beta} + \Gamma^{\alpha}_{\lambda[\gamma}\Gamma^{\lambda}_{\delta]\beta}$, with $\nabla_{\beta}V^{\alpha} = \partial_{\beta}V^{\alpha} + \Gamma^{\alpha}_{\beta\gamma}V^{\gamma}$. Abbreviation BH stands for Black Hole, GR stands for general relativity, and QFT stands for Quantum Field Theory.

[4]AMPS is the abbreviation of names of the four authors who proposed this argument

Chapter 2

Fundamentals: quantum field theory in curved background

Quantum field theory in curved spacetime is often viewed as an effective field theory, where we treat spacetime as fixed classical background and matter fields as quantum objects. In this chapter, we give a short introduction to these mathematical tools.

The physics community believe quantum gravity effects are small under a certain limit. Any free flat space field theory has Fourier modes with wavelengths all the way to zero. If we do need the full details (including physics for wavelength shorter than Planck scale) to describe any process, then we could not do any calculation without having major discrepancy. The limit at which we need not consider quantum gravity effects is called 'solar system limit' by S. Mathur [10, 11]. We believe that quantum field theory in curved spacetime is valid in this limit, and a locally well-defined approximate evolution equation is available [10, 11]. This belief originates from the rather successful tests of semi-classical approaches in the early days of quantum mechanics. Recently, this belief seems to be challenged by the firewall argument by AMPS [15]. We show via examples that some interesting and puzzling results occur, even with a minor quantum correction. The changes in QFT that result from introducing curved spacetime are listed below.

1. The first is the problem of the vacuum, meaning there is no unique vacuum for all observers. A perfect example is the Unruh effect [20, 21], where an accelerating observer in Minkowski vacuum sees a thermal bath of particles. Because of the general feature of not having a unique vacuum for all observers, we also cannot agree on a unique number operator. A good example is cosmological particle creation, where a spacetime patch stretches to generate particle flows [22, 23]. Operationally, we can deal with the particle number problem by using a particle detector [20, 21], which measures the transition probability in its rest frame.

2. The second is related to the problem of the vacuum. It says different frames may not agree on the same positive frequency modes. A positive frequency mode in one frame could have negative frequency components in another frame. In Minkowski spacetime, the timelike Killing vector ∂_t ensures Poincaré symmetry, so we can agree on positive and negative frequencies across all inertial frames. In general spacetime, Poincaré symmetry is lost and there is no preferred set of modes.

3. The third is the problem of renormalization [23]. Unfortunately, divergences persist and are actually harder for QFT in curved spacetime. For QFT in flat spacetime, one can simply cut off at a reasonable energy scale. However, since GR suggests energy being the source of gravity, we cannot throw away infinite energy with a cutoff. This indicates that we can impose a local (any small smooth patch of spacetime) cutoff and discard it in renormalization, but we cannot impose a global cutoff.

In this chapter we briefly discuss the problems of vacuum and modes, while leaving renormalization out because of its complexity.

2.1 Scalar field in curved spacetime

In quantum field theory, it has long been known that a time-dependent boundary condition or metric can create particle and energy flows. One of the earliest works was pioneered by Parker in 1969, which showed that a Klein-Gordon field on an expanding spacetime patch undergoes particle creation [24]. In the year that followed, Moore uncovered particle emission with an adjustable-length cavity [25]. Then in 1977, Candelas and Deutsch discovered the so-called Dynamical Casimir Effect [26], which states that a single accelerating mirror can trigger particle/energy outflow [26]. This was observed in 2011 using a photon analogue system [27]. The long lasting puzzle, however, is Hawking's prediction of BH radiation [7] that puts quantum theory and GR in direct conflict. This eventually led to the AMPS firewall proposal [15].

In this section, we incorporate the curved background into standard QFT and explain cosmological particle creation through examples. We add to the scalar field Lagrangian the Einstein-Hilbert Lagrangian and a coupling term (that couples gravity/Ricci scalar and the scalar field). We then solve the modified scalar field equation by choosing a fixed metric with no back-reaction.

The following formulation of scalar field theory in curved spacetime follows that of Parker and Toms [22].

We start by considering a scalar field in flat spacetime, the action is defined as

$$S = \int d^4x \mathcal{L} \tag{2.1.1}$$

with Lagrangian density

$$\mathcal{L} = \frac{1}{2}\Big(\eta^{\mu\nu}\partial_\mu\phi\partial_\nu\phi - m^2\phi^2\Big)\,. \tag{2.1.2}$$

Here, $\eta_{\mu\nu}$ is the Minkowski metric $diag(1,-1,-1,-1)$ and ∂_μ is the Minkowski partial derivative. The goal is to promote all quantities to general spacetime while keeping S invariant under coordinate transformations. We accomplish this by changing the Minkowski metric to general metric, partial derivative to covariant derivative, and integration measure to volume density:

$$\eta_{\mu\nu} \to g_{\mu\nu}, \quad \partial \to \nabla, \quad d^4x \to \sqrt{-g}d^4x\,. \tag{2.1.3}$$

We introduce the simplest coupling term $\xi R\phi^2$, where ξ is the coupling constant and R is the Ricci tensor. The Lagrangian density becomes

$$\mathcal{L} = \frac{1}{2}\sqrt{-g}\Big(g^{\mu\nu}\nabla_\mu\phi\nabla_\nu\phi - m^2\phi^2 - \xi R\phi^2 + \frac{R}{16\pi G}\Big)\,, \tag{2.1.4}$$

where the last term is the usual Einstein action. The dynamical equation is derived by variation of the field ϕ

$$(\Box + m^2 + \xi R)\phi = 0\,. \tag{2.1.5}$$

Covariant scalar inner product is defined as an integral over a spacelike hypersurface

$$(\phi_1,\phi_2) := i\int d^{n-1}x\sqrt{-g}n^\nu(\overline{\phi_1}\partial_\nu\phi_2 - (\partial_\nu\overline{\phi_1})\phi_2)\,, \tag{2.1.6}$$

where n_ν is a timelike vector and ϕ_1,ϕ_2 are solutions of eq.(2.1.5). The inner product, by definition, is not positive definite but is linear in both arguments and satisfies $(\phi_1,\phi_2) = \overline{(\phi_2,\phi_1)}$.

A general field can be expanded as

$$\phi = \sum_k [A_k f_k(x) + A_k^\dagger \overline{f_k}(x)]\,, \tag{2.1.7}$$

where $f_k(x)$ are the modes of eq.(2.1.5) with annihilation and creation operators $A_k, A_k^\dagger$. The vacuum state $|0\rangle$ is defined by

$$A_k|0\rangle = 0\,. \tag{2.1.8}$$

So far everything parallels quantum field theory on a flat background.

The presence of a non-trivial background geometry does however have a major effect.

Consider the time-dependent Friedman-Robertson-Walker metric:

$$ds^2 = dt^2 - a^2(t)(dx^2 + \cdots) \tag{2.1.9}$$

$$a(t) \sim \begin{cases} a_1 & \text{when} \quad t \to -\infty \\ a_2 & \text{when} \quad t \to +\infty \,, \end{cases} \tag{2.1.10}$$

we take the limit where $a(t)$ evolves so slow (adiabatic limit) that at any point in time the field perceives spacetime as Minkowski.

In the minimal coupling regime (where $\xi = 0$), the dynamical equation reduces to

$$a^{-3}\partial_t(a^3\partial_t\phi) - a^{-2}\sum_i \partial_i^2\phi = 0\,. \tag{2.1.11}$$

Then we propose the ansatz (with V being the total volume)

$$f_k = V^{-1/2}e^{i\vec{k}\cdot\vec{x}}\psi_k(\tau) \tag{2.1.12}$$

and substitute it into equation (2.1.11). The result reads

$$(\frac{d^2}{d\tau^2} + k^2a^4)\psi_k = 0, \qquad \tau = \int^t a^{-3}(t)dt\,. \tag{2.1.13}$$

We want to look at two different sets of modes corresponding to the limits $t \to \pm\infty$:

$$t \to -\infty, \quad f_k^{(1)} \sim (Va_1^3)^{-1/2}(2k/a_1)^{-1/2}e^{i(\vec{k}\cdot\vec{x} - \frac{k}{a_1}t)} \tag{2.1.14}$$

$$t \to +\infty, \quad f_k^{(2)} \sim (Va_2^3)^{-1/2}(2k/a_2)^{-1/2}e^{i(\vec{k}\cdot\vec{x} - \frac{k}{a_2}t)}\,. \tag{2.1.15}$$

Either set is a complete basis to describe the evolution of the field. However, due to difference in the mode functions, these two sets of modes have two different vacua.

We proceed with canonical quantization. Annihilation operators $A_k^{(1)}$ of modes $f_k^{(1)}$ are defined by

$$A_k^{(1)}|0_{-\infty}\rangle = 0 \tag{2.1.16}$$

and annihilation operators $A_k^{(2)}$ of modes $f_k^{(2)}$ are defined by

$$A_k^{(2)}|0_{+\infty}\rangle = 0\,, \tag{2.1.17}$$

where $|0_{-\infty}\rangle$ and $|0_{+\infty}\rangle$ are vacuum states of the early and late time respectively.

Since either set (of modes) is complete, we can expand the field as

$$\phi = \sum_k A_k^{(1)} f_k^{(1)} + A_k^{(1)\dagger} \overline{f_k^{(1)}} = \sum_k A_k^{(2)} f_k^{(2)} + A_k^{(2)\dagger} \overline{f_k^{(2)}} \,. \tag{2.1.18}$$

Expanding modes $f_k^{(1)}$ in terms of modes $f_k^{(2)}$

$$f_k^{(1)} \sim \alpha_k f_k^{(2)} + \beta_k \overline{f_k^{(2)}}, \tag{2.1.19}$$

we get

$$A_k^{(2)} = \alpha_k A_k^{(1)} + \beta_k A_k^{(1)\dagger} \,. \tag{2.1.20}$$

Equation (2.1.20) is called a Bogoliubov transformation [22].

By using commutators $[A_k^{(1)}, A_{k'}^{(1)\dagger}] = \delta_{kk'}$ and $[A_k^{(2)}, A_{k'}^{(2)\dagger}] = \delta_{kk'}$, we also get

$$|\alpha_k|^2 - |\beta_k|^2 = 1 \,. \tag{2.1.21}$$

We compare the expectation value of particle numbers in state $|0_{-\infty}\rangle$ at early and late times

$$\langle 0_{-\infty} | A_k^{(1)\dagger} A_k^{(1)} | 0_{-\infty} \rangle = 0 \tag{2.1.22}$$

versus

$$\langle 0_{-\infty} | A_k^{(2)\dagger} A_k^{(2)} | 0_{-\infty} \rangle = |\beta_k|^2 \,. \tag{2.1.23}$$

Equation (2.1.23) is an example of cosmological particle creation [22].

We notice that the definitions of particles are different between the early and late time observers, due to the difference in the early and late time vacua $|0_{-\infty}\rangle$ and $|0_{+\infty}\rangle$. Particularly, there is no unique vacuum for all observers. This apparent ambiguity in the definition of a particle leads us to an operational definition: particle detector.

2.2 Particle detector

Defining particles through creation/annihilation operator does not specify where a particle is [28]. We can tell the total particle number and the total energy, but we cannot say for sure whether two observers at different spacetime points agree on their observations of the field. In this sense, the concept of particle is subjective. This is illustrated with the simple example in the previous section. From an operational point of view, a particle is what a particle detector 'sees'. Therefore, defining a particle by the clicks of a particle detector is completely unambiguous.

In the late 1970s, Unruh proposed a model particle detector which was later simplified by DeWitt, this model detector is what we now call Unruh-DeWitt detector [20, 23]: an interaction Lagrangian of a field coupling to a two-state system. So when the field is excited or particles are created, the two-state system will transfer from low to high energy. It models mathematically what happens in a real particle detector.

The Lagrangian for field and moment coupling (in the same fashion that a magnetic moment couples to magnetic field) is

$$\mathcal{L}_{int}(\tau) = cm(\tau)\partial_\tau^{(p)}\phi(x(\tau)), \tag{2.2.1}$$

where c is not the speed of light but the coupling constant and $\partial_\tau^{(p)}$ is the p-th order proper time derivative. The first order transition amplitude reads [23, 29]

$$\mathcal{A}^{(1)}\Big(|E_0,0\rangle \to |E,\psi\rangle\Big) = ic\langle E,\psi| \int_{-\infty}^{\infty} d\tau m(\tau)\partial_\tau^{(p)}\phi(\tau)|0,E_0\rangle\,, \tag{2.2.2}$$

where $|0\rangle, |\psi\rangle$ are states of the field, $m(\tau)$ is the Heisenberg operator of a moment that couples to the field, and $|E\rangle, |E_0\rangle$ are the detector's eigenstates. The symbol $|0,E_0\rangle$ means $|0\rangle \otimes |E_0\rangle$. When $p=0$, it is called non-derivative coupling detector.

We choose to use non-derivative coupling detector from last paragraph. Factoring eq.(2.2.2) with $p=0$, we rewrite it as

$$\mathcal{A}^{(1)}\Big(E_0,|0\rangle \to E,|\psi\rangle\Big) = ic\langle E|m(0)|E_0\rangle \int_{-\infty}^{\infty} d\tau e^{i(E-E_0)\tau}\langle\psi|\phi(x)|0\rangle\,. \tag{2.2.3}$$

This leads to the first order transition probability

$$\sum_{E,|\psi\rangle}\Big|\mathcal{A}^{(1)}\Big(E_0,|0\rangle \to E,|\psi\rangle\Big)\Big|^2 = c^2\sum_E |\langle E|m(0)|E_0\rangle|^2\mathcal{F}(E-E_0)\,, \tag{2.2.4}$$

where the response function $\mathcal{F}(E-E_0)$ is defined by

$$\mathcal{F}(E-E_0) := \int_{-\infty}^{\infty} d\tau \int_{-\infty}^{\infty} d\tau' e^{-i(E-E_0)(\tau-\tau')}\langle 0|\phi(x)\phi(x')|0\rangle\,. \tag{2.2.5}$$

Equation (2.2.5) indicates that the response function is an intrinsic measure of the field, because it is independent of how the monopole couples to the field. We usually refer to eq.(2.2.5) as the response function, because the factor $\sum_E |\langle E|m(0)|E_0\rangle|^2$ only represents the selectivity of the detector. The function

$$\mathcal{W}(x,x') := \langle 0|\phi(x)\phi(x')|0\rangle \tag{2.2.6}$$

is called the Wightman function.

If the field is time-translation invariant $\langle 0|\phi(x)\phi(x')|0\rangle = \mathcal{W}(\tau - \tau')$, then the transition rate becomes

$$c^2 \sum_E |\langle E|m(0)|E_0\rangle|^2 \int_{-\infty}^{\infty} dt e^{-i(E-E_0)t} \mathcal{W}(t)\,. \tag{2.2.7}$$

The detector response is the Fourier transformation of the two point correlation function of the field. It is also possible for detectors moving with different trajectories to respond differently, see Appendix A.1.

2.3 Klein-Gordon modes in Schwarzschild metric

An extraordinary result of GR is the Schwarzschild metric. It describes the exterior of geometry of any spherically symmetric mass distribution, and also describes the complete spacetime of an eternal black hole. The metric outside a spherical object of mass M is

$$ds^2 = \Big(1 - \frac{2GM}{r}\Big)dt^2 - \Big(1 - \frac{2GM}{r}\Big)^{-1} dr^2 - r^2(d\theta^2 + \sin^2\theta d\varphi^2)\,, \tag{2.3.1}$$

where there is a coordinate singularity at $r = 2GM$. We introduce Newton's constant G so that when $r \to \infty$ Newtonian gravity is recovered. The Schwarzschild metric is the only spherical symmetric vacuum solution, which is a result of Birkhoff's theorem [2].

We notice that the metric is not well-defined at the Schwarzschild radius $r_s = 2GM$. The ill-defined metric at radius $r = 2GM$ seems to suggest that it breaks down for $r \leq 2GM$. However, this is not the case, because we can choose a different coordinate system in which the metric is well-defined [2]. We introduce the tortoise coordinate

$$r_* = r + 2GM \ln\Big|\frac{r}{2GM} - 1\Big|\,, \tag{2.3.2}$$

and rewrite the metric as

$$ds^2 = \frac{r - 2GM}{r}(dt^2 - dr_*^2) - r^2(d\theta^2 + \sin^2\theta d\varphi^2)\,. \tag{2.3.3}$$

The vanishing determinant of the metric at $r = 2GM$ is not physical, it will be finite if we choose a different coordinate system. However, at the origin $r = 0$, we can see a physical singularity because the curvature and many other scalars (such as Kretschmann scalar) diverge. We can switch to Kruskal coordinates [2] and find out nothing is unusual at $r = 2GM$, except that the light cones tip over.

The Penrose diagram of the Schwarzschild metric of an eternal black hole is shown in

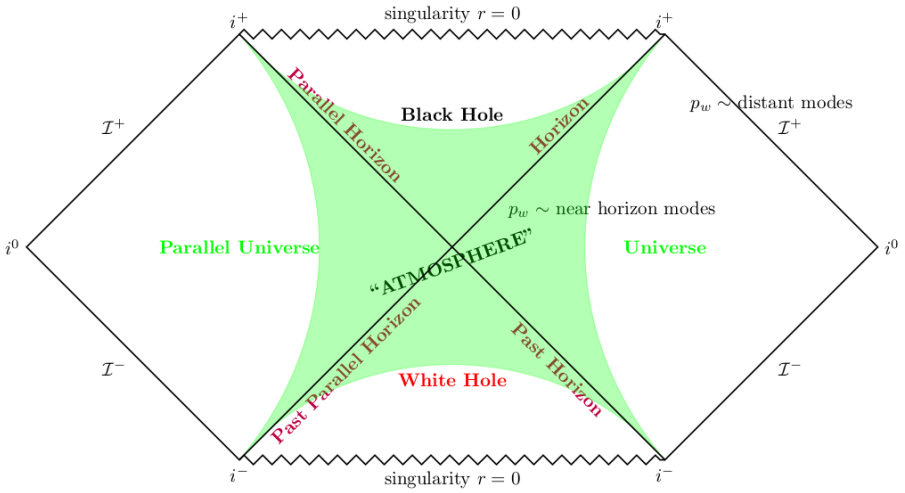

Figure 2.1: Penrose diagram of an eternal Schwarschild black hole. There are two singularities, two horizons, and two exterior regions of which one is the parallel universe [2]. Of the four regions, the right diamond-shaped region describes the exterior of a black hole in our universe. Near-horizon modes live mostly in the shaded region in this diamond and decay exponentially in the outside. Distant modes can travel to the white region of the diamond. The green shaded region is also called the **'atmosphere'** [6].

Figure 2.1. It is easy to tell the difference from Minkowski Penrose diagram, see Appendix A.2.

Now we consider a free scalar field ϕ in this metric [6]

$$\frac{1}{\sqrt{-g}}\partial_\mu(\sqrt{-g}g^{\mu\nu}\partial_v\phi) = \tilde{m}^2\phi\,, \tag{2.3.4}$$

where $g^{\mu\nu}$ is the inverse metric, $\sqrt{-g}$ is the determinant, and $\tilde{m}$ is the mass (of the field). Noticing the right exterior of the Penrose diagram in Figure 2.1 is covered by coordinates (t, r, φ, θ), a trial solution is given as

$$f_{\omega lm} = \frac{1}{r}Y_{lm}(\Omega)e^{-i\omega t}\psi_{\omega l}(r)\,. \tag{2.3.5}$$

The effective Schrödinger equation for $\psi_{\omega l}$ is

$$-\frac{d^2}{dr_*^2}\psi_{\omega l} + V(r)\psi_{\omega l} = \omega^2\psi_{\omega l}\,, \tag{2.3.6}$$

with

$$V(r) = \frac{r - 2GM}{r^3}\Big(\tilde{m}^2 r^2 + l(l+1) + \frac{2GM}{r}\Big)\,. \tag{2.3.7}$$

We discuss this potential in more detail, because it is crucial in categorizing the mode functions [6].

We show that only massless modes are important in the discussion of BH radiation by explaining why massive particles are not important.

First, we notice that radiation is carried by modes that can travel far from the BH, these modes must satisfy $\omega > \tilde{m}$ (by taking $r \gg 2GM$ and letting the potential go to constant $\tilde{m}^2$).

Next, we consider two limits: Compton wavelength $1/\tilde{m} \gg r_s = 2GM$ and Compton wavelength $1/\tilde{m} << r_s = 2GM$. The first limit is essentially setting $\tilde{m} \approx 0$ and the second limit is for massive particles.

For massive particles $\tilde{m} \gg 1/2GM$, in order for the mode to propagate to infinity, we need to have frequency $\omega > \tilde{m} \gg 1/2GM$. However, according to Hawking [7], black holes have temperature of the order of the inverse Schwarzschild radius $T_{Hawking} \sim 1/2GM$. This means large frequencies $\omega \gg T_{Hawking}$ are exponentially suppressed. Due to the small nature of the quantity $1/2GM$, most of the massive fields have much larger energy scale than $1/2GM$. Heavy massive fields are mostly confined around the Schwarschild radius and do not interact because of the difference in energy scales. So we are restricted to considering massless scalar field.

For a massless field, the effective potential has two limits

$$V \approx \begin{cases} \frac{l(l+1)}{r_*^2} & r_* \to \infty \\ (l^2 + l + 1)e^{r_* - 1} & r_* \to -\infty\,. \end{cases} \tag{2.3.8}$$

It vanishes polynomially in r_* at spatial infinity and exponentially in r_* near the horizon. In between these two regions there is a barrier, whose peak has a height of order l^2 and is at radius $r \approx 3GM$ (see Figure 2.2). According to references [6, 30], this potential divides the spacetime outside the horizon into two regions. The geometry is very similar to the Minkowski geometry in the region $r \gg 3GM$ (distant region), while the geometry differs significantly from Minkowski geometry in the region $2GM < r < 3GM$ (near-horizon region). As a result, the distant modes are not much different from the Minkowski modes and can propagate to infinity, but the majority of the near-horizon modes are confined in the shaded region of the right diamond in Figure 2.1. The near-horizon modes are sometimes called the 'atmosphere' [6].

Solving for the modes of the effective Schrödinger equation eq.(2.3.6) now becomes a 1-dimensional scattering problem. Modes that travel to null infinity could come from null infinity but are reflected back, or from near the horizon and tunnel through the barrier.

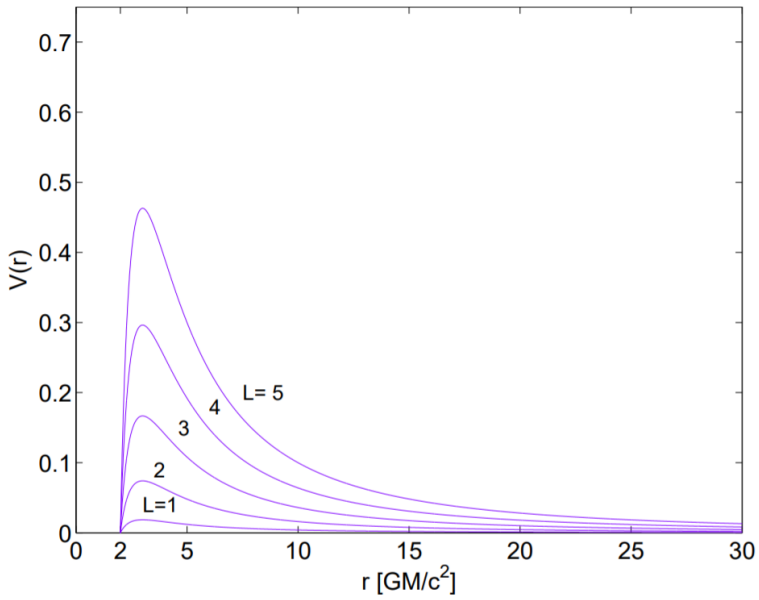

Figure 2.2: A plot of potential from [31]: effective potential as a function of r for $l = \{1, 2, 3, 4, 5\}$, where r is in units of GM.

2.4 Hawking radiation

We now consider spacetime where an infinitely large shell of matter starts to collapse at time $t \sim -\infty$. Inside the shell, the space is Minkowski. Outside the shell, due to spherical symmetry, it should be Schwarzschild. The Penrose diagram of a black hole formed from a collapsing shell is given by sewing the Minkowski Penrose diagram of Figure A.2 and the two upper right regions of Figure 2.1 together. It is shown in Figure 2.3.

To study the mathematical relationships of different modes, we use the detailed diagram of Figure 2.4, where different modes are labeled. We emphasize that f_ω is the initial ingoing Minkowski mode. Modes p_ω consist of both near-horizon modes (in the 'atmosphere') and distant modes. We do not have an accurate expression for near-horizon modes.

When $t \to -\infty$, there is only ingoing massless particles with positive energy near the past null infinity $\mathcal{I}_-$. The ingoing modes are Minkowski-like [22]

$$f_\omega \sim \omega^{-1/2} r^{-1} \exp(-i\omega(t+r)) S(\varphi, \theta)\,, \tag{2.4.1}$$

where $S(\varphi, \theta)$ is the angular distribution of the modes and f_ω satisfies the orthonormality condition $(f_\omega, f_{\omega'}) = \delta(\omega - \omega')$.

From a distant observer's point of view, when $t \to +\infty$, any null ray either goes to future null infinity $\mathcal{I}_+$ or ends up on the BH horizon H_+. The distant modes portion of p_ω is also Minkowski-like (no explicit expression for near-horizon mode and modes q_ω behind the horizon):

$$p_\omega \sim \omega^{-1/2} r^{-1} \exp(-i\omega(t-r)) S(\varphi,\theta)\,. \tag{2.4.2}$$

Both p_ω and q_ω satisfy orthonormality conditions $(p_\omega, p_{\omega'}) = \delta(\omega-\omega')$, $(q_\omega, q_{\omega'}) = \delta(\omega-\omega')$, $(p_\omega, q_{\omega'}) = 0$.

Given these expressions, any field can be expanded as

$$t \to -\infty : \qquad \phi = \int d\omega (a_\omega f_\omega + c.c) \tag{2.4.3}$$

or

$$t \to +\infty : \qquad \phi = \int d\omega (b_\omega p_\omega + c_\omega q_\omega + c.c)\,, \tag{2.4.4}$$

where $c.c$ means complex conjugate. Similar to eq.(2.1.20), we calculate the Bogoliubov transformation between the operators. According to eq.(2.1.23), it turns out that an empty space at past null infinity is filled with particles from the point of view of a later time observer. These late time particles are what we call Hawking radiation [7, 22, 23].

The physical idea is recapitulated below. We define the state in such a way that at early times there are no excited Minkowski modes f_ω below the shell (this was done when the shell was infinitely big, so the entire space is inside the shell). Because of the mixing of modes q_ω and p_ω, a positive frequency Schwarzschild mode p_ω is excited. This is the part we call Hawking radiation.

Hawking's remarkable work tells how the Schwarzschild modes are excited [7]. The energy flux from a BH [7, 22, 23, 6] is given as a thermal distribution:

$$\frac{dE}{dt} = \frac{\omega d\omega}{2\pi} \frac{P_{abs}(\omega, l)}{e^{\beta\omega} - 1}\,, \tag{2.4.5}$$

where $P_{abs}(\omega, l)$ is the absorption probability of the potential barrier in Figure 2.2 (often called a graybody factor), and $\beta = 1/T_{BH}$ is the inverse Hawking temperature where $T_{BH} = 1/2GM$.

Hawking radiation is derived from the technical assumption of an approximately stationary black hole. As the black hole radiates, this assumption breaks down and the radiation must slowly change in some way. We give more thoughts on this question in the following chapter. From now on, we call the radiation that **does not carry information**[1] as "unentangled Hawking radiation", and the radiation in general as "Hawking radiation".

[1] By the definition in chapter three, this means maximum entropy.

We calculate the total amount of energy leaving a black hole

$$\frac{d}{dt}E = \sum_{l,m} \int_0^\infty \frac{d\omega}{2\pi} \frac{\omega P_{abs}(\omega, l)}{e^{\beta\omega} - 1} \,, \tag{2.4.6}$$

where $P_{abs}(\omega, l)$ is called the graybody factor. A naive estimation by setting $l = 0$ gives $P_{abs}(\omega, 0) \sim (\omega r_s)^2$. Thus we have

$$\frac{dE}{dt} \approx -\frac{C}{(GM)^2} \tag{2.4.7}$$

with C being a constant, so the lifetime of mass M black hole is

$$t_{evap} \sim G^2 M^3 \,. \tag{2.4.8}$$

We can also derive t_{evap} using the Stefan-Boltzmann law.

For a black hole weighing a hundred tons (mass of a blue whale), its life time is about 0.01 second. For mountain sized black hole, its life time is about 10^{12} years. For a solar mass black hole, its life time is about 10^{66} years compared to the universe's age 10^{10} years [35]. If we can create a black hole in the Large Hadron Collider (LHC), it would be relatively easy to watch it evaporate and disappear. We also want to emphasize that Hawking's result of t_{evap} is derived by considering a stationary and relatively large black hole. Whereas any black hole in reality is dynamical, so the semi-classical approximation breaks down.

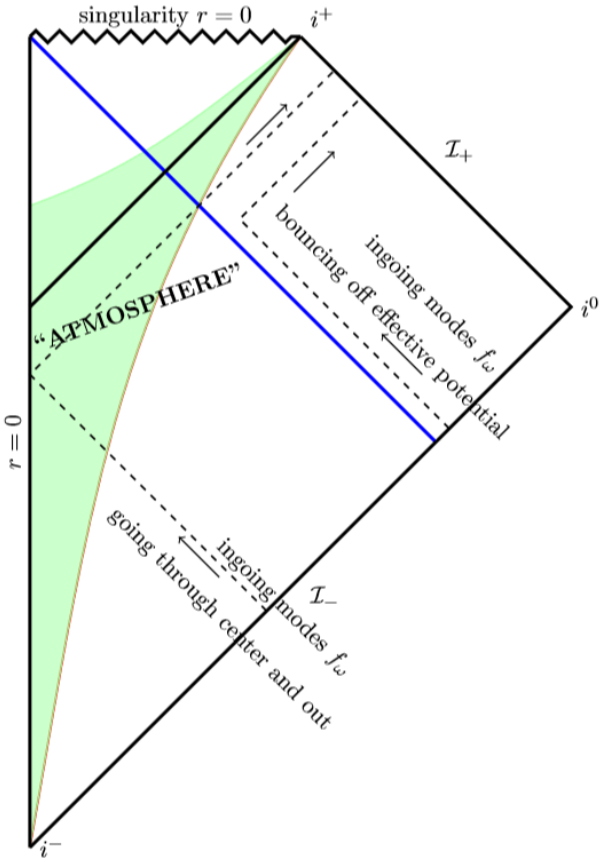

Figure 2.3: Penrose diagram of a black hole formed from collapsing matter. The green region is called the '**atmosphere**'. The blue line describes a collapsing null shell, the backward evolution of the outgoing modes are in dotted lines. Part of the outgoing modes are from the initial ingoing Minkowski modes: below the blue line. Part of the outgoing modes are from ingoing modes being scattered off the potential barrier of Figure 2.2: above the blue line.

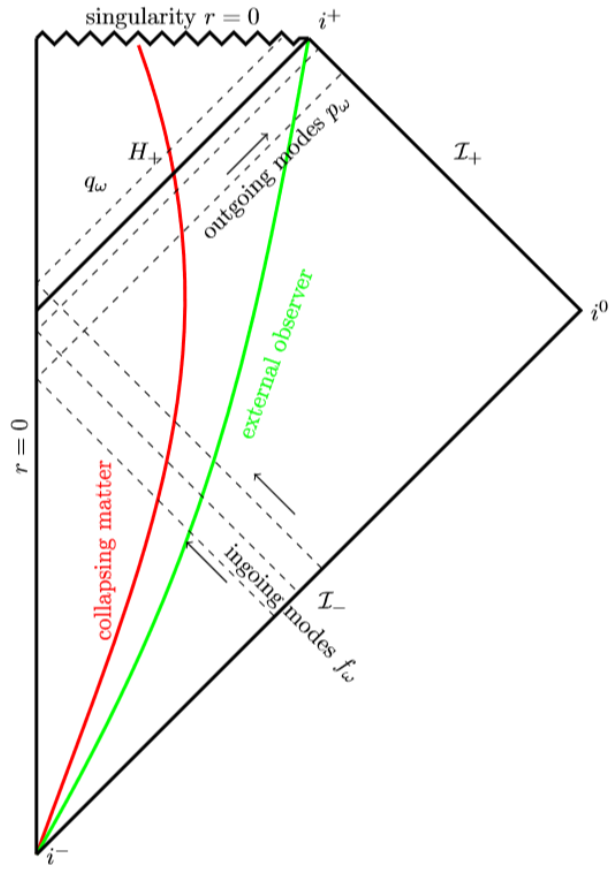

Figure 2.4: Penrose diagram of a black hole. H_+ is the event horizon, $\mathcal{I}_+$ is future null infinity, $\mathcal{I}_-$ is past null infinity, i^- is past time infinity $t \sim -\infty$, i^+ is future time infinity $t \sim +\infty$, i^0 is space infinity. f_ω are ingoing modes, p_ω are outgoing modes, q_ω are modes behind the horizon. The solid line of collapsing matter describes massive particles falling through the horizon until reaching the singularity. We did not include modes bouncing off the effective potential of Figure 2.2. From Figure 2.1, modes p_ω have two contributions: those in the 'atmosphere' and those that can propagate to distant regions. We do not usually have explicit expressions for modes in the 'atmosphere', while for modes in distant regions we often assume they are Minkowski-like.

Chapter 3

Introduction to the firewall

We outline this chapter as follows.

- We discuss Hawking radiation in the context of black hole thermodynamics and quantum field theory in curved spacetime, and explain the connection to the information loss conundrum.
- Then we introduce Page's argument on black hole entropy. It states that the entanglement entropy of a black hole first increases steadily from zero then decreases starting from Page time t_{Page}. On one hand, Hawking radiation should no longer be purely thermal after Page time, because by then there is entanglement with the early radiations (entanglement entropy starts decreasing). On the other hand, for a big black hole, Hawking's calculation should still hold at Page time (because the black hole is still big), and Hawking radiation should still be purely thermal.

  There is obviously a contradiction on whether Hawking radiation is purely thermal. Should the Hawking radiation hold for big black holes after Page time?
- Then we consider the physics for an infalling observer, which violates quantum no-cloning theorem globally. But locally, for each observer alone, there is no violation.
- To incorporate a set of locally self-consistent laws of physics, we introduce black hole complimentarity. However, black hole complimentarity still has problem. As a result, we introduce the black hole firewall.

3.1 Black hole thermodynamics

Now that we have established some facts about the Schwarzschild black hole, we want to discuss the general properties of black holes.

Classically, four laws were formulated for black hole mechanics under various conditions [2, 32]:

1. Surface gravity [32] κ (acceleration of a static object near the horizon measured by a distant observer) of a stationary black hole is uniform across the horizon. This law resembles the law of thermal equilibrium where temperature is uniform among different systems in equilibrium.

2. For perturbations of a stationary black holes: the change in its energy E is related to the changes of its horizon area A, total angular momentum J, and electric charge Q through formula (note that κ is surface gravity)

$$dE = \frac{\kappa}{8\pi} dA + \Omega dJ + \Phi dQ \,. \tag{3.1.1}$$

   It describes when the system is rotating with angular frequency Ω and charged up to an electric potential Φ, the changes in its angular momentum J and charge Q contribute to energy change dE.

3. Horizon area of a black hole is non-decreasing:

$$\frac{d}{dt} A \geq 0 \,. \tag{3.1.2}$$

4. Zero surface gravity is un-achievable within finite time.

The first term of eq.(3.1.1) $\frac{\kappa}{8\pi} dA$ resembles TdS in thermodynamics, so not surprisingly κ is proportional to Hawking temperature and A is proportional to Bekenstein-Hawking entropy.

Historically, this law was the key for Jacob Bekenstein to suggest black holes entropy [33] (that is proportional to the area of its event horizon), which further lead to the discovery of Hawking radiation.

These four laws are strikingly similar to the four laws of thermodynamics [33]: surface gravity behaves like the temperature of a black hole, horizon area is related to the measure of some kind of entropy [4], and black hole mass is a measure of the total energy. For a black hole, thermal equilibrium corresponds to it being stationary. A thermal equilibrium with Hawking radiation can be reached by adding a thermal reservoir at spatial infinity. But this equilibrium is unstable because a black hole has negative specific heat (i.e. if it loses energy it radiates even more).

The striking similarities between the laws of black hole mechanics and the laws of thermodynamics [33] were originally considered purely mathematical by most physicists. It was

Hawking's ground-breaking work on black hole radiation [7] and entropy [34] that finally 'proved' the laws of black hole mechanics are in fact thermodynamic laws.

We derive the entropy using the first law of thermodynamics

$$\frac{dS}{dE} = \frac{1}{T_{Hawking}} \,. \tag{3.1.3}$$

We have the Bekenstein-Hawking entropy [34] below:

$$S_{BH} = \frac{A}{4l_p^2} = \frac{A}{4G} \,, \tag{3.1.4}$$

where l_p is Plank length, $A = 16\pi(GM)^2$ is area of the event horizon. Surprisingly, the entropy is not proportional to the volume of the black hole but to the area of its boundary.

Reference [4] shows the entanglement entropy of a quantum field with spherical boundary, where a general feature of the entanglement entropy is that it is proportional to the area of the boundary. As a result, relationships like eq.(3.1.4) are quite general.

- **Assumptions:**

  Hawking radiation is based on the low energy effective field theory (EFT) near the horizon of a large black hole. By a large black hole we mean the curvature near its horizon is small and Planck scale physics can be ignored. There is no reason to believe Hawking radiation is not valid for large black holes.

- **Conclusions & problems:**

  If Hawking radiation continues until the black hole reaches Planck size, whatever is left has a huge amount of entropy comparing to its tiny mass [34]. However, there is an upper limit on the entropy of any bounded system, called Bekenstein bound [57]. How can such tiny mass has entropy exceeding the bound?

3.2 Information loss paradox and two attempted solutions

We define information following reference [5], where it is defined as the deviation of the Von Neumann entropy from maximum.

Let's briefly review the information loss conundrum through an example [10, 11].

Consider a system of particle pairs 'a, b' in a pure state near event horizon, where particle 'a' falls into the horizon while particle 'b' remains outside. Mathematically, this process is represented as follows.

For system with one particle pair, the system is in a pure state described by the wave-function [10]

$$|\psi\rangle = \frac{1}{\sqrt{2}}\Big(|0_a\rangle \otimes |0_b\rangle + |1_a\rangle \otimes |1_b\rangle\Big)\,. \tag{3.2.1}$$

The (reduced) density matrix of particle 'b' is

$$|\psi\rangle\langle\psi| \to \rho_b = \mathrm{Tr}_a|\psi\rangle\langle\psi| = \frac{1}{2}\Big(|0_b\rangle\langle 0_b| + |1_b\rangle\langle 1_b|\Big)\,, \tag{3.2.2}$$

and it is a mixed state because $\rho_b^2 \neq \rho_b$. Trace over 'a' comes from the assumption that particle 'a' falls into the black hole and becomes inaccessible to distant observers.

Quantum unitary evolutions tells us that pure states only evolves into pure states. But if the semi-classical form of Hawking radiation continues, there is no mechanism for transferring the correlation between particle 'a' and 'b' to the Hawking radiation, suggesting that the initial pure state of the BH + radiation will evolve into a mixed state. Clearly, this process is non-unitary [34].

It might be possible to avoid the information loss problem if the Hawking radiation stops before evaporation is complete, and leaves behind a remnant, which strongly entangles with the early radiation [14, 8]. Another proposal is that a baby universe is created inside the black hole [8]. The basic idea behind both of these scenarios is that the radiation could form an entangled pure state together with whatever is left of (or in) the black hole. However, there are major difficulties associated with both of these approaches.

- **Assumptions:**

  Hawking radiation (thermal) is valid as long as effective field theory is valid near the black hole horizon.

  Effective field theory should be valid until quantum gravity comes in, which is when the black hole reaches Planck size.

- **Conclusions:**

  There could be a (microscopic or macroscopic) remnant or baby universe. A Planck sized remnant does not seem plausible because it holds a macroscopic amount of entropy and might exceed Bekenstein bound [57]. But macroscopic remnant also poses problem, because it means effective field theory breaks down before Planck stage.

3.3 Page's argument

We ended last section with the possibility that a remnant or a baby universe might solve the information loss conundrum. However, an unexpected problem shows up if we really look into when Hawking radiation stops.

The idea is to find out when the entanglement is restored. Essentially, if Hawking radiation (pure thermal) fails, we have a good reason to not trust effective field theories. The moment entanglement starts restoring is the moment effective field theory stops being valid.

Here is Don Page's observation.

1. Bekenstein-Hawking entropy eq.(3.1.4) satisfies the first and second laws of thermodynamics, it is natural to assume it is a thermodynamic entropy and comes from state counting. The dimensions of a black hole's Hilbert space is $\exp[S_{BH}]$. So eq.(3.1.4) should be an upper limit of the von Neumann entropy $-\mathrm{Tr}(\rho \ln \rho)$ of a black hole.

2. However, as the black hole evaporates, Bekenstein-Hawking entropy S_{BH} decreases because the black hole shrinks, while the von Neumann entropy of the black hole increases [10]. But the von Neumann entropy should always be smaller than the Bekenstein-Hawking entropy [10, 11]. At some point in time, von Neumann entropy is going to decrease. The decrease of von Neumann entropy corresponds to the restoration of entanglement, or information. See figure 3.1.

This point in time is called Page time, and it is typically of order $t_{Page} \sim (GM)^3/l_P^2$, where l_P is Planck length. For a big black hole, at Page time t_{Page}, its radius is approximately half its original size. So if the black hole is still big, why would semi-classical approximation break down? One would never imagine the effective field theory or semi-classical approximation breaks down for such a big black hole. This is quite different from our expectation of effective field theory being valid till the black hole is Planck sized [7, 9]. Therefore, for quite a few long years, the conflict between Page's entropy argument and Hawking's semi-classical argument just continued.

- **Assumptions:**

  The exponential of Bekenstein-Hawking entropy is the number of internal degrees of freedom of a black hole, or the dimensions of the black hole's Hilbert space.

  Bekenstein entropy is the upper bound of von Neumann entropy.

  For a young black hole, as it evaporates, Bekenstein-Hawking entropy decreases while the von Neumann entropy increases.

  As the black hole ages it reaches a point where its von Neumann entropy starts decreasing, and its entanglement starts restoring.

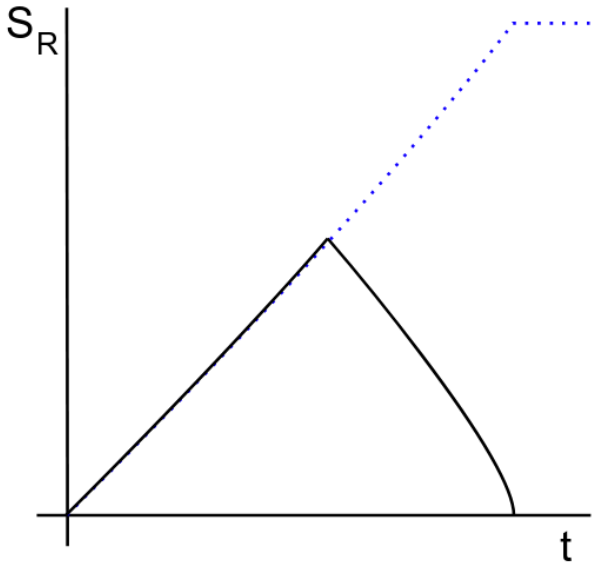

Figure 3.1: From [6]: In black, entropy of the radiation S_R versus time. The blue dotted line describes a steady increasing radiation entropy, which follows Hawking's argument. The maximum amount entropy radiation can have is the Bekenstein-Hawking entropy, which is given as the horizontal line. The turning point in time is called the Page time. If we can calculate the entire Page curve, then we are capable of understanding black hole evaporation. For some particular theory, Andrew Strominger argued that being able to compute the Page curve is equivalent to solving the information paradox [6]. Typical Page time of a solar mass black hole is of order 10^{66} years [13], while the age of our universe is 10^{10} years.

Hawking radiation (effective field theory) starts breaking down when entanglement starts restoring.

- **Conclusions & problems:**

  We cannot trust low energy effective field theory even when the black hole is still big (with half its original S_{BH} entropy & low curvature near the horizon). Then when can we use effective field theory?

3.4 Quantum no-cloning

From the last two sections, studies of Hawking radiation and Page's argument seem to suggest something is seriously wrong in our understanding of the black holes. Would effective field theory work near a black hole horizon? Would the theory depart significantly from low

energy effective field theory at Page time (when the black hole is still big)? Naturally, one would ask about the experiences of an infalling observer. Would an infalling observer go through the horizon smoothly?

We consider an infalling observer sitting on a collapsing matter shell, which collapses to form a black hole. The infalling observer can read the information of the matter shell. A distant observer can read information of the matter shell from studying the entanglement of the radiation (after Page time). If we reflect the radiation back to the black hole with a mirror, the infalling observer sees two copies of the same information: his own copy and one copy from reflection. This contradicts the no-cloning theorem [6]. The process is shown in Figure 3.2.

For a distant observer, information is stored in the entanglement between the late-time radiation and the initial Hawking radiation. For an infalling observer, the equivalence principle is preserved. A distant observer has to wait until past Page time to retrieve information from the radiation, by then it is too late to jump in the black hole and see the second copy [6].

Laws of nature work just well to prevent the infalling observer from seeing two copies, see [6] and references therein. For any individual observer, no-cloning theorem is not violated after all. This suggests no-cloning theorem is valid only locally.

- **Assumptions:**

  We assume the infalling observer sees nothing out of the ordinary. Laws of quantum physics continue to be valid and quantum cloning is forbidden.

- **Conclusions:**

  There are two copies of the same information on the green slice of Figure 3.2. But each observer can only see one copy of the same information, so unitarity is preserved for each observer. No-cloning theorem only holds locally.

3.5 Black hole complimentarity

To be consistent with the no-cloning theorem, Susskind, Thorlacius and Uglum proposed [36, 37] that no single observer can see both copies of information on the green slice in Figure 3.2. This is commonly called black hole complementarity, which is a set of consistent statements to make sure no single observer ever sees any violation of laws of the nature [30].

We introduce a rigorous description of black hole complementarity as the following [15, 35]:

1. Postulate 1: From a distant observer's point of view, the formation and evaporation of black holes can be described entirely within the context of standard quantum theory.

Mathematically, an S-matrix can describe the evolution from infalling matter to outgoing Hawking-like radiation. For each observer, it says the evolution from red slice to green slice is unitary, see Figure 3.2.

2. Postulate 2: Outside the horizon of a massive black hole, physics is well approximated by a set of semi-classical field equations. This means a low energy effective field theory with local Lorentz invariance is available.

3. Postulate 3: For a distant observer, a black hole appears to be a quantum system with discrete energy levels. The dimensions of the subspace of states for a mass M black hole is the exponential of Bekenstein-Hawking entropy $\exp[S_{BH}(M)]$.

4. Postulate 4: A free falling/infalling observer experiences nothing unusual at the horizon until the singularity is approached. This postulate justifies that the inside of a black hole is entangled with late-time Hawking radiation, namely the systems 'A' and 'B' of figure 3.3. because the infalling observer sees a smooth horizon (meaning entanglement across the horizon).

3.6 Firewall conjecture

3.6.1 The AMPS argument

For black holes older than Page time, Almheiri et al (AMPS) [15] argue that the postulates of black hole complementarity are not mutually consistent.

We use the notations in Figure 2.4. Initially, modes q_ω and p_ω are very entangled. Modes p_ω are mainly in the 'atmosphere' because there is no radiation yet. As the black hole radiates, modes q_ω 'leak' out and become radiations in modes p_ω. We point out that modes q_ω in Figure 2.4 corresponds to A in Figure 3.3, and modes p_ω in Figure 2.4 corresponds to $B\,, R$ in Figure 3.3. Page's theorem indicates that after Page time p_ω in the 'atmosphere' and p_ω in the radiations are very entangled [35, 5] (since most of q_ω radiate out with very few degrees of freedom left). A contradiction occurs for the infalling observer.

We explain the argument with Figure 3.3, where $A\,, B\,, R$ stand for modes behind the horizon, in the 'atmosphere' and in distant region respectively.

- For an old black hole (after Page time), Page's theorem indicates that $B\,, R$ are maximally entangled. For example, the state may resemble $|\psi\rangle \sim |A\rangle \otimes (|B\rangle + |R\rangle)$ to leading order.

- For the same old black hole, because it is still quite big, the equivalence principle suggests that an infalling observer experiences a smooth horizon. Therefore $A\,, B$ are

maximally entangled. For example, the state may look like $|\psi\rangle \sim (|A\rangle + |B\rangle) \otimes |R\rangle$ to leading order. See [10].

However, according to monogamy theorem in Appendix A.3, modes B can only be maximally entangled with either R or A. The two points above obviously contradict each other.

To reconcile with monogamy theorem, AMPS [15] conjectured that an infalling observer runs into a firewall right outside the black hole horizon. This firewall is such a singular structure that it incinerates even the entanglement between A, B. We may have a violent horizon. It is not clear whether an infalling observer is suddenly terminated, or merely experience abnormalities at the black hole horizon [35].

AMPS argue that a firewall is the most likely resolution to the information paradox, but they do not suggest that it is the only option [15, 35]. So the nature of the horizon is still unknown.

3.6.2 Implications:

The firewall conjecture hints at a drastic change in the concept of black hole horizon [35]. This is historically somewhat similar to wave-particle duality, which introduced the idea that the concept of individual particles is not meaningful [6].

Firewalls serve as disruptive boundaries of black holes to ensure no entanglement exists between the two sides of a horizon. The lack of entanglement between the two sides of a boundary, as Czech et al suggested [38, 39], means the space behind this boundary does not exist. Therefore, the space behind a black hole firewall/horizon potentially does not even exist [35], see Figure 3.5. This is a major departure from the spacetime structure in Figure 3.3. Some hypothetical changes are shown in Figure 3.4 and Figure 3.5.

3.7 Summary

We summarize as follows.

1. We introduced Hawking radiation in the low energy effective field theory (we still do not know when effective field theory breaks down), which naturally leads to what remains after a black hole evaporates. Two of the options are some kind of remnant and baby universe.

2. We looked at the black hole evaporation from an entropic perspective, where we introduced Page's argument about entropy that challenges the validity of effective field theory.

3. We introduced the concept of quantum no-cloning, which leads to black hole complimentarity.

4. Finally we introduced the firewall argument, which changes black hole complimentarity.

We stop at the firewall argument, because the focus of this thesis is the mechanism of firewall creation. In particular, we attempt to model firewall creation using time-dependent boundary condition.

Our research studies further one possible mechanism [17, 40] of firewall creation, which makes use of time dependent boundary conditions. The goal is to study the singularity structure of the energy density and detector response [15]. We confirm that time dependent boundary conditions indeed create energy pulses. These energy pulses have divergent energy density even when the boundary conditions evolve smoothly. However, the total energy fails to be finite when the metric is fixed [17, 18]. Also, except in special cases, the detector response is not singular enough.

In the following chapters, we discuss some of the simplest firewall models [15]. Our results are mathematically rigorous, but the models are not quite so because all three models in references [17, 18, 19] assume fixed Minkowski metric. Any realistic model should include interactions between the metric and the matter field. However, we do not consider metric back-reactions in this thesis.

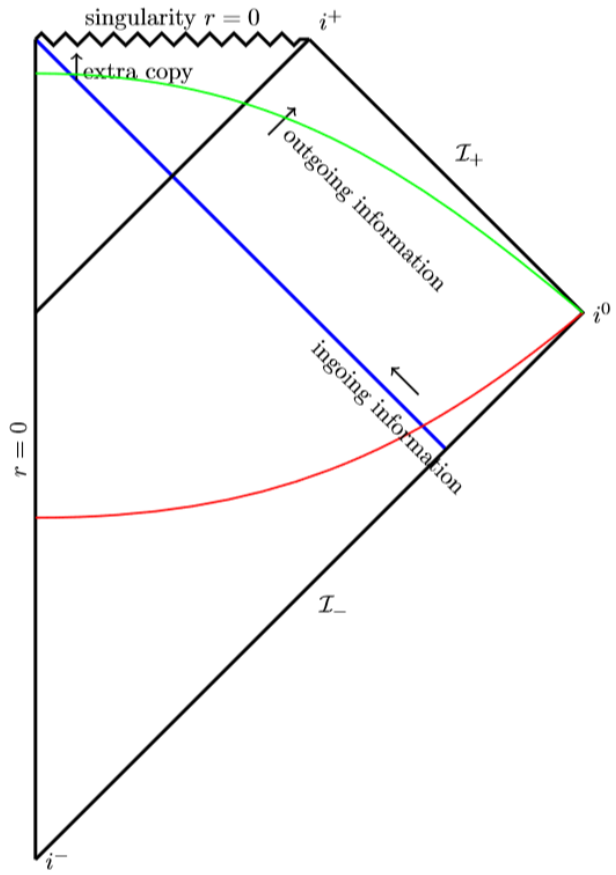

Figure 3.2: Black hole cloning. Information on the red slice is carried onto the green slice. Both the infalling observer and the distant observer see the same information, which means there are two copies of the same information on green slice [6]. But this does not violate no-cloning theorem because each observer can only see one copy.

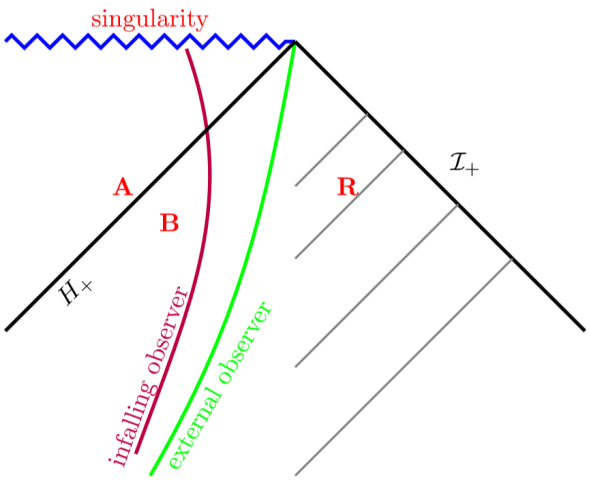

Figure 3.3: A zoom-in of the upper right corner of a Penrose diagram of Schwarzschild geometry, where A are the modes inside the horizon, B are the modes just outside the horizon, R is the radiation. (1) For a young black hole, a distant observer sees A and B heavily entangled with each other (there is basically no radiation R). So a partial trace of A gives a thermal distribution in B (Hawking radiation). (2) For an old black hole (past Page time), Page's theorem says enough of A modes should have come out that B and R are very entangled. Whereas the equivalence principle (postulate 4) says A, B are very entangled (as long as the black hole is big enough), because an infalling observer should encounter a smooth horizon [35]. Accordingly, the equivalence principle contradicts with monogamy theorem Appendix.A.3 in the infalling observer's frame.

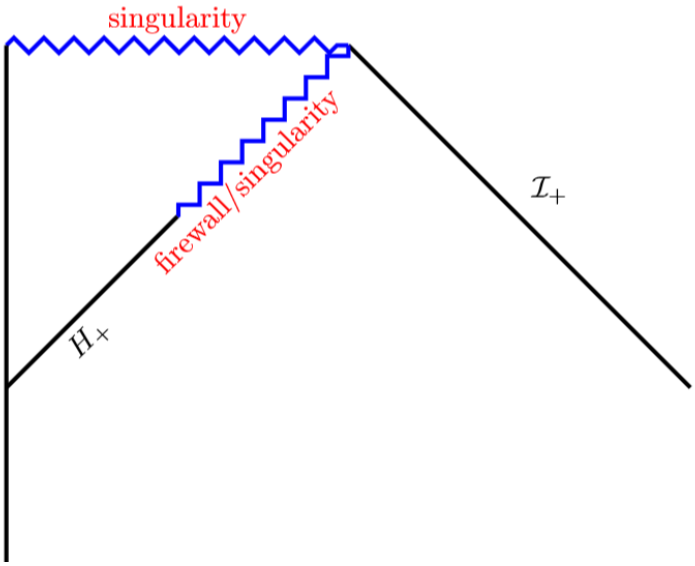

Figure 3.4: Firewall, if exist, would alter the horizon. So it becomes part of the singularity. An infalling observer sees this naked singularity as firewall [35].

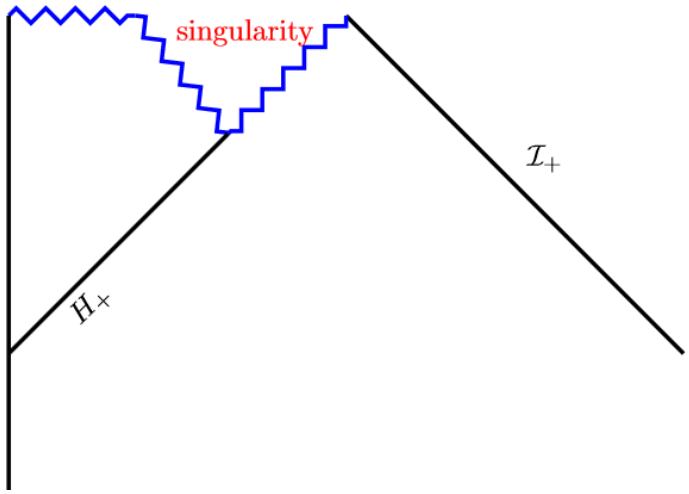

Figure 3.5: According to Czech et al [38, 39], the lack of entanglement means space behind the firewall does not exist. Firewall is the result of singularity shifts towards the horizon [35].

Chapter 4

Modeling the firewall in 1+1 dimensions

It was proposed in [10, 15, 16, 6, 41, 42, 43] (and reviewed in the last chapter) that the horizon of a radiating BH could be more singular than general relativity suggests, although the mechanism remains unknown. In this chapter, we discuss a model for this singularity. For simplicity, we start from quantum field theory in Minkowski spacetime, since back-reaction of the metric remains elusive except in a few situations such as the CGHS model [44].

There are two different approaches known to the author. One is to write down by hand a quantum state in which the correlations are absent [29, 40, 45]. Another is to allow an impermeable wall to develop where initially there was none [28, 17, 46, 47]. This thesis tries to address the latter scenario.

To include time dependence in the boundary condition, Brown and Louko used self-adjoint operator extension [48]. Specifically, they studied the smooth creation of a reflecting wall (Dirichlet) at the origin in a 1+1 dimensional massless scalar quantum field [17]. As expected, time evolution of the boundary conditions creates outgoing energy pulses. where the energy density is positively divergent. This divergence cannot be smoothed out by manipulating the boundary condition (see Appendix B.4). This somewhat counterintuitive fact may be evidence of a black hole firewall, if not for the finite Unruh-DeWitt detector response when passing through the energy burst.

In this chapter, we review Brown and Louko's work on time dependent boundary condition in a 1+1 dimensional massless scalar field [17].

We derive a boundary condition for time-evolving source creation. To be specific, we extend the definitions of the self-adjoint operator ∂_x^2. We derive a boundary condition that describes a smooth time evolution from Neumann to Dirichlet in a finite period of time. We solve the 1+1 dimensional scalar field Klein-Gordon equation under this boundary condition.

We expect the time-evolution of the scalar field to create some outgoing energy pulses along the null directions [47, 26, 25]. We search the existence and properties of the outgoing energy pulses, which model the behaviour of a 'firewall'. We emphasize that the 'firewall' is not the Dirchlet boundary condition at the origin, but the outgoing pulses of energy.

We discuss the infrared divergence of the energy density and discover that it is infrared cutoff dependent, where the cutoff is just a parameter. The total energy is divergent when there is a sudden switch of the boundary condition from Neumann to Dirichlet. Despite the divergence in the energy density, the response of a detector that passes through the pulse is finite, and therefore wall creation does not break quantum entanglement. In addition, the need to introduce artificially an infrared cutoff is an indication that the 1+1 dimensional theory misses important physics.

In Section 4.1, we introduce the rigorous procedure of self-adjoint operator extension. In Section 4.2, we solve for the mode functions of a massless Klein-Gordon equation and verify the orthonormality. In Section 4.3, we investigate the stress-energy tensor, where detailed calculations on the energy density are given in the first subsection and the rapid creation limit is given in the second subsection. Appendix B.4 shows that even for smooth wall creation, the energy density is positively divergent. In the last section 4.4, we discuss the detector response. When the boundary condition is suddenly switched from Neumann to Dirichlet, we find that the detector response remains finite despite the energy density diverges.

We state that an overline denotes complex conjugation. A continuous function of a real variable is said to be C^0. A function that is $n \in \mathbb{N} = \{1, 2, \ldots\}$ times continuously differentiable is said to be C^n. A function that has all derivatives is said to be C^∞ or smooth.

4.1 Operator extension in 1+1 dimensions

Naturally, the definition of an operator includes the set of functions the operator acts on. This set of functions is called the operator's domain. Two domains are different when the functions therein have different boundary conditions. For instance, operator $-i\partial_x$ defined on domain $\{f \in \mathcal{L}^2([0, L])\,; f(0) = f(L) = 0\}$ is different from operator $-i\partial_x$ defined domain $\{f \in \mathcal{L}^2([0, L])\,; f(0) = -f(L)\}$. A great many misunderstandings in quantum mechanics come from the negligence of a rigorous definition of quantum operators [48]. In this section, we derive a time-evolving boundary condition from self-adjoint operator extension.

For example [48], the Hamiltonian operator $H = -\frac{\hbar^2}{2m}\partial_x^2$ is defined as

$$H = -\frac{\hbar^2}{2m}\partial_x^2\,, \mathcal{D}(H) = \left\{\phi\,, H\phi \in \mathcal{L}^2(-\frac{a}{2}, \frac{a}{2})\,, \phi(\pm\frac{a}{2}) = 0\right\}, \tag{4.1.1}$$

where $\mathcal{D}(H)$ is the domain of H and $\phi(\pm\frac{a}{2}) = 0$ is the boundary condition.

Time dependency comes in from operator extension, which we outline as the following steps.

1. Identify self-adjoint condition. For example: we want ∂_x^2 to be self-adjoint on $[a, b]$

$$\int_a^b dx[\overline{\psi}\partial_x^2\psi - (\partial_x^2\overline{\psi})\psi] = [\overline{\psi}\partial_x\psi - (\partial_x\overline{\psi})\psi]\Big|_a^b = 0\,.$$

   As long as $[\overline{\psi}\partial_x\psi - (\partial_x\overline{\psi})\psi]\Big|_a^b = 0$ is satisfied, the operator is self-adjoint.

2. Rewrite the boundary condition. We rewrite the boundary condition as (with $\psi' := \partial_x\psi$)

$$|i\psi(a) + L\psi'(a)|^2 + |i\psi(b) - L\psi'(b)|^2 = |i\psi(a) - L\psi'(a)|^2 + |i\psi(b) + L\psi'(b)|^2\,,$$

$$\begin{pmatrix} L\phi'(b) - i\phi(b) \\ L\phi'(a) + i\phi(a) \end{pmatrix} = U(\alpha, \beta, \gamma) \begin{pmatrix} L\phi'(b) + i\phi(b) \\ L\phi'(a) - i\phi(a) \end{pmatrix}\,,$$

   where L is a positive constant of dimension length, U is a unitary matrix with parameters α, β, γ.

3. Choose the parametrization. For example: $U = \mathrm{diag}(1, 1)$ leads to periodic boundary condition $\psi(a) = \psi(b) = 0$.

We evolve the boundary condition at the origin from Neumann to Dirichlet. Neumann boundary condition states that spatial derivative of the field vanishes on either side of the origin, while Dirichlet boundary condition states that the field itself vanishes on either side of the origin. They are

$$\text{Neumann: } \partial_x\phi|_{x=0^-} = \partial_x\phi|_{x=0^+} = 0 \tag{4.1.2}$$

$$\text{Dirichlet: } \phi_{x=0^-} = \phi_{x=0^+} = 0\,. \tag{4.1.3}$$

We define self-adjoint operator $-\partial_x^2$ on $\mathcal{L}^2(\mathbb{R}\setminus\{0\})$ [48]. The definition gives

$$0 = \int_{-\infty}^{0^-} + \int_{0^+}^{+\infty} dx[\overline{\psi}\partial_x^2\phi - (\partial_x^2\overline{\psi})\phi]\,, \tag{4.1.4}$$

where $\psi\,, \phi$ are square integrable and defined on the real axis excluding the origin. We notice

that square integrability means $\psi_{x\sim\infty} = 0\,, \phi_{x\sim\infty} = 0$. Eq.(4.1.4) reduces to

$$[\overline{\phi_-}(\partial_x\phi_-) - (\partial_x\overline{\phi_-})\phi_-] = [\overline{\phi_+}(\partial_x\phi_+) - (\partial_x\overline{\phi_+})\phi_+]\,, \tag{4.1.5}$$

where we set $\psi = \phi, \phi_\pm = \phi(0_\pm)$ and discard extra terms using $\psi_{x\sim\infty} = 0\,, \phi_{x\sim\infty} = 0$.

Using notations $\phi' = \partial_x\phi\,, \phi_\pm = \phi(0_\pm)$, we rewrite eq.(4.1.5) as

$$\frac{1}{2iL}\Big[|L\phi'_- - i\phi_-|^2 - |L\phi'_- + i\phi_-|^2\Big] = \frac{1}{2iL}\Big[|L\phi'_+ - i\phi_+|^2 - |L\phi'_+ + i\phi_+|^2\Big]\,. \tag{4.1.6}$$

Eq(4.1.6) takes a simpler form when we rewrite it using a matrix notation as

$$\begin{pmatrix} L\phi'_+ - i\phi_+ \\ L\phi'_- + i\phi_- \end{pmatrix} = U \begin{pmatrix} L\phi'_+ + i\phi_+ \\ L\phi'_- - i\phi_- \end{pmatrix}\,, \tag{4.1.7}$$

where U is a 2 by 2 unitary matrix with parametrization $U(\theta)\,, \theta \in [0, \pi)$.

We notice that eq.(4.1.6) is automatically satisfied for odd solutions, so we focus on the even modes where $\phi_+ = \phi_-$ and $\phi'_+ = -\phi'_-$.

We parametrize U as

$$U = e^{-i\theta}\begin{pmatrix} \cos\theta & i\sin\theta \\ i\sin\theta & \cos\theta \end{pmatrix}\,. \tag{4.1.8}$$

We use this specific parametrization to derive the boundary condition for the even sector of the field

$$\frac{\phi'_+}{\phi_+} = \frac{\cot\theta(t)}{L}\,. \tag{4.1.9}$$

This is the simplest boundary condition for this model.

We notice that eq.(4.1.6) can also be solved by separating odd and even sectors. For odd sector of the field, eq.(4.1.6) is automatically satisfied. For even sector of the field, using $\phi_+ = \phi_-$ and $\phi'_+ = -\phi'_-$, we have

$$\begin{aligned} |L\phi'_- - i\phi_-|^2 &= |L\phi'_+ + i\phi_+|^2 \\ |L\phi'_- + i\phi_-|^2 &= |L\phi'_+ - i\phi_+|^2\,. \end{aligned} \tag{4.1.10}$$

Therefore, we rewrite eq.(4.1.6) as

$$\begin{aligned}
&|L\phi'_- - i\phi_-|^2 - |L\phi'_- + i\phi_-|^2 = |L\phi'_+ - i\phi_+|^2 - |L\phi'_+ + i\phi_+|^2 \\
\Rightarrow &|L\phi'_- - i\phi_-|^2 = |L\phi'_+ - i\phi_+|^2 \\
\Rightarrow &L\phi'_- - i\phi_- = -e^{2i\tilde{\theta}}[L\phi'_+ - i\phi_+] \\
\Rightarrow &i\phi_+[e^{2i\tilde{\theta}} + 1] = [e^{2i\tilde{\theta}} - 1]L\phi'_+ \\
\Rightarrow &\frac{\phi'_+}{\phi_+} = \frac{\cot\tilde{\theta}}{L}\,.
\end{aligned} \tag{4.1.11}$$

This is again eq.(4.1.9).

4.2 Wall creation in 1+1 dimensions

4.2.1 Field equation and boundary condition

We notice the odd solutions automatically satisfy eq.(4.1.7), so the boundary condition cannot change it. We discuss the even sector of the field, specifically solutions on the positive half space. We seek solutions of the Klein-Gordon (KG) equation with the boundary condition eq.(4.1.9).

The field equation and boundary conditions are

$$[\partial_t^2 - \partial_x^2]\phi = 0 \qquad \frac{\phi'(0_+)}{\phi(0_+)} = \frac{\cot\theta(t)}{L}\,, \tag{4.2.1}$$

with

$$\theta(t) = \begin{cases} \pi/2 & t \le 0 \\ \text{smooth in between} & \\ 0 & t \ge 1/\lambda\,. \end{cases} \tag{4.2.2}$$

Some authors [17] use the notation $\Delta_{\theta(t)}$ for Laplace operator with a boundary condition and parametrization $\theta(t)$, i. e.

$$[\partial_t^2 - \Delta_{\theta(t)}]\phi = 0\,. \tag{4.2.3}$$

The unique self-adjoint extension $\theta(t) = \pi/2$ corresponds to no wall, while $\theta(t) = 0$ corresponds to Dirichlet boundary condition on each side of the origin (impenetrable wall). We choose $\theta \in (0, \pi/2)$ [17] to keep the field amplitude finite, otherwise tachyon-like instabilities

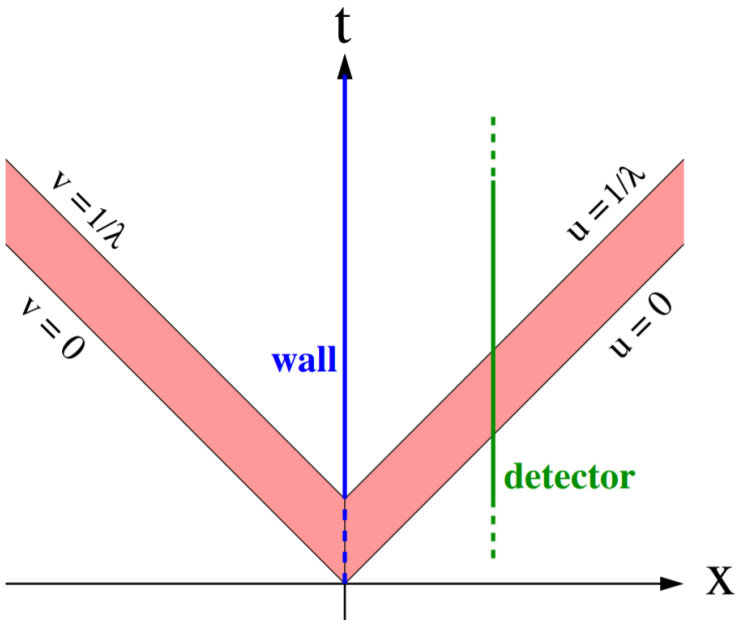

Figure 4.1: Diagram of wall creation in 1+1 dimensional scalar quantum field theory [17]. The time-dependent boundary condition at the origin generates two energy pulses going symmetrically to the right and left. The total energy, however, is infrared divergent. When the wall is suddenly turned on, the total energy is divergent even with an infrared cut-off.

would appear, see Appendix E.2. We introduce λ to control how fast the boundary condition evolves, where bigger λ means faster evolution.

We introduce light-cone coordinates

$$u := t - x \tag{4.2.4a}$$
$$v := t + x \,. \tag{4.2.4b}$$

The general solution of KG equation is

$$\phi_k = F_k(v) + E_k(u) \,, \tag{4.2.5}$$

where $F_k(v)\,, E_k(u)$ are the left and right movers. We only discuss solutions on the positive axis, solutions on the negative axis can be recovered by taking mirror image across the t axis. See Figure 4.1.

On the positive axis, the left-mover comes from positive infinity so it should be a plane wave. The right-mover has 'felt' the boundary condition at the origin so it cannot be plane

wave. We use the trial solution

$$\phi_k(u,v) = \frac{1}{\sqrt{8\pi k}}[e^{-ikv} + E_k(u)]\,, \tag{4.2.6}$$

where $k > 0$ and $E_k(u)$ is to be found [17].

We need to satisfy the boundary condition in eq.(4.1.9)

$$L\sin\theta(t)\frac{d}{dt}[e^{-ikt} - E_k(t)] = \cos\theta(t)[e^{-ikt} + E_k(t)]\,, \tag{4.2.7}$$

where we have used $\frac{\partial}{\partial x}E_k(u) = -\frac{\partial}{\partial t}E_k(u)$. I want to point out that the constant L has been introduced for dimensional convenience and its value is considered fixed [17].

This equation can be rewritten by introducing a dimensionless function $B(y)$, with dimensionless $y = \lambda t$, which is defined as the solution to the differential equation

$$\frac{\cot(\theta(t))}{L} = \lambda\cot(h(\lambda t)) = \frac{\partial_t B(\lambda t)}{B(\lambda t)}\,, \tag{4.2.8}$$

with the boundary condition B(0)=1. We want to emphasize that function $B(y)$ and its argument y are both dimensionless. We choose $y = \lambda t$ in the expression above because λt is dimensionless. All terms in eq.(4.2.8) have the same dimension of inverse length.

$h(y)$ is assumed to be a **smooth C^∞ function** over its entire domain $-\infty < y < \infty$ (including $y = 0$ and $y = 1$) and monotonous (see Appendix B.5) over $0 < y < 1$, with the properties

$$h(y) = \pi/2 \qquad \text{for } y \le 0 \tag{4.2.9a}$$
$$0 < h(y) < \pi/2 \qquad \text{for } 0 < y < 1 \tag{4.2.9b}$$
$$h(y) = 0 \qquad \text{for } y \ge 1\,. \tag{4.2.9c}$$

In particular, since all derivatives of $h(y)$ vanish for $y < 0$ and $y > 1$, for them to be continuous at $y = 0$ and $y = 1$, we need all derivatives of $h(y)$ to vanish for $y = 0_+$ and for $y = 1_-$. In Appendix B.2.1, it is shown that $1/B(y)$ and all of its derivatives approach zero as $y \to 1_-$.

4.2.2 Mode functions

We have the solution

$$E_k(u) = R_{k/\lambda}(\lambda u) \tag{4.2.10}$$

$$R_K(y) = \begin{cases} e^{-iKy} & y \leq 0 \\ e^{-iKy} - \frac{2}{B(y)} \int_0^y dz B'(z) e^{-iKz} & 0 < y < 1 \\ -e^{-iKy} & y \geq 1\,. \end{cases} \tag{4.2.11}$$

It is straightforward to show by substitution that these expressions for $R_K(y)$, when inserted in eq.(4.2.10) to give $E_k(y)$, solve eq.(4.2.7).

An alternative expression for $R_K(y)$ is derived by integration by parts

$$R_K(y) = -e^{-iKy} + \frac{2}{B(y)} - \frac{2iK}{B(y)} \int_0^y dz B(z) e^{-iKz}\,, \tag{4.2.12}$$

where $0 < y < 1$.

For $u \leq 0$ and $u \geq 1/\lambda$, using equations (4.2.10) and (4.2.11) in (4.2.6) we obtain

$$\phi_k = \begin{cases} \frac{e^{-ikt}\cos(kx)}{\sqrt{4\pi k}} & \text{for } u \leq 0 \\ -\frac{ie^{-ikt}\sin(kx)}{\sqrt{4\pi k}} & \text{for } u \geq 1/\lambda\,. \end{cases} \tag{4.2.13}$$

These solutions are interpreted as follows. When $u \leq 0$, the mode is Minkowski because it is in the region before the boundary condition starts evolving. When $u \geq 1/\lambda$, the mode vanishes at the spatial origin because the effect of a Dirichlet boundary condition has been imposed. The full solution is reached by simple reflecting through a mirror at the origin.

In Appendix B.1 and B.2.2, we verify that the mode function is both orthonormalized and smooth. We have the orthonormality condition

$$(\phi_k, \phi_{k'}) = \delta(k - k') \tag{4.2.14}$$

$$(\overline{\phi_k}, \overline{\phi_{k'}}) = -\delta(k - k') \tag{4.2.15}$$

$$(\phi_k, \overline{\phi_{k'}}) = 0\,, \tag{4.2.16}$$

where overline represents complex conjugation and $(\cdot\,,\cdot)$ represents the Klein-Gordon inner product.

4.3 Energy density

4.3.1 Derivation

We first need to quantize the field. Following the standard procedure of canonical quantization, we write the field as

$$\phi = \int_0^{+\infty} dk \Big(a_k \phi_k + a_k^\dagger \overline{\phi_k} \Big) \,, \tag{4.3.1}$$

where the non-vanishing commutator of the annihilation and creation operators is $[a_k, a_{k'}^\dagger] = \delta(k - k')$. The integral limits are 0 and $+\infty$ because we have separated the right-movers from the left-movers. We only look at the even section of the field, because the odd section is Minkowski.

We introduce the Minkowski vacuum state notation $|0_M\rangle$, which satisfies the relation $a_k|0_M\rangle = 0$ for $t < |x|$ due to the spacetime being Minkowski. The vacuum state $|0\rangle$ is generally different from the Minkowski vacuum.

The classical stress-energy tensor of a scalar field is

$$T^{\mu\nu} = \partial^\mu \phi \partial^\nu \phi - \frac{1}{2} g^{\mu\nu} (\partial^\alpha \phi)(\partial_\alpha \phi) \,. \tag{4.3.2}$$

Using lightcone coordinate u, v, the spacetime interval is $ds^2 = dudv$ and the metric is

$$g_{\mu\nu} = \begin{pmatrix} 0 & 1/2 \\ 1/2 & 0 \end{pmatrix} .$$

In this coordinate system, we have $\partial^u \phi = 2\partial_v \phi \,, \partial^v \phi = 2\partial_u \phi$ and $(\partial^\alpha \phi)(\partial_\alpha \phi) = 4(\partial_u \phi)(\partial_v \phi)$. We rewrite eq.(4.3.2) as

$$T_{uu} = \partial_u \phi \partial_u \phi \,, \tag{4.3.3}$$

$$T_{vv} = \partial_v \phi \partial_v \phi \,, \tag{4.3.4}$$

$$T_{uv} = 0 \,. \tag{4.3.5}$$

We need to renormalize $T_{\mu\nu}$ to get the physical expression. This requires us to subtract the expectation value of $T_{\mu\nu}$ in Minkowski spacetime from that in curved spacetime, because we are only interested in the difference. This is merely a subtraction in Minkowski spacetime, but remains unclear [22, 23, 49] in curved spacetime.

I. First we calculate the expectation value of T_{uu} and T_{vv} in state $|0\rangle$:

$$\begin{aligned}\langle 0|T_{uu}|0\rangle &= \langle 0|\partial_u\phi\partial_u\phi|0\rangle = \int_0^\infty dk\frac{1}{8\pi k}|E_k'(u)|^2\\ \langle 0|T_{vv}|0\rangle &= \int_0^\infty dk\frac{1}{8\pi k}k^2\,.\end{aligned} \tag{4.3.6}$$

II. Then we set $E_k(u) = e^{-iku}$ to derive the corresponding Minkowski expressions

$$\begin{aligned}\langle 0_M|T_{uu}|0_M\rangle &= \int_0^\infty dk\frac{1}{8\pi k}|E_k'(u)|^2 = \int_0^\infty dk\frac{1}{8\pi k}k^2\\ \langle 0_M|T_{vv}|0_M\rangle &= \int_0^\infty dk\frac{1}{8\pi k}k^2\,.\end{aligned} \tag{4.3.7}$$

III. Lastly, we renormalize by subtracting the Minkowski expressions

$$\begin{aligned}\langle T_{uu}\rangle &= \int_\mu^\infty dk\frac{1}{8\pi k}(|E_k'(u)|^2 - k^2)\\ \langle T_{vv}\rangle &= \langle T_{uv}\rangle = 0\,.\end{aligned} \tag{4.3.8}$$

We note that μ is infrared cutoff[1] inserted by hand. The necessity of an infrared cutoff is explained as follows. Mode function eq.(4.2.6) has asymptotic expansions $|E_k'(u)|^2 = k^2 + O(k^{-2})$ and $|E_k'(u)|^2 = 4\lambda^2[B'(\lambda u)]^2[B^4(\lambda u)]^{-4} + O(k^2)$, so the integral $\int dk\frac{1}{8\pi k}(|E_k'(u)|^2 - k^2)$ is convergent for $k\to\infty$ but divergent for $k\to 0$. Therefore we introduce a cutoff at the lower integral limit to make the integral finite.

The divergence as $k\to 0$ is a feature of 1+1 dimensions. We show in later chapters that infrared cutoff is not needed in 3+1 dimensions.

We calculate the quantized expression of stress-energy tensor the following way

$$\langle T_{uu}\rangle = \lim_{u_1,u_2\to u}\partial_{u_1}\partial_{u_2}\Big[\langle 0|\phi(v_1,u_1)\phi(v_2,u_2)|0\rangle - \langle 0_M|\phi(v_1,u_1)\phi(v_2,u_2)|0_M\rangle\Big]\,, \tag{4.3.9}$$

$$\langle T_{vv}\rangle = \lim_{v_1,v_2\to v}\partial_{v_1}\partial_{v_2}\Big[\langle 0|\phi(v_1,u_1)\phi(v_2,u_2)|0\rangle - \langle 0_M|\phi(v_1,u_1)\phi(v_2,u_2)|0_M\rangle\Big]\,, \tag{4.3.10}$$

$$\langle T_{uv}\rangle = 0\,, \tag{4.3.11}$$

where $\langle\cdots\rangle$ on the left hand side means renormalization by subtracting the corresponding Minkowski value. The technique $\lim_{u_1,u_2\to u}\partial_{u_1}\partial_{u_2}$ in eq.(4.3.9) is called point splitting. It is useful because all we need to calculate is the Wightman function $\langle 0|\phi(v_1,u_1)\phi(v_2,u_2)|0\rangle$.

[1] the letter μ is also sometimes used for a 4-index

Figure 4.1 describes eq.(4.3.8), where the pink pulses are the only region with non-vanishing energy density. The total energy is

$$\begin{aligned} \Delta E_{total} &= \int_{\Sigma} dx \langle T_{tt} \rangle \\ &= 2 \int_0^{1/\lambda} du \langle T_{uu} \rangle \,, \end{aligned} \tag{4.3.12}$$

where Σ is a constant time hypersurface in the region $t > 1/\lambda$. From the first to the second line, the non-vanishing contribution is from $t - 1/\lambda < x < t$ and its mirror image in the negative half space. We also change integration variable from x to u, as a result of time being constant $dx = -du$. The integrand change is from $T_{tt} = T_{uu} + T_{vv}$ where $\langle T_{vv} \rangle$ is zero.

The total energy is

$$\begin{aligned} \Delta E_{total} &= 2 \int_0^{1/\lambda} du \int_{\mu}^{\infty} \frac{dk}{8\pi k} \Big(|E_k'(u)|^2 - k^2 \Big) \\ &= \frac{\lambda}{4\pi} \int_0^1 dy \int_{\mu/\lambda}^{\infty} \frac{dK}{K} \Big(|R_K'(y)|^2 - K^2 \Big) \,, \end{aligned} \tag{4.3.13}$$

where we use new variable $y = \lambda u$.

We discuss the divergence of the stress-energy tensor in the Appendix B.4, where we show that the energy density is unbounded along the null line $t \pm x = 1/\lambda$ even when the boundary condition evolves smoothly.

4.3.2 Rapid wall creation limit

We have large λ for rapid wall creation, so the lower integral limit μ/λ is very small. We separate the K-integral into two parts: $\int_{\mu/\lambda}^1 dK$ and $\int_1^{\infty} dK$.

For the first K-integral $\int_{\mu/\lambda}^1 dK$, we use small K expansion (Appendix B.3)

$$|R_K'(y)|^2 = 4|B'(y)|^2 [B(y)]^{-4} + O(K^2) \,, \tag{4.3.14}$$

which is from expanding eq.(4.2.12) in powers of K. Because the integral of eq.(4.3.8) does not converge when $k \to 0$, a positive infrared cutoff is required to make $\langle T_{ab} \rangle$ finite.

For the second K-integral $\int_1^{\infty} dK$, we use the large K expansion (Appendix B.3)

$$|R_K'(y)|^2 = K^2 + O(K^{-2}) \,, \tag{4.3.15}$$

which is obtained from repeated integration by parts of eq.(4.2.11).

The total energy is

$$\begin{aligned}\Delta E_{total} &= \frac{\lambda}{4\pi}\int_0^1 dy \int_{\mu/\lambda}^1 \frac{dK}{K}\left(|R'_K(y)|^2 - K^2\right) + \frac{\lambda}{4\pi}\int_0^1 dy \int_1^\infty \frac{dK}{K}\left(|R'_K(y)|^2 - K^2\right) \\ &= \frac{\lambda}{\pi}\int_0^1 dy \int_{\mu/\lambda}^1 \frac{dK}{K}|B'(y)|^2[B(y)]^{-4} + \frac{\lambda}{4\pi}\int_0^1 dy \int_{\mu/\lambda}^1 \frac{dK}{K}O(K^2) \\ &\quad + \frac{\lambda}{4\pi}\int_0^1 dy \int_1^\infty \frac{dK}{K}O(K^{-2})\,.\end{aligned} \tag{4.3.16}$$

In Appendix B.4, we show the integral $\int_1^\infty \frac{dK}{K}O(K^{-2})$ is positive divergent just before the light cone where the wall creation ends. An integral on hypersurface $t = T > 0$ in an arbitrary small neighborhood of $x = \pm T$ gives positive infinite energy.

4.4 Response of an Unruh-DeWitt detector

Unfortunately, the response function of a non-derivative coupling detector is ambiguous. We can see this ambiguity by considering [29]

$$\mathcal{F}^{(0)}(\omega) = \int_{-\infty}^{\infty} d\tau_2 \int_{-\infty}^{\infty} d\tau_1 e^{-i\omega(\tau_2-\tau_1)}\chi(\tau_1)\chi(\tau_2)\mathcal{W}(\tau_1,\tau_2)\,, \tag{4.4.1}$$

where $\chi(\tau_{1,2})$ is called the switching function and describes how the detector is turned on and off. $\mathcal{W}(\tau_1,\tau_2)$ is the so-called Wightman function.

Using Minkowski mode, the Wightman function is

$$\mathcal{W}(\tau_1,\tau_2) = -(4\pi)^{-1}\ln[i\mu(\Delta u - i0_+)] - (4\pi)^{-1}\ln[i\mu(\Delta v - i0_+)]\,, \tag{4.4.2}$$

with $\Delta u = u(\tau_1) - u(\tau_2)$, $\Delta v = v(\tau_1) - v(\tau_2)$. Here μ is the infrared cutoff and the logarithm is taken in its principal branch. The Wightman function generates an ambiguous term proportional to $\ln[i\mu]$ when we substitute it into eq.(4.4.1).

Because of the infrared ambiguity, Brown and Louko chose the first order derivative coupling detector [17]. The response function is defined as

$$\mathcal{F}^{(1)}(\omega) = \int_{-\infty}^{\infty} d\tau_2 \int_{-\infty}^{\infty} d\tau_1 e^{-i\omega(\tau_2-\tau_1)}\chi(\tau_1)\chi(\tau_2)\ \partial_{\tau_1}\partial_{\tau_2}\mathcal{W}(\tau_1,\tau_2)\,, \tag{4.4.3}$$

where $x(\tau_{1,2})$ parametrizes the detector's world line. The authors selected a detector trajec-

tory

$$(t, x) = (\tau + d, d)\,, \tag{4.4.4}$$

with $d > 0$ being a constant. The detector stays at fixed space location and waits for the energy burst to pass through. See Figure 4.1.

In Minkowski vacuum, the detector response is [29]

$$\mathcal{F}^{(1)}_{Mink}(\omega) = -\omega\Theta(-\omega)\int_{-\infty}^{\infty} du[\chi(u)]^2 + \frac{1}{\pi}\int_0^{\infty} ds\frac{\cos(\omega s)}{s^2}\int_{-\infty}^{\infty} du\chi(u)[\chi(u) - \chi(u-s)]\,, \tag{4.4.5}$$

and is independent of infrared cutoff μ. Θ is the Heaviside step function.

After a Dirichlet boundary condition establishes at the origin $x = 0$, the response function is [17]

$$\mathcal{F}^{(1)}_{Dir} = \mathcal{F}^{(1)}_{Mink} + \Delta\mathcal{F}^{(1)}\,, \tag{4.4.6}$$

with

$$\Delta\mathcal{F}^{(1)} = \frac{1}{2\pi}\mathrm{Re}\left[e^{-2i\omega d}\left(i\pi G_\omega(2d) + \int_0^{\infty} ds\frac{e^{-i\omega s}G_\omega(2d+s) - e^{i\omega s}G_\omega(2d-s)}{s}\right)\right] \tag{4.4.7}$$

and

$$G_\omega(y) = \int_{-\infty}^{\infty} du[\chi'(u) - i\omega\chi(u)]\chi(u-y)\,. \tag{4.4.8}$$

This is also independent of infrared cutoff.

We notice that the detector response obviously does not depend on parameter λ, because the second line of mode function eq.(4.2.13) does not depend on λ. Therefore, it is finite even in the fast wall creation limit with $\lambda \to \infty$.

4.5 Summary and discussion

In this chapter, we set up and solved a Klein-Gordon equation with time dependent boundary condition. We chose the boundary condition through self-adjoint operator extension, which describes the transition from Neumann to Dirichlet boundary condition at the space origin.

Under technical assumption $g'''(y) < 0$ for $0 < y < 1$, we verified that an infinite energy density occurs in the model. See eq.(B.4.21). According to Appendix B.4, this energy density [17] diverges where the boundary condition approaches its final value, just before the light cone of event $(x = 0, t = 1/\lambda)$. Even when the boundary condition evolves smoothly, there are still two points $(x = \pm|T - 1/\lambda|)$ on any constant time (with $t = T > 1/\lambda$) hypersurface with divergent energy density.

Although the divergence in energy density seems to suggest that a firewall that breaks entanglement could exist, the detector response does not support this: there is no way the detector response can diverge.

In addition to the finite detector response, the appearance of an infrared cutoff in the stress-energy tensor and Wightman function also indicates that this model is not physical.

We want to investigate higher dimensional models because of the infrared cutoff and finite detector response. We ask if a cutoff in the Wightman function is essential. If not, would the detector response diverge at some point? We suspect metric back-reaction could keep the total energy finite, but we have to work with fixed metric models for now because they are analytically solvable. In the next two chapters, we generalize the firewall model to two 3+1 dimensional models with fixed Minkowski metric: one for a source creation at the space origin, one for shell creation at a fixed radius.

To sum up, this 1+1 dimensional model does not have a firewall-like structure. For general relativity to undergo drastic amendment in 1+1 dimensions to produce a firewall structure, a more exotic model may be needed.

Chapter 5

Modeling firewalls with a pointlike source in 3+1 dimensions

The results from last chapter give us plenty of motivation to generalize the model to higher dimensions. We want to specify some terms and symbols. We use the same parameters λ and μ as in the last chapter, where λ measures how fast the boundary condition evolves with $\lambda \to \infty$ meaning the boundary condition switches suddenly, and the symbol μ for infrared cutoff or a 4-index depending on the context. The infrared cutoff is often shortened to 'cutoff' and we use the term 'infrared ambiguity' to indicate the existence of such cutoff. Since the boundary condition is defined at one point, we use the term 'pointlike source' which is usually shortened to 'source'.

A major motivation is the unexpected behavior that in the 1+1 dimensional case the detector registers finite readings [17] even at rapid creation limit $\lambda \to \infty$. This finite detector response could be the result of derivative coupling detector, where the λ- dependence is lost once we take the derivative of Wightman function. We wonder what would happen if using a non-derivative coupling operator.

Another reason for the generalization to 3+1 dimensional spacetime is that we might not need an infrared cutoff μ. This comes from the observation that the first line of the 1+1 dimensional mode function eq.(4.2.13) is divergent as $k \to 0$. Could mode functions in higher dimensions be finite when $k \to 0$? We investigate whether the cutoff μ is a feature of 1+1 dimensions or it persists in higher dimensions.

In this chapter, we generalize the scalar field model with time dependent boundary condition to 3+1 dimensions. We consider a massless scalar field in 3+1 dimensional Minkowski spacetime, where the field is square integrable. We introduce a Laplace operator defined in all space except at the origin. By allowing this Laplace operator to be Hermitian at any instant of time, we derive a time dependent boundary condition at the space origin $r = 0$. This boundary condition is then imposed upon the numerator f of a field $\phi = f/r$, describing

the time evolution of a f evolving from zero amplitude (Dirichlet type) to zero derivative of the f (Neumann type). Because the boundary condition is given at one spatial point, the physical interpretation is the smooth creation of a pointlike source rather than a wall. We want to see what happens at the rapid source creation limit, where the boundary condition is switched instantly from Dirichlet type to Neumann type. Specifically, we investigate the energy density and the Unruh-DeWitt detector response.

The results about energy density $\langle T_{00}\rangle$ are summarized in this paragraph. Similar to the 1+1 dimensional case, the energy density is not bounded even when the wall is smoothly developed, see Appendix C.2. In the outgoing pulse generated by the evolving source, $\langle T_{00}\rangle$ is negatively divergent to the immediate future of the light cone of the point where the boundary condition starts to change, with the total energy in the pulse being negative infinity. After the pulse has gone, $\langle T_{00}\rangle$ is nonzero and it diverges at $r \to 0$ proportionally to $-(\ln r)/r^4$. This shows a cloud of positive energy lingering near the source after it is fully formed, with the total energy of this cloud being positive infinity. The cloud of energy lingering near the source is new compared to the the 1+1 dimensional case, as it is related to vacuum polarization which has no counter part in 1+1 dimensions. Further, at a fixed r, $\langle T_{00}\rangle$ is not static and it diverges at $t \to \infty$ proportionally to $\ln t$. In the limit of rapid source creation, $\langle T_{00}\rangle$ diverges everywhere in the timelike future of the creation event. The source creation hence leaves in the late time region a large energetic memory, which has no counterpart in the 1+1 dimensional analysis of [17]. The persistence of large late time effects is perhaps particularly reminiscent of the energetic curtain scenario proposed in [16].

The response of an Unruh-DeWitt detector is described as follows. In Section 5.4 and [17], the Unruh-DeWitt detector is set static and waiting for an outgoing pulse of energy (i.e. firewall). The Wightman function is well-defined everywhere except at the origin and no infrared cutoff is needed. The energy density and detector response are also well defined with no cutoff. We use a non-derivative coupling detector because no cutoff appears in the Wightman function. The response of a detector is divergent when the source creation is instantaneous, consequently it may be able to break entanglement in a quantum state in the way that has been proposed in references [10, 15, 16, 6, 41, 42, 43]. We find that the response of a detector that operates only in the late time region mimics $\langle T_{00}\rangle$ closely, both in the late time limit and in the limit of rapid source creation, where the response has a logarithmic divergence. We have not addressed the response of a detector that goes through the pulse, but the behavior in the post-pulse region is sufficient to establish that the response does not remain finite in the limit of rapid source creation.

In Section 5.1, we extend the operator in the spherical sector of a general n-dimensional Laplace operator. In Section 5.2.1, we set up a classical scalar field equation under a time-dependent boundary condition at the spatial origin, then we solve it in Section 5.2.2. Section 5.3 introduces the quantized field and evaluates the energy density $\langle T_{00}\rangle$. Section 5.4 discusses the response of an Unruh-DeWitt detector. Section 5.5 gives a brief summary and

discussion.

5.1 Operator extension: punctured Laplace operator

In this section we record relevant properties of the scalar Laplacian on punctured Euclidean space $\mathbb{R}^3$. We use spherical coordinates in which r is the radial coordinate and the puncture is at $r = 0$. The scalar Laplacian reads

$$\nabla^2 = \frac{1}{r^2}\partial_r\big(r^2\partial_r\big) + \frac{1}{r^2}\nabla^2_{S^2}\,, \tag{5.1.1}$$

where $\nabla^2_{S^2}$ is the Laplacian on unit sphere S^2. The L_2 inner product can be scaled using $g = f/r$

$$(g_1, g_2) = \int_0^\infty dr \int_{S^2} d\varphi d\theta \overline{f_1} f_2 \xrightarrow{\text{spherical symmetry}} 4\pi \int_0^\infty dr \overline{f_1} f_2\,. \tag{5.1.2}$$

Laplace operator ∇^2 can be scaled to

$$\nabla^2_{sc} = \partial_r^2 + \frac{1}{r^2}\nabla^2_{S^2} \xrightarrow{\text{spherical symmetry}} \partial_r^2\,. \tag{5.1.3}$$

After decomposing into spherical harmonics and choosing the spherical symmetric sector, the inner product $(\,\cdot\,,\,\cdot\,)_{sc}$ reduces to the standard $\mathcal{L}^2$ inner product on the positive half-line. The Laplace operator reduces to standard one dimensional Laplace operator on a half-line.

A rigorous treatment of a general n- dimensional Laplacian and inner product on punctured Euclidean space $\mathbb{R}^n$ can be found in reference [18, 48, 50]. The self-adjoint extension is unique except for the spherically symmetric sector for $n = 2$ and $n = 3$, see references [51, 52]. In each of these two cases there is a $U(1)$ family of self-adjoint extensions, characterized by a boundary condition at the origin [18, 50].

In the $n = 3$ spherically symmetric sector, the boundary condition is derived in a similar fashion to that of the 1+1 dimensions

$$\cos\theta \lim_{r\to 0} f(r) = L \sin\theta \lim_{r\to 0} f'(r)\,, \tag{5.1.4}$$

where L is a positive constant of dimension length, and $\theta \in [0, \pi)$ is the parameter that specifies the extension. At time $t = 0$, we choose the wave function $g = f/r$ to be well-defined in the entire space, so that $f(t, r)|_{r=0} = 0$. At time $t = 1/\lambda$, we choose $\partial_r f(t, r)|_{r=0} = 0$. As a result, the wave function $g = f/r$ at the spatial origin is well-defined in the beginning but ill-defined after time $t = 1/\lambda$. Therefore, the boundary condition on $f(t, r)$ evolves from

Dirichlet to Neumann, which is a time reverse of the boundary condition evolution in 1+1 dimensions.

For $\theta \in [0, \pi/2]$ the spectrum consists of the negative continuum. For $\theta \in (\pi/2, \pi)$ there is one proper eigenvalue, which is positive and nondegenerate. The case $\theta = 0$ reduces to the essentially self-adjoint operator ∇^2 on $\mathcal{L}^2(\mathbb{R}^3)$.

5.2 Pointlike source creation in $3+1$ dimensions

5.2.1 Field equation and boundary conditions

We consider a real massless scalar field ϕ in 3+1 dimensional Minkowski spacetime from which the spatial origin has been distinguished. The field equation is

$$(\partial_t^2 - \nabla^2)\phi = 0\,, \tag{5.2.1}$$

where ∇^2 is Laplace operator in spherical coordinates.

To specify the dynamics, we need to define ∇^2 at each t as a self-adjoint operator. After decomposition into spherical harmonics, the only freedom is in the spherically symmetric sector. Writing

$$\phi(t, r) = \frac{f(t, r)}{\sqrt{4\pi}\, r}\,, \tag{5.2.2}$$

the eigenfunctions of ∇^2 must satisfy the boundary condition

$$\frac{\cot\theta(t)}{L} = \lim_{r\to 0} \frac{\partial_r f(t, r)}{f(t, r)}\,, \tag{5.2.3}$$

where L is a positive constant of dimension length introduced for dimensional convenience. The prescribed function $\theta(t)$, taking values in $[0, \pi)$, specifies at each t the self-adjoint extension of ∇^2. We denote this extension by $\Delta_{\theta(t)}$. Δ_0 coincides with the unique self-adjoint extension of ∇^2 on $L_2(\mathbb{R}^3)$, yielding usual scalar field dynamics on full Minkowski space.

For $\theta \in (\pi/2, \pi)$, Δ_θ has a positive proper eigenvalue, which gives a tachyonic instability [17]. This instability appears when we set $h(y) \in (\pi/2, \pi)$, where $h(y)$ will be given in eq.(5.2.13), which naturally leads to $B(1) = 0$ because we choose $B(0) = 1$. Therefore, the mode function $R_K(y)$ in eq.(5.2.15) diverges as $y \to 1$. This means the wave functions diverges and the we cannot interpret it as the probability amplitude. We therefore always assume $\theta \in [0, \pi/2]$, in which case the spectrum of Δ_θ consists of the negative continuum.

We choose a $\theta(t)$ that interpolates between $\theta = 0$ and $\theta = \pi/2$ over a finite interval of

time. The parametrization of $\theta(t)$ is similar to that of the last chapter, but time reversed

$$\frac{\cot\theta(t)}{L} = \begin{cases} \infty & \text{for } t \le 0 \ , \\ \lambda \cot\big(h(\lambda t)\big) & \text{for } 0 < t < \lambda^{-1} \ , \\ 0 & \text{for } t \ge \lambda^{-1} \ . \end{cases} \tag{5.2.4}$$

λ is a positive constant of dimension inverse length and $h : \mathbb{R} \to \mathbb{R}$ is a smooth function such that

$$h(y) = 0 \qquad \text{for } y \le 0 \ , \tag{5.2.5a}$$
$$0 < h(y) < \pi/2 \quad \text{for } 0 < y < 1 \ , \tag{5.2.5b}$$
$$h(y) = \pi/2 \qquad \text{for } y \ge 1 \ . \tag{5.2.5c}$$

We point out that unlike the 1+1 dimensional and 3+1 shell case, $h(y)$ does not need to be monotonous.This is because we only require $g'''(y) \ge 0$ for sufficiently small positive y in Appendix C.2.2. We note that $h(y)$ of eq.(4.2.9) and eq.(5.2.5) are "reverse" to each other in the sense that $h(0)$ in eq.(4.2.9) has the same value as $h(1)$ in eq.(5.2.5) and vice versa.

Over the interval $0 < t < \lambda^{-1}$, the boundary condition eq.(5.2.3) reads

$$\lim_{r\to 0} \frac{\partial_r f(t,r)}{f(t,r)} = \lambda \cot\big(h(\lambda t)\big) \ . \tag{5.2.6}$$

The boundary condition interpolation takes place over time λ^{-1} while the interpolation profile is determined by the dimensionless function $h(y)$. The limit of rapid interpolation with fixed profile is that of $\lambda \to \infty$.

5.2.2 Mode functions

We write down the mode functions that reduce to the usual Minkowski modes when $t \le 0$. We consider only the spherically symmetric sector.

We work in the radial null coordinates $u := t - r$ and $v := t + r$, in which $t = (v+u)/2$ and $r = (v-u)/2$. Taking ϕ to be spherically symmetric, the field equation (5.2.1) becomes

$$\partial_u \partial_v (r\phi) = 0 \, . \tag{5.2.7}$$

We seek mode functions with the Ansatz

$$\phi_k = \frac{f_k}{\sqrt{4\pi}\, r} \, , \tag{5.2.8}$$

where

$$f_k(u,v) = \frac{1}{\sqrt{4\pi k}} \left[e^{-ikv} + E_k(u)\right] \,, \tag{5.2.9}$$

$k > 0$, and E_k is to be found.

Since any choice for $E_k(u)$ satisfies the wave equation, we determine $E_k(u)$ so that the boundary condition (5.2.3) is satisfied for all t and the usual Minkowski modes are obtained for $t \leq 0$. Substituting eq.(5.2.9) into eq.(5.2.3), we get an ordinary differential equation

$$L \sin\big(\theta(t)\big) \frac{d}{dt} \left[e^{-ikt} - E_k(t)\right] = \cos\big(\theta(t)\big) \left[e^{-ikt} + E_k(t)\right] \,. \tag{5.2.10}$$

We use eq.(5.2.4) and re-parametrize $E_k(u)$ with the dimensionless frequency $K = k/\lambda > 0$ and dimensionless null coordinate $y = \lambda u$

$$E_k(u) = R_K(y) := R_{k/\lambda}(\lambda u) \,. \tag{5.2.11}$$

Equation (5.2.10) is rearranged to

$$\sin\big(h(y)\big) \frac{d}{dy} \left[e^{-iKy} - R_K(y)\right] = \cos\big(h(y)\big) \left[e^{-iKy} + R_K(y)\right] \,. \tag{5.2.12}$$

To solve eq.(5.2.12), we introduce the auxiliary function $B(y)$

$$\frac{B'(y)}{B(y)} := \cot\big(h(y)\big) \,,\; B(0) = 1 \,, \tag{5.2.13}$$

so that $B(y)$ is a function changing smoothly from $B(y) = 1$ for $y \leq 0$ to $B(y) = 0$ for $y \geq 1$. The intermediate part of this function is

$$B(y) = \exp\left(-\int_y^1 \cot\big(h(z)\big)\, dz\right) , \quad \text{for } 0 < y < 1 \,. \tag{5.2.14}$$

It is shown in Appendix C.1 that $B(y)$ is smooth everywhere, including $y = 0$ and $y = 1$.

It follows that the solution to eq.(5.2.12) is

$$R_K(y) = \begin{cases} -e^{-iKy} & \text{for } y \leq 0 \,, \\ e^{-iKy} - \dfrac{2}{B(y)} \displaystyle\int_0^y B'(z)\, e^{-iKz}\, dz & \text{for } 0 < y < 1 \,, \\ e^{-iKy} - 2C_K & \text{for } y \geq 1 \,, \end{cases} \tag{5.2.15}$$

where

$$C_K = \int_0^1 B'(z)\, e^{-iKz}\, dz\,. \tag{5.2.16}$$

It is verified by repeated integration by parts [53], that C_K is smooth in K, $C_0 = 1$, $C_K \to 0$ faster than any inverse power of K as $K \to \infty$.

An alternative expression for $R_K(y)$ which will be useful later can be obtained by integrating by parts

$$R_K(y) = \begin{cases} -e^{-iKy} & \text{for } y \le 0\ , \\ -e^{-iKy} - \dfrac{2iK}{B(y)} \displaystyle\int_0^y B(z)\, e^{-iKz}\, dz & \text{for } 0 < y < \infty\ . \end{cases} \tag{5.2.17}$$

From eq.(5.2.17) and the smoothness of B, we see that $R_K(y)$ is smooth everywhere except possibly at $y = 0$. We verify in Appendix C.1 that $R_K(y)$ is C^{25} (has continuous derivative till the 25th order) at $y = 0$. It follows that the mode functions are smooth everywhere except possibly at $r = t$, and they are at least C^{25} at $r = t$.

When $u \le 0$ and $u \ge \lambda^{-1}$, the mode functions ϕ_k in eq.(5.2.8) reduce to

$$\phi_k(t,r) = \begin{cases} -\dfrac{ie^{-ikt}\sin(kr)}{2\pi\sqrt{k}\, r} & \text{for } u \le 0\ , \\ \dfrac{e^{-ikt}\cos(kr) - C_{k/\lambda}}{2\pi\sqrt{k}\, r} & \text{for } u \ge \lambda^{-1}\ . \end{cases} \tag{5.2.18}$$

$\phi_k(t,r)$ coincide with the usual Minkowski space mode functions for $u \le 0$. Evaluating the Klein-Gordon inner product on a hypersurface of constant negative t shows that the normalization is $(\phi_k, \phi_{k'})_{KG} = \delta(k - k')$. Comparing eq.(5.2.18) with eq.(4.2.13), we notice that it is well-defined for both $K \to 0$ and $K \to \infty$. It is reasonable to anticipate that the Wightman function is not infrared singular, such as in eq.(4.3.8). Indeed, we show in later sections that no infrared cutoff is needed.

For $u \ge \lambda^{-1}$, the r-dependence in the numerator of $\phi_k(t,r)$ contains the term $\cos(kr)$, which one would expect from the boundary condition eq.(5.2.3) with $\theta = \pi/2$, but it contains also the additive memory term $-C_{k/\lambda}$, which carries a recollection of how the boundary condition evolved from $\theta = 0$ to $\theta = \pi/2$. For fixed λ, the memory term is hence insignificant at large frequencies but significant at low frequencies. We will show in Section 5.3 that the memory term has significant effects on the stress-energy tensor and the Wightman function.

A spacetime diagram is shown in Figure 5.1, with three regions $u < 0$, $0 < u < \lambda^{-1}$ and $u > \lambda^{-1}$.

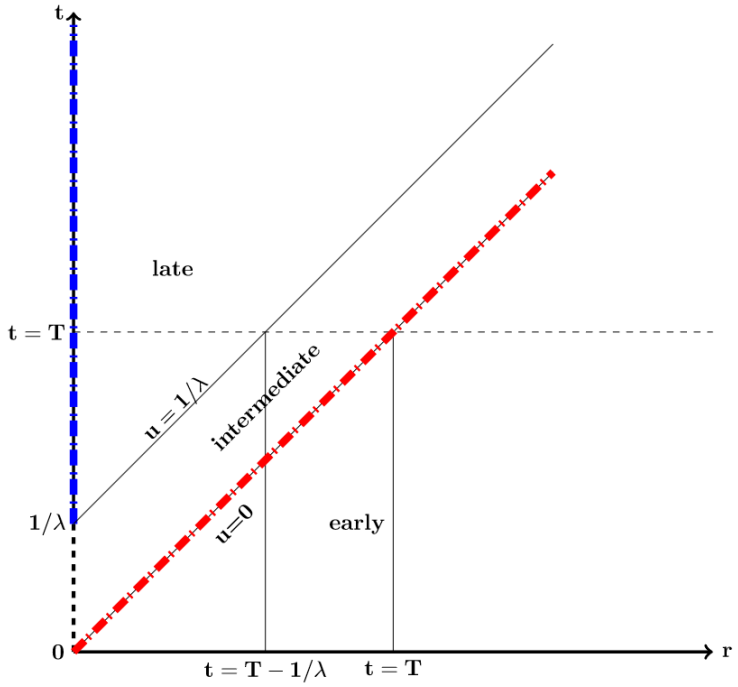

Figure 5.1: Spacetime diagram of the time-dependent boundary condition eq.(5.2.3) at $r = 0$, with the angular dimensions suppressed. The interpolation between $\theta = 0$ and $\theta = \pi/2$ at $r = 0$ occurs over $0 < t < \lambda^{-1}$. The early region $u < 0$ is outside the light cone of $(t, r) = (0, 0)$, where the mode functions coincide with those of the Minkowski space. The mode functions in the late region $u > \lambda^{-1}$ carry a memory of the field evolution. The infinities in the energy density at $r = 0$ (positive infinity) and $r = t$ (negative infinity) are along the blue and red dashed lines. The spacelike hypersurface $t = T > \lambda^{-1}$ (horizontal dashed line) intersects all three regions.

5.3 Energy density

5.3.1 Expression for the energy density

We quantize the field with the spherically symmetric mode functions in Section 5.2.2 and treat the nonzero angular momentum sectors as in ordinary Minkowski space. We are interested in the effects due to the evolving boundary condition, and we only give the expressions in the spherically symmetric sector.

We expand the spherically symmetric sector of the quantized field as

$$\phi = \int_0^\infty \left(a_k \phi_k + a_k^\dagger \overline{\phi}_k\right) dk \,, \tag{5.3.1}$$

where the annihilation and creation operators have the commutators $\left[a_k, a_{k'}^\dagger\right] = \delta(k-k')$. The normalization of the mode functions gives the field and its time derivative the correct equal-time commutator. We denote by $|0\rangle$ the state that is annihilated by all a_k and by all the annihilation operators of the nonzero angular momentum sectors. In the region $u < 0$, $|0\rangle$ coincides with the usual Minkowski vacuum, which we denote by $|0_M\rangle$.

In the Lorentz frame of the Minkowski metric, the energy density of the classical scalar field is given in terms of the energy-momentum tensor by

$$T_{00} = T_{uu} + T_{vv} + 2T_{uv} \,, \tag{5.3.2}$$

where [23]

$$T_{uu} = (\partial_u \phi)^2 \,, \tag{5.3.3a}$$
$$T_{vv} = (\partial_v \phi)^2 \,, \tag{5.3.3b}$$
$$T_{uv} = T_{vu} = \frac{1}{4r^2}\left[(\partial_\theta \phi)^2 + (\sin\theta)^{-2}(\partial_\varphi \phi)^2\right] \,. \tag{5.3.3c}$$

To obtain the renormalized energy density of the field $\langle T_{00}\rangle := \langle 0|T_{00}|0\rangle_{\rm ren}$, we point-split the expressions in eq.(5.3.3), take the expectation value in $|0\rangle$ then subtract the corresponding expectation value in $|0_M\rangle$, and finally take the coincidence limit. Since $|0\rangle$ and $|0_M\rangle$ differ only in the spherically symmetric sector, we have $\langle T_{uv}\rangle = 0$ and

$$\langle T_{00}\rangle = \lim_{\substack{u_1,u_2\to u \\ v_1,v_2\to v}} (\partial_{u_1}\partial_{u_2} + \partial_{v_1}\partial_{v_2})\Big[\langle 0|\phi(v_1,u_1)\phi(v_2,u_2)|0\rangle - \langle 0_M|\phi(v_1,u_1)\phi(v_2,u_2)|0_M\rangle\Big] \,, \tag{5.3.4}$$

where ϕ denotes the spherically symmetric quantum field eq.(5.3.1).

To evaluate eq.(5.3.4), we write ϕ in terms of f as in eq.(5.2.2). Recalling that $r = (v-u)/2$, we have

$$\langle T_{00}\rangle = \frac{1}{4\pi}\left[\frac{\langle(\partial_u f)^2\rangle}{r^2} + \frac{\langle(\partial_v f)^2\rangle}{r^2} + \frac{\langle f(\partial_u f - \partial_v f)\rangle + \langle(\partial_u f - \partial_v f)f\rangle}{2r^3} + \frac{\langle f^2\rangle}{2r^4}\right] . \tag{5.3.5}$$

From eq.(5.2.2), eq.(5.2.8) and eq.(5.3.1), f has the expansion

$$f = \int_0^\infty \big(a_k f_k + a_k^\dagger \overline{f_k}\big)\, dk\,. \tag{5.3.6}$$

From eq.(5.2.9), eq.(5.2.11) and eq.(5.3.6), we obtain for $\langle T_{00}\rangle$ the final expression

$$\langle T_{00}\rangle = \frac{\lambda^2}{16\pi^2 r^2}\int_0^\infty \frac{dK}{K}\Big[\big|R_K'\big(\lambda(t-r)\big)\big|^2 - K^2\Big] - \frac{1}{32\pi^2 r^2}\,\frac{\partial}{\partial r}\left(\frac{\mathcal{G}_\lambda(t,r)}{r}\right), \tag{5.3.7}$$

where the prime on R_K denotes the derivative with respect to the argument. The first term in eq.(5.3.7) comes from the first term of eq.(5.3.5), the second term in eq.(5.3.7) comes from the last two terms of eq.(5.3.5), and the second term of eq.(5.3.5) vanishes.

The explicit expression of $\mathcal{G}_\lambda(t,r)$ is

$$\begin{aligned}\mathcal{G}_\lambda(t,r) = \int_0^\infty \frac{dK}{K}\Big[&\big|R_K\big(\lambda(t-r)\big)\big|^2 + 2\cos(2K\lambda r) - 1 \\ &+ R_K\big(\lambda(t-r)\big)e^{iK\lambda(t+r)} + \overline{R_K\big(\lambda(t-r)\big)}e^{-iK\lambda(t+r)}\Big],\end{aligned} \tag{5.3.8}$$

and we note that $\mathcal{G}_\lambda$ is related to the renormalized vacuum polarization $\langle\phi^2\rangle$ by

$$\langle\phi^2\rangle = \frac{\mathcal{G}_\lambda(t,r)}{16\pi^2 r^2}\,. \tag{5.3.9}$$

5.3.2 Energy density in the early, late and intermediate regions

We consider $\langle T_{00}\rangle$ separately in the early region, $t < r$, in the late region, $t > r + \lambda^{-1}$, and in the intermediate region, $r \le t \le r + \lambda^{-1}$.

In the early region, $t < r$, $|0\rangle$ coincides with $|0_M\rangle$ and $\langle T_{00}\rangle$ vanishes. This is seen immediately from eq.(5.3.4), and also by substituting eq.(5.2.17) into eq.(5.3.7) and eq.(5.3.8).

In the late region, $t > r + \lambda^{-1}$, the first term in eq.(5.3.7) vanishes. It suffices to consider $\mathcal{G}_\lambda$ eq.(5.3.8), which (by the last line of eq.(5.2.15)) reduces to

$$\mathcal{G}_\lambda(t,r) = 4\int_0^\infty \frac{dK}{K}\Big[|C_K|^2 + \cos(2K\lambda r) - \big(C_K e^{iK\lambda t} + \overline{C}_K e^{-iK\lambda t}\big)\cos(K\lambda r)\Big], \tag{5.3.10}$$

where the integral is convergent (at large K in the sense of an improper Riemann integral) by the properties of C_K in Section 5.2.2: C_K is smooth in K, $C_0 = 1$, and $C_K \to 0$ faster than any inverse power of K as $K \to \infty$. We notice that every term of the integrand is divergent when $K \to 0$, so some carefully rearrangements are needed to identify finite combinations.

We rearrange the integrand of eq.(5.3.10)

$$\begin{aligned}\mathcal{G}_\lambda(t,r) = 4\int_0^\infty \frac{dK}{K}\Big[(1-C_K)\,e^{iK\lambda t} + (1-\overline{C}_K)\,e^{-iK\lambda t}\Big]\cos(K\lambda r)\\ + 2\int_0^\infty \frac{dK}{K}\Big[|C_K|^2 - \cos\big(K\lambda(t+r)\big)\Big]\\ + 2\int_0^\infty \frac{dK}{K}\Big[|C_K|^2 - \cos\big(K\lambda(t-r)\big)\Big]\\ + 2\int_0^\infty \frac{dK}{K}\Big[\cos\big(2K\lambda r\big) - \cos\big(K\lambda(t+r)\big)\Big]\\ + 2\int_0^\infty \frac{dK}{K}\Big[\cos\big(2K\lambda r\big) - \cos\big(K\lambda(t-r)\big)\Big]\,. \qquad (5.3.11)\end{aligned}$$

The integrals are evaluated using Appendix C.3

$$\begin{aligned}\mathcal{G}_\lambda(t,r) = 2H\big(\lambda(t+r)\big) + 2H\big(\lambda(t-r)\big) + 2H\big(\lambda(t+r)\big) + 2H\big(\lambda(t-r)\big)\\ + 4\ln\left(\frac{\lambda(t^2-r^2)}{r}\right) - 4\ln 2 + 4k_1\,, \qquad (5.3.12)\end{aligned}$$

where the function H is defined in Proposition C.3.3 and the constant k_1 is given by eq.(C.3.2). By Proposition C.3.2, when $t \to \infty$ or $r \to 0$, the logarithmic term in eq.(5.3.12) is dominant. Therefore, we can derive the following asymptotic expressions,

$$\langle T_{00}\rangle \sim \frac{\ln(\lambda t)}{4\pi^2 r^4} \quad \text{as } t\to\infty \text{ with } r \text{ fixed}, \qquad (5.3.13a)$$

$$\langle T_{00}\rangle \sim -\frac{\ln(\lambda r)}{8\pi^2 r^4} \quad \text{as } r\to 0 \text{ with } t \text{ fixed}. \qquad (5.3.13b)$$

On the hypersurface of $t = T =$ constant with $T > \lambda^{-1}$ (see Figure 5.1), every ball with radius less than $T - \lambda^{-1}$ contains positive infinite amount of energy, due to the divergence of $\langle T_{00}\rangle$ when $r \to 0$.

In the intermediate region, $r \le t \le r + \lambda^{-1}$, we show in Appendix C.2 that $\langle T_{00}\rangle$ is a pointwise well defined function, and it is continuous in r for $t > r$. Under the technical assumption that the third derivative of $\tan\big(h(y)\big)$ is non-negative for sufficiently small positive y, we show that $\langle T_{00}\rangle$ is also well defined at $t = r$ (where it vanishes). However, due to contributions from the first term in eq.(5.3.7), $\langle T_{00}\rangle$ tends to negative infinity as $r \to t_-$, faster than any negative multiple of $1/h\big(\lambda(t-r)\big)$. In particular, $\langle T_{00}\rangle$ is not continuous at $r = t$. We get negative infinity when we integrate $\langle T_{00}\rangle$ in a small neighborhood of $r = T$ on

a hypersurface of $t = T =$ constant > 0. The time-dependent boundary condition generates a negative infinite pulse of energy, immediately to the future of the light cone of the point $(t, r) = (0, 0)$ where the boundary condition starts to change.

Considering that $h(y)$ of eq.(4.2.9) and eq.(5.2.5) are "reverse" to each other in the sense explained beneath eq.(5.2.5), it is not surprising that there are the following two differences. First, the signs of the energy density/pulse of the 3+1 dimensional source creation and the 1+1 dimensional wall creation are opposite. Second, the divergence in energy density of the 1+1 dimensional wall creation is at the immediate past of the light cone of where the boundary condition finishes changing, but the divergence in the energy density of the 3+1 source creation is at the immediate future of the light cone of where the boundary condition starts changing.

Combining the results of the two previous paragraphs, the total energy on the hypersurface of $t = T =$ constant with $T > \lambda^{-1}$ is not defined, although $\langle T_{00} \rangle$ is defined every point. Given an $r_0 \in (0, T)$, the total energy for $r \leq r_0$ is positive infinite, due to a large positive contribution from $r \to 0$. While the total energy for $r \geq r_0$ is negative infinite, due to a large negative contribution from $r \to T_-$.

5.3.3 Rapid boundary condition change

Finally, consider the limit in which the boundary condition changes rapidly, $\lambda \to \infty$. At each given point in the region $t > r$, the first term of eq.(5.3.7) vanishes while the second term contributes to a divergence. The only divergence comes from $\mathcal{G}_\lambda(t, r)|_{\lambda \to \infty} \sim 4 \ln \lambda$ by Proposition C.3.2, with the asymptotic form

$$\langle T_{00} \rangle \sim \frac{\ln \lambda}{8\pi^2 r^4} \,. \tag{5.3.14}$$

In the limit of rapid source creation, $\langle T_{00} \rangle$ hence diverges everywhere inside the light cone of the creation event. This is drastically different from the 1+1 dimensional wall creation, where $\langle T_{00} \rangle$ vanishes inside the light cone of the creation event [17].

5.4 Response of an Unruh-DeWitt detector

In this section, we study the response of an inertial Unruh-DeWitt (UDW) detector [20, 54] at fixed locations.

We investigate all the Wightman functions to make sure no cutoff is needed. By the definition of eq.(2.2.6), the arguments $x = (t, r), x' = (t', r')$ of the following expression

$$\langle 0 | \phi(t, r) \phi(t', r') | 0 \rangle$$

can be in any of the three regions of Figure 5.1. We end up with nine combinations in total, the Wightman function is cutoff independent if and only if all nine Wightman functions are cutoff independent.

We consider an example where $x = (t, r)$ is in '**late**' region in Figure 5.1 and $x' = (t', r')$ is in '**early**' region ins Figure 5.1. We calculate

$$\begin{aligned} \langle 0|\phi(t,r)\phi(t',r')|0\rangle &= \int dk \overline{\phi_k(t,r)}\phi_k(t',r') \\ &= -\frac{1}{4\pi^2 r^2}\int_\mu^\infty \frac{dk}{k}\Big[e^{ikt}\cos(kr) - \overline{C_{k/\lambda}}\Big] i e^{-ikt}\sin(kr)\,, \end{aligned} \tag{5.4.1}$$

where eq.(5.3.1) is used. When $k \to 0$, the integrand of eq.(5.4.1) is well-defined, so we do not need an infrared cutoff. When $k \to \infty$, the integrand behaves like $e^{ik\times\mathbf{const}}/k$ with fast changing numerator and a large denominator, so we do not need an ultraviolet cutoff. For the same reason, all the other eight Wightman functions are also well-defined with no cutoff.

We consider a detector that is coupled linearly to the quantum field. Within 1st-order perturbation theory, the probability of the detector to undergo a transition from a state with energy 0 to a state with energy ω is proportional to the response function, given by [20, 23, 49, 54]

$$\mathcal{F}(\omega) = \int_{-\infty}^{\infty} dt_1 \int_{-\infty}^{\infty} dt_2\, e^{-i\omega(t_1-t_2)}\,\chi(t_1)\chi(t_2)\,\mathcal{W}(t_1,t_2)\,, \tag{5.4.2}$$

where the smooth real-valued switching function χ specifies how the detector's interaction with the field is turned on and off, and $\mathcal{W}$ is field's Wightman function on the detector's worldline.

Denoting by $\mathcal{F}_{|0_M\rangle}$ the response function in the state $|0_M\rangle$ and by $\mathcal{F}_{|0\rangle}$ the response function in the state $|0\rangle$, we have

$$\Delta\mathcal{F}(\omega) = \int_{-\infty}^{\infty} dt_1 \int_{-\infty}^{\infty} dt_2\, e^{-i\omega(t_1-t_2)}\,\chi(t_1)\chi(t_2)\,\Delta\mathcal{W}(t_1,t_2)\,, \tag{5.4.3}$$

where

$$\begin{aligned} \Delta\mathcal{W}(t_1,t_2) = \frac{1}{4\pi r^2}\int_0^\infty \Big(& f_k(t_1-r,t_1+r)\overline{f_k(t_2-r,t_2+r)} \\ & - f_k^M(t_1-r,t_1+r)\overline{f_k^M(t_2-r,t_2+r)}\Big)\,dk\,, \end{aligned} \tag{5.4.4}$$

r is the location of the detector, f^M is as in eq.(5.2.9) but with $E_k(u) = -e^{-iku}$ for all u. Note that $\Delta\mathcal{W}(t_1,t_2)$ vanishes when $t_1, t_2 \le r$.

We consider a detector that operates only in the future region, $t > r + \lambda^{-1}$. For $t_1, t_2 > r + \lambda^{-1}$, the integrand in eq.(5.4.4) can be rearranged and split to give

$$\begin{aligned}
4\pi^2 r^2 \Delta\mathcal{W}(t_1,t_2) = &\int_0^\infty \frac{dK}{K}\Big[(1-C_K)\,e^{iK\lambda t_2} + (1-\overline{C}_K)\,e^{-iK\lambda t_1}\Big]\cos(K\lambda r)\\
&+\int_0^\infty \frac{dK}{K}\Big[|C_K|^2 - \cos(K\lambda r)\Big]\\
&+\int_0^\infty \frac{dK}{K}\Big[\big(1-e^{iK\lambda t_2}\big) + \big(1-e^{-iK\lambda t_1}\big)\Big]\cos(K\lambda r)\\
&+\int_0^\infty \frac{dK}{K}\big(e^{-iK\lambda(t_1-t_2)}-1\big)\cos(2K\lambda r)\\
&+\int_0^\infty \frac{dK}{K}\big[\cos(2K\lambda r) - \cos(K\lambda r)\big]\,. \qquad (5.4.5)
\end{aligned}$$

The integrals can be evaluated by the formulas of Appendix C.3, with the result

$$\begin{aligned}
8\pi^2 r^2 \Delta\mathcal{W}(t_1,t_2) = &\,H\big(\lambda(t_2+r)\big) + H\big(\lambda(t_2-r)\big) + H\big(\lambda(t_1+r)\big) + H\big(\lambda(t_1-r)\big)\\
&+\ln\left(\frac{\lambda^2\big(t_1^2-r^2\big)\big(t_2^2-r^2\big)}{\big|4r^2-(t_1-t_2)^2\big|}\right)\\
&+i\pi\big[\Theta(t_2-t_1-2r)-\Theta(t_1-t_2-2r)\big] + 2k_1\,, \qquad (5.4.6)
\end{aligned}$$

where the function H is defined in Proposition C.3.2 and the constant k_1 is given by (C.3.2). Note that $\mathcal{W}(t_1,t_2)$ has singularities at $|t_1-t_2| = 2r$, which is when the two points are separated by a null geodesic that bounces off the origin, but this singularity is only logarithmic. Note also that the first four terms in (5.4.6) are real because $t_1, t_2 > r + \lambda^{-1}$ by assumption and $H(\alpha)$ is real for $\alpha \geq 1$ by (C.3.4).

We consider two limits.

First, suppose that the support of χ is contained in some finite interval of fixed length, centered at $t = t_c$, and consider the limit $t_c \to \infty$. By the large argument expansion of H in (C.3.5), the contribution from the H-terms in (5.4.6) vanishes in this limit, and we have

$$\Delta\mathcal{F}(\omega) \sim \frac{(\ln t_c)\big|\widehat{\chi}(\omega)\big|^2}{2\pi^2 r^2}\,, \qquad (5.4.7)$$

where the hat denotes the Fourier transform $\widehat{\chi}(\omega) := \int_{-\infty}^{\infty} e^{-i\omega t}\,\chi(t)\,dt$. $\Delta\mathcal{F}$ hence diverges in this limit and is proportional to $\ln t_c$. This is similar to the late time divergence of $\langle T_{00}\rangle$ (5.3.13a).

Second, consider the limit of large λ. We assume that the support of χ is in $[r+a, \infty)$, where a is a positive constant, and we take λ large enough that $\lambda^{-1} < a$. By similar arguments, we find

$$\Delta\mathcal{F}(\omega) = \frac{(\ln\lambda)\left|\widehat{\chi}(\omega)\right|^2}{4\pi^2 r^2} \; + \; O(1)\,. \tag{5.4.8}$$

The $\ln\lambda$ divergence in (5.4.8) at $\lambda \to \infty$ resembles the $\ln\lambda$ divergence of $\langle T_{00}\rangle$ in (5.3.14).

5.5 Summary and discussion

As was intended, we found that point source creation is significantly more singular than the corresponding wall creation in 1+1 dimensional Minkowski spacetime [17]. While $\langle T_{00}\rangle$ is well defined away from the source, it is unbounded from above and below: there is a pulse of infinite negative energy traveling outwards, and there is a cloud of infinite positive energy lingering around the source. We emphasized that the infinite negative energy radiating from the evolving source is localized to the immediate future of the light cone (of the point where the boundary condition starts to change), and this negative energy cannot become finite by slowing down the boundary condition change. In the rapid source creation limit, $\langle T_{00}\rangle$ diverges everywhere in the timelike future of the creation event, and so does the response of an Unruh-DeWitt detector that operates in the same spacetime region.

Three technical reasons have led to the difference between the 3+1 dimensional source creation and the 1+1 dimensional wall creation. First, the boundary condition resembles the removal of a 1+1 dimensional wall rather than its creation [47]. We can see this by comparing the time dependence of function $h(y)$ of eq.(4.2.9) with that of eq.(5.2.5). Second, the boundary condition of this chapter is at a single spatial point, it does not divide the space into two regions. Third, the 3+1 dimensional $\langle T_{00}\rangle$ in eq.(5.3.7) contains terms that have no counterpart in $1+1$ dimensions, i.e. $\mathcal{G}_\lambda(t,r)$ term, and these additional terms are especially significant near the source.

The existence and the sign of the infinity in the energy density come from the first technical reason of last paragraph. Since the 3+1 dimensional point source creation resembles the removal of a 1+1 dimensional wall, we understand the boundary condition in this chapter as a "reverse" of the boundary condition in the last chapter. A "reverse" produces a negative sign on the energy density: positively divergent in the energy pulse (in the last chapter) comparing to negatively divergent in the outgoing energy pulse (in this chapter). The same "reverse" also switches the divergence from the immediate past (of the light cone of $t = 1/\lambda\,, r = 0$) to the immediate future (of the light cone of $t = 0\,, r = 0$).

Our results, including the divergent negative energy near $r = t$, suggest that the creation of a pointlike source may be sufficiently singular to model the breaking of correlations that has

been proposed to happen at the horizon of an evaporating BH [10, 15, 16, 6, 41, 42, 43]. It is possible that the divergence near $r = t$ cancels the divergence near $r = 0$ and produces finite total energy, but such a cancellation requires a nonlocal correlation between the regulator near $r = t$ and the regulator near $r = 0$.

Finally, the techniques in this chapter can be adapted to an evolving boundary condition on a spherical shell. In particular, will the time-dependent boundary condition at the shell lead to divergent detector response? This is the subject of the next chapter.

To sum up, the calculations show that a firewall-like singular structure could exist in 3+1 dimensions, which could modify general relativity if we can generalize it to curved spacetime. However, to verify that this is indeed so, we still need to consider a second possibility in 3+1 dimensions where the model is set up slightly different.

Chapter 6

Modeling firewalls with spherical shell creation in 3+1 dimensions

We confirm from the last chapter that point source creation in 3+1 dimensions models firewall in Minkowski space very well. We desire the following features: divergent outgoing energy pulse in radial null direction, divergent Unruh-DeWitt detector response when the boundary condition is suddenly switched on.

These favorable results toward firewall [15] rely on the memory term C_K of eq.(5.2.15), which has no correspondence in $1+1$ dimensions. The memory term C_K is important at small K despite being insignificant at large K. Besides having no cutoff, the energy density is also unbounded even when the boundary condition evolves smoothly.

In this chapter, we look further into source creation in $3+1$ dimensions and study the effect of a time evolving boundary condition at finite radius $r = a$. We grant the name "shell creation" to this model. To be specific, we follow the standard procedures: (1) set up Klein-Gordon equation with a time dependent boundary condition at finite radius $r = a$; (2) solve for the mode functions then quantize the field and investigate the divergence structure of its energy density and detector response. Since there may be infinite total energy in the point source model, it would be an improvement if the shell creation gives finite total energy while keeping other desirable features of the point source model.

We start by solving for the mode functions of Klein-Gordon equation with a boundary condition at finite radius $r = a$, then we quantize to derive the energy density. There is an expression inside the shell ($0 < r < a$) and a different expression outside ($r > a$) the shell. We propose Ansatz eq.(6.2.8) whose expression for $r < a$ is valid till time $t = a$, which is the time when the reflection occurs at the origin. The expression for $r > a$ should always be valid since there is no probability flow across the shell (at $r = a$) once it is formed. The detector response is discussed at the end.

We show that the mode functions in eq.(6.2.13) do not contain C_K-like term as in eq.(5.2.16). Consequently, the detector response is finite and does not depend on the parameter λ, which describes how fast the boundary condition evolves. The energy density in the outgoing/ingoing pulse is unbounded, just like the other two models. Beside the divergence in the energy pulses, vacuum polarization terms eq.(6.3.4) and eq.(6.3.6) also produce divergences unique to the models. The divergence in the outgoing/ingoing energy pulse is common across all three models and it is related to the properties of function $h(y)$ in eq.(6.2.5).

A key feature of the shell creation is the existence of an inner region $r < a$, where the energy density is also divergent in the ingoing pulse. The energy pulses for the shell creation resemble that of the 1+1 dimensions, because the energy density in the ingoing/left-moving and outgoing/right-moving pulses have the same positive sign. On the constant time $t = T$ (with $1/\lambda < T < a$) hypersurface, integrating the energy density in a volume containing the outgoing energy pulse (from radius $r = R_1 > a$ to space infinity), we get positive infinite energy. Similarly, integrating in a volume containing the ingoing energy pulse (from the space origin to radius $r = R_2 < a$), we also get positive infinite energy. Integrating the energy density in a small region around $r = a$ on the constant time $t = T > 1/\lambda$ hypersurface, we get finite energy because the divergence at $r = a_+$ and $r = a_-$ cancel out.

6.1 Operator extension: Laplacian with a shell

The spherical symmetric Laplacian in 3 dimensions is

$$\nabla^2 = \frac{1}{r^2}\partial_r(r^2\partial_r) + \frac{1}{r^2}\nabla^2_{\mathcal{S}^2}\,. \tag{6.1.1}$$

The $\mathcal{L}^2$ inner product is

$$(\phi_1, \phi_2) = \int_{\mathcal{S}^2} d\theta d\varphi \fint dr r^2 \overline{\phi_1}\phi_2\,, \tag{6.1.2}$$

with the shorthand notation $\fint_0^\infty dr = \int_0^{a^-} + \int_{a^+}^\infty$.

Decomposing the mode function with spherical harmonics and taking the spherical symmetric sector $\phi(t, r) := f(t, r)/\sqrt{4\pi}r$, the self-adjointness condition is

$$(f_1, \nabla^2 f_2) - (\nabla^2 f_1, f_2) = \fint_0^\infty dr \partial_r[\overline{f_1}(\partial_r f_2) - (\partial_r \overline{f_1})f_2] = 0\,. \tag{6.1.3}$$

By setting $f_1 = f_2$, equation (6.1.3) reduces to

$$\begin{aligned}&\frac{1}{2iL}\left[|Lf'_- - if_-|^2 - |Lf'_- + if_-|^2\right] - \frac{1}{2iL}\left[|Lf'_0 - if_0|^2 - |Lf'_+ if_0|^2\right]\\ =&\frac{1}{2iL}\left[|Lf'_+ - if_+|^2 - |Lf'_+ + if_+|^2\right],\end{aligned} \tag{6.1.4}$$

with $f' = \partial_r f$ and $f_\pm = f(t, a_\pm)\,, f_0 = f(t, 0_+)$. Similar to eq.(4.1.6), we write the equations in matrix form:

$$\begin{pmatrix} Lf'_+ - if_+ \\ Lf'_- + if_- \\ Lf'_0 - if_0 \end{pmatrix} = U \begin{pmatrix} Lf'_+ + if_+ \\ Lf'_- - if_- \\ Lf'_0 + if_0 \end{pmatrix}, \tag{6.1.5}$$

where different choices of the matrix U lead to different boundary conditions. This matrix can be decomposed using Gell-man matrices with eight independent parameters. We choose a matrix that is most similar to the corresponding matrix in 1+1 dimensions

$$U = \begin{pmatrix} e^{-i\theta(t)} \begin{pmatrix} \cos\theta(t) & i\sin\theta(t) \\ i\sin\theta(t) & \cos\theta(t) \end{pmatrix} & \\ & 1 \end{pmatrix}, \tag{6.1.6}$$

which leads to

$$f_0 = 0 \tag{6.1.7a}$$

$$f_- = f_+ \tag{6.1.7b}$$

$$\frac{f'_+}{f_+} - \frac{f'_-}{f_-} = \frac{2\cot\theta(t)}{L}\,. \tag{6.1.7c}$$

We note that the continuity requirement in eq.(6.1.7b) comes from the special choice of matrix U in eq.(6.1.6). This indicates that continuity is not necessary for the Laplace operator to be Hermitian. The continuity requirement further selects the right boundary condition from the Hermitian set.

6.2 Shell creation in 3+1 dimensions

6.2.1 Field equation and boundary conditions

We consider a real massless Klein-Gordon field ϕ in 3+1 dimensional Minkowski space

$$[\partial_t^2 - \nabla^2]\phi = 0\,. \tag{6.2.1}$$

After decomposing the field into spherical harmonics and assuming spherical symmetry, the field equation is reduced to

$$[\partial_t^2 - \partial_r^2]f = 0\,, \tag{6.2.2}$$

where we have used eq.(6.1.1) and $f(t,r) = \sqrt{4\pi}r\phi(t,r)$.

The boundary conditions for shell formation in the time bracket $t \in (0, 1/\lambda)$ are

$$\begin{aligned} &f(t,0) = 0 \\ &f(t,a_-) = f(t,a_+) \\ &\frac{f'(t,a_+)}{f(t,a_+)} - \frac{f'(t,a_-)}{f(t,a_-)} = \frac{2\cot\theta(t)}{L}\,, \end{aligned} \tag{6.2.3}$$

with

$$\theta(t) = \begin{cases} \pi/2 & t \le 0 \\ \text{smooth inbetween} & \\ 0 & t \ge 1/\lambda\,. \end{cases} \tag{6.2.4}$$

We call the boundary condition in the beginning 'Neumann type', where the derivatives of the wave functions coincide but are not necessarily zero. And we call the boundary condition in the end 'Dirichlet type'.

We parametrize $\theta(t) = \cot^{-1}[L\lambda\cot(h(\lambda t))]$ with dimensionless function $h(y)$

$$h(y) = \pi/2 \qquad \text{for } y \le 0 \tag{6.2.5a}$$
$$0 < h(y) < \pi/2 \qquad \text{for } 0 < y < 1 \tag{6.2.5b}$$
$$h(y) = 0 \qquad \text{for } y \ge 1\,, \tag{6.2.5c}$$

as in eq.(4.2.9). Therefore, $h(y)$ is smooth over its entire domain, including $y = 0$ and $y = 1$. $h(y)$ is also monotonous according to Appendix B.5.

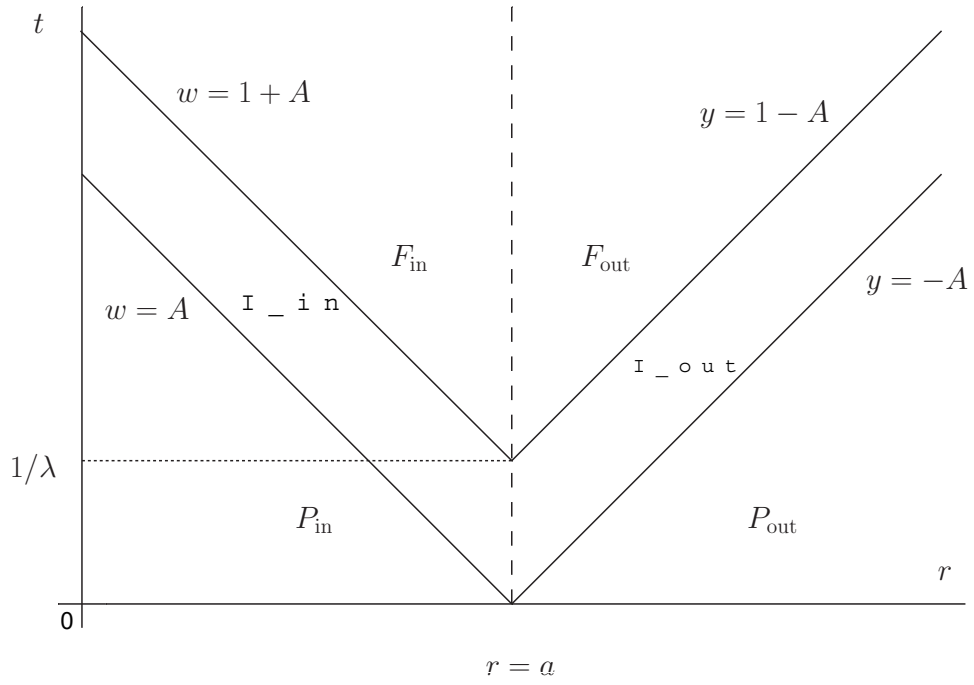

Figure 6.1: Spacetime diagram of shell creation.

Diagram of the shell formation in 3+1 dimensions, where the shell radius a is greater than the time $1/\lambda$ for the complete formation of the shell. The shell formation begins at $t = 0, r = a$ and is completed at $t = 1/\lambda, r = a$.
We label six different regions.
• P_{in} is at $r < a$ and $t < a - r$, inside the radius of shell and spacelike separated from the formation of the shell.
• P_{out} is at $r > a$ and $t < r - a$, outside the radius of the shell and also spacelike separated from the formation of the shell.
• I_{in} is at $r < a$ and $a - r < t < 1/\lambda + a - r$, inside the shell and to the causal future of part but not all of the shell formation process ($0 < t < 1/\lambda, r = a$).
• I_{out} is at $r > a$ and $r - a < t < 1/\lambda + r - a$, outside the shell and to the causal future of part but not all of the shell formation process.
• F_{in} is at $r < a$ and $t > 1/\lambda + a - r$, inside the shell and to the causal future of the entire shell formation process (at the same angular coordinates (θ, φ)).
• F_{out} is at $r > a$ and $t > 1/\lambda + r - a$, outside the shell and to the causal future of the entire shell formation process (at the same angular coordinates).

(continued)

The ingoing spherical null cone from the beginning of the shell formation at $t = 0, r = a$, which has $r = a - t < a$ and is the initial boundary of the ingoing energy pulse which occurs in the region I_{in}, is labeled $w = A = \lambda a$.
The ingoing spherical null cone from the end of the shell formation at $t = 1/\lambda, r = a$, which has $r = 1/\lambda + a - t < a$ and is the final boundary of the ingoing energy pulse in the region I_{in}, is labeled $w = 1 + A$.
The outgoing spherical null cone from the beginning of the shell formation at $t = 0, r = a$, which has $r = a + t > a$ and is the initial boundary of the outgoing energy pulse, which occurs in the region I_{out}, is labeled by $y = -A = -\lambda a$.
The outgoing spherical null cone from the end of the shell formation at $t = 1/\lambda, r = a$, which has $r = a + t - 1/\lambda > a$ and is the final boundary of the outgoing energy pulse in the region I_{out}, is labeled by $y = 1 - A$.
In the rapid shell creation limit, we have $\lambda \to \infty$ so that the energy pulse has zero width. We note that the second line of Ansatz eq.(6.2.8) is valid in the region $t < r + a < 2a$, where it is too early for a signal to come in from the shell, reflect off the origin, and get back to some $0 < r < a$.
The energy density is positively divergent just inside the shell $r = a_-$ and is negatively divergent just outside the shell $r = a_+$, for $0 < t < 1/\lambda$. Also, the energy density is positively divergent just before the null cones $w = 1 + A$ and $y = 1 - A$ from the completion of the shell formation at $t = 1/\lambda, r = a$.

6.2.2 Mode functions

We introduce the radial null coordinates $u := t - r\,, v := t + r$ to rewrite the Klein-Gordon equation as

$$\partial_u \partial_v f = 0\,. \tag{6.2.6}$$

For the outside region $r > a$, a wave packet coming from spacial infinity would not 'know' the boundary condition at $r = a$, while a wave packet going to spacial infinity would have 'known' the boundary condition. For the inside region $r < a$, an ingoing wave packet would have 'known' the boundary condition while an outgoing wave packet would not. We seek solution with the Ansatz

$$\phi_k = \frac{f_k}{\sqrt{4\pi} r} \tag{6.2.7}$$

where

$$f_k(t, r) = \begin{cases} \frac{1}{\sqrt{4\pi k}} \big(e^{-ikv} + E_k(u)\big) & \text{for } r > a\ , \\ \frac{1}{\sqrt{4\pi k}} \big(G_k(v) - e^{-iku}\big) & \text{for } t < r + a < 2a\,, \end{cases} \tag{6.2.8}$$

with $k > 0$, and $E_k(u)\,, G_k(v)$ to be found. The second line of the Ansatz eq.(6.2.8) is only

valid for $t < a$, because otherwise we end up with reflecting wave packets in the outgoing direction and the plane wave assumption e^{-iku} is invalid. We assume $a > 1/\lambda$, so that by the time the ingoing wave packet $G_k(v)$ reaches the origin, the boundary condition has finished evolving.

We highlight that the Ansatz which works for the entire time range is

$$f_k(t,r) = \begin{cases} \frac{1}{\sqrt{4\pi k}}\big(e^{-ikv} + E_k(u)\big) & \text{for } r > a \ , \\ \frac{1}{\sqrt{4\pi k}}\big(\tilde{G}_k(v) - \tilde{G}_k(u)\big) & \text{for } 0 < r < a \, , \end{cases} \tag{6.2.9}$$

and it automatically satisfies eq.(6.1.7a). We replace Ansatz (6.2.9) with (6.2.8) because (6.2.9) leads to equations that are not analytically solvable.

The analytical expression in the late time region F_{in} of Figure 6.1 is not known, due to the observation that waves are reflected at the origin and the failure of Ansatz eq.(6.2.8). The analytical expression in the late time region F_{out} should satisfy Ansatz eq.(6.2.8), which is a result of zero probability flow between F_{in} and F_{out} once the shell is formed.

Substituting the Ansatz into eq.(6.1.7b) and eq.(6.1.7c), while keeping eq.(6.1.7a) satisfied, we have

$$-e^{-ik(t-a)} + G_k(t+a) = e^{-ik(t+a)} + E_k(t-a) \tag{6.2.10a}$$

$$2\lambda \cot h(\lambda t) = \frac{-ike^{-ik(t+a)} - E_k'(t-a)}{e^{-ik(t+a)} + E_k(t-a)} - \frac{-ike^{-ik(t-a)} + G_k'(t+a)}{-e^{-ik(t-a)} + G_k(t+a)} \tag{6.2.10b}$$

where the prime indicates differentiation with respect to the argument. To solve for eq.(6.2.10), it is crucial to define the auxiliary function $B(y)$ with dimensionless variable y

$$B(y) = \begin{cases} 1 & \text{for } y \leq 0 \ , \\ \exp\left(\int_0^y \cot\big(h(z)\big)\, dz\right) & \text{for } 0 < y < 1 \ . \end{cases} \tag{6.2.11}$$

It is easy to see that $B(0) = 1$ and that for $0 \leq y < 1$, $B(y)$ is smooth and satisfies

$$\frac{B'(y)}{B(y)} = \cot\big(h(y)\big) \, . \tag{6.2.12}$$

Following the same logic as Appendix B.2.1, $1/B(y)$ and all of its derivatives approach zero as $y \to 1_-$. Therefore $1/B(y)$ is smooth at $y = 1$.

Rearranging eq.(6.2.10), we obtain first order differential equations of $E_k(t,a)$ and $G_k(t,a)$. Introducing the additional dimensionless variables $K = k/\lambda$ and $A = a\lambda$, $y = \lambda u$ and $w = \lambda v$,

and defining the functions $R_K(y) = E_k(u)$ and $S_K(w) = G_k(v)$, we obtain

$$R_K(y) = \begin{cases} -e^{-iKy} & y < -A \\ -e^{-iKy} + \frac{2i\sin(AK)}{B(y+A)} \int_0^{y+A} e^{-iKz} B'(z)\, dz & y \in (-A, 1-A) \\ -e^{-iK(y+2A)} & y > 1-A\,, \end{cases} \tag{6.2.13}$$

$$S_K(w) = \begin{cases} e^{-iKw} & w < A \\ e^{-iKw} + \frac{2i\sin(AK)}{B(w-A)} \int_0^{w-A} e^{-iKz} B'(z)\, dz & w \in (A, 1+A) \\ e^{-iK(w-2A)} & w > 1+A\,. \end{cases} \tag{6.2.14}$$

Substituting these expressions into eq.(6.2.8), we obtain expressions for the mode functions in regions inside and outside of the shell.

It is easy to see that $R_K(y)$ is smooth for $y < 1 - A$. From the conclusions of Appendix B.2.2 and Appendix D.2, it is also smooth at $y = 1 - A$. The same argument shows $S_K(w)$ is smooth for $w \leq 1 + A$.

For $t < a$, we have

$$\lim_{r \to a_-} \left(G_k(v) - e^{-iku} \right) = \lim_{r \to a_+} \left(e^{-ikv} + E_k(u) \right)$$

and therefore the mode functions $f_k(t, r)$ are continuous at the location of the shell $r = a$. It is not difficult to verify the normalization

$$(\phi_k, \phi_{k'}) = i \int_0^\infty dr\, r^2 \int_{S^2} d\Omega \, \left(\overline{\phi_k} \partial_t \phi_{k'} - (\partial_t \overline{\phi_k}) \phi_{k'} \right) = \delta(k - k')$$

for any constant time hypersurface with $t < \lambda^{-1}$.

To investigate the smoothness of our solutions, some alternative expressions for the functions $R_K(y)$ and $S_K(w)$ are obtained by integrating the middle lines of eq.(6.2.13) and eq.(6.2.14) by parts:

$$R_K(y) = -e^{-iK(y+2A)} - \frac{2i\sin(AK)}{B(y+A)} - \frac{2K\sin(AK)}{B(y+A)} \int_0^{y+A} e^{-iKz} B(z)\, dz\,, \tag{6.2.15}$$

$$S_K(w) = e^{-iK(w-2A)} - \frac{2i\sin(AK)}{B(w-A)} - \frac{2K\sin(AK)}{B(w-A)} \int_0^{w-A} e^{-iKz} B(z)\, dz\,. \tag{6.2.16}$$

We state some features of the mode functions.

1. The regions in Figure 6.1 marked P_{out} and P_{in} correspond to the early time regions,

relative to the wall creation. The top line of either eq.(6.2.13) or eq.(6.2.14) gives the mode functions in these regions, which are just those of the Minkowski vacuum: $f_k(t,r) = -\frac{ie^{-ikt}\sin(kr)}{\sqrt{\pi k}}$. Since our Ansatz eq.(6.2.8) is valid only for time $t < a$, the boundary condition eq.(6.1.7a) at the origin is automatically satisfied for $t < a$.

2. The regions in Figure 6.1 marked $F_{\rm out}$ and $F_{\rm in}$ correspond to the late, or future time regions, relative to the wall creation. The mode functions in these two regions are obtained from the bottom lines of equations (6.2.13,6.2.14), which lead to

$$\begin{aligned} f_k(t,r) &= \frac{-ie^{-ik(t+a)}\sin[k(r-a)]}{\sqrt{\pi k}}\,, \quad y > 1-A\,, t < a \text{ and } r > a \quad [\text{region} \quad F_{\rm out}]\,, \\ f_k(t,r) &= \frac{-ie^{-ik(t-a)}\sin[k(r-a)]}{\sqrt{\pi k}}\,, \quad w > 1+A\,, t < a \text{ and } r < a \quad [\text{region} \quad F_{\rm in}]\,. \end{aligned}$$

   The above expressions reduce to standard Minkowski mode when $ka = 2n\pi$, physically this means wall formation at the node of an original mode does not affect the mode.

3. The third line of eq.(6.2.13) does not have a "memory term C_K" as in eq.(5.2.15), but has a phase factor e^{2iKA} which is independent of λ. Consequently, the detector response function would not contain λ and is therefore insensitive to how fast the boundary condition evolves.

We emphasize that in order to write equations in a more compact form, a shorthand notation in which functions that depend only on $y + A$ are written without their arguments, for example $B := B(y + A)$. This notation is used throughout the chapter and Appendix D.

6.3 Energy density

6.3.1 Expression for the energy density

We quantize the scalar field by writing

$$\begin{aligned} &\phi(t,r) = \int_0^\infty \left(a_k \phi_k(t,r) + a_k^\dagger \overline{\phi}_k(t,r)\right) dk\,, \qquad (6.3.1) \\ &\text{with} \quad \phi_k(t,r) = \frac{f_k(t,r)}{\sqrt{4\pi r}}\,, \end{aligned}$$

where the annihilation and creation operators have the commutators $\left[a_k, a_{k'}^\dagger\right] = \delta(k-k')$. The mode functions $\phi_k(t,r)$ are normalized so that the field and its time derivative have the correct equal-time commutator. The vacuum $|0\rangle$ is the state that is annihilated by all a_k.

The expression for the energy density outside of the shell in terms of the mode functions $R_K(y)$ has exactly the same form as in reference [18]. We summarize the calculation and give the result below. The renormalized energy density of the quantized field in the state $|0\rangle$ is obtained by point-splitting the field operators, taking the expectation value in $|0\rangle$, subtracting the corresponding expectation value in the Minkowski vacuum $|0\rangle_M$, and taking the coincidence limit. This gives

$$\begin{aligned}\langle T_{00}\rangle &= \lim_{\substack{u_1,u_2\to u\\ v_1,v_2\to v}}(\partial_{u_1}\partial_{u_2}+\partial_{v_1}\partial_{v_2})\Big[\langle 0|\phi(1)\phi(2)|0\rangle - \langle 0_M|\phi(1)\phi(2)|0_M\rangle\Big]\\ &= \frac{1}{4\pi}\left(\frac{\langle(\partial_u f)^2\rangle}{r^2}+\frac{\langle f(\partial_u f-\partial_v f)\rangle + c.c}{2r^3}+\frac{\langle f^2\rangle}{2r^4}\right). \qquad (6.3.2)\end{aligned}$$

Using eq.(6.3.1) and the first line of eq.(6.2.8) we obtain in the outside region ($r > a$)

$$\langle T_{00}\rangle = \frac{\lambda^2}{16\pi^2 r^2}\int_0^\infty \frac{dK}{K}[|R'_K(y)|^2 - K^2] - \frac{1}{32\pi^2 r^2}\frac{\partial}{\partial r}\Big(\frac{\mathcal{G}_{\rm out}(t,r)}{r}\Big), \qquad (6.3.3)$$

where $\mathcal{G}_{\rm out}$ is defined as

$$\mathcal{G}_{\rm out} = \int_0^\infty \frac{dK}{K}\Big[|e^{-iKw}+R_K(y)|^2 - |e^{-iKw}-e^{-iKy}|^2\Big]. \qquad (6.3.4)$$

The second line of eq.(6.2.8) gives for the inside region ($r < a$)

$$\langle T_{00}\rangle = \frac{\lambda^2}{16\pi^2 r^2}\int_0^\infty \frac{dK}{K}[|S'_K(w)|^2 - K^2] - \frac{1}{32\pi^2 r^2}\frac{\partial}{\partial r}\Big(\frac{\mathcal{G}_{\rm in}(t,r)}{r}\Big), \qquad (6.3.5)$$

with the definition

$$\mathcal{G}_{\rm in} = \int_0^\infty \frac{dK}{K}\Big[|S_K(w)-e^{-iKy}|^2 - |e^{-iKw}-e^{-iKy}|^2\Big]. \qquad (6.3.6)$$

In the early time regions, which are denoted $P_{\rm out}$ and $P_{\rm in}$ in Figure 6.1, $\langle T_{00}\rangle$ vanishes by construction. In the late time regions $F_{\rm out}$ and $F_{\rm in}$, the first terms in eq.(6.3.3) and eq.(6.3.5) vanish but the second terms stay, as a result of eq.(6.2.13, 6.2.14). The functions $\mathcal{G}_{\rm out}$ and $\mathcal{G}_{\rm in}$ are easily calculated. We obtain

$$\mathcal{G}_{\rm out}|_{F_{\rm out}} = \mathcal{G}_{\rm in}|_{F_{\rm in}} = \ln\big[(r-a)^2\big] - \ln(r^2) \qquad (6.3.7)$$

$$\langle T_{00}\rangle_{\rm future} = \frac{1}{16\pi^2 r^4}\Big(\ln|r-a| - \ln(r)\Big) - \frac{1}{16\pi^2 r^3}\Big(\frac{1}{r-a}-\frac{1}{r}\Big), \qquad (6.3.8)$$

where $\mathcal{G}_{\rm out}|_{F_{\rm out}}, \mathcal{G}_{\rm in}|_{F_{\rm in}}$ are the $\mathcal{G}$ functions in the $F_{\rm out}$ and $F_{\rm in}$ regions respectively. $\langle T_{00}\rangle_{\rm future}$

is the energy density in both F_{out} and F_{in} regions. The energy density is positively divergent just inside the shell and negatively divergent just outside the shell. We could get finite energy if integrating on a constant time hypersurface in a small region around $r = a$.

In Appendix D.3, we consider the continuity of the energy density in the intermediate outside region: $r > a$ and $-A < y < 1 - A$. We find out that the energy density is positively divergent just before light cone of the point where shell creation ends. This divergence suggests that wall creation on a spherical shell could cut off quantum entanglement, but the problem of finite detector response persists.

A spacetime diagram is shown in Figure 6.1.

6.3.2 Energy density inside the shell $r < a$

In this section we look at the energy density in the region $r < a$, before time $t = a$. The idea is to see if there is a symmetry between the inside and outside regions that would allow us to extract the final result for the inside region from the results outside the shell.

The results turn out to be just as expected (for $t < a$). Once we have the energy density results for the outside region, we can deduce its inside region behavior accordingly by changing sign $A \to -A$ and switching variables $(w, y) \to (y, w)$, then dropping the imaginary terms produced. We find out the energy density is also positively divergent along the ingoing null line just before the light cone of the point where wall creation ends.

For convenience we rewrite some equations in appendix D.3 for the four different contributions to the energy density outside the shell, equations (D.3.12, D.3.17, D.3.39, D.3.40 and D.3.42), and then compare with the corresponding expressions inside the shell.

From equations (D.4.2, D.4.4, D.4.5, D.4.6), the energy density inside the shell is obtained from the outside results by performing the transformation $(y, w, A) \to (w, y, -A)$ and dropping any imaginary parts that are produced.

6.4 Response of an Unruh-DeWitt detector

We consider an inertial Unruh-DeWitt detector [20, 54] that linearly couples to the quantum field at a fixed spatial location. The probability of a detector transitioning from a state of energy 0 to a state of energy ω is proportional to the response function [20, 23, 49, 54]

$$\mathcal{F}(\omega) = \int_{-\infty}^{\infty} dt_1 \int_{-\infty}^{\infty} dt_2 \, e^{-i\omega(t_1 - t_2)} \, \chi(t_1)\chi(t_2) \, \mathcal{W}(t_1, t_2) \, . \tag{6.4.1}$$

The smooth real-valued function χ specifies how the detector's interaction with the field is turned on and off. Function $\mathcal{W}$ is the pull-back of the field's Wightman function to the

detector's worldline. We consider a detector located outside the spherical shell and in the future region $F_{\rm out}$ in Figure 6.1. The response function has the same form as eq.(5.4.3), and the change in Wightman function has the same form as eq.(5.4.4). The functions f_k and $\overline{f_k}$ are obtained from the first line of eq.(6.2.8); f_k^M and $\overline{f_k^M}$ are obtained in the same way except using the first line of eq.(6.2.13). Substituting these expressions and collecting terms, we find

$$16\pi^2 r^2 \Delta\mathcal{W}(t_1,t_2) = \int_0^\infty \frac{dk}{k}\left(e^{ik(2r-t_1+t_2)} + e^{-ik(2r+t_1-t_2)} - e^{ik(2a-2r-t_1+t_2)} - e^{-ik(2a-2r+t_1-t_2)}\right) . \tag{6.4.2}$$

Finishing the k integral we get

$$16\pi^2 r^2 \Delta\mathcal{W}(t_1,t_2) = \ln\left[\frac{|e_1|\,|e_3|}{|e_2|\,|e_4|}\right] + i\pi\left[\theta(e_1)\,\theta(e_2)\,\theta(-e_3)\,\theta(e_4) - \theta(-e_1)\,\theta(e_2)\,\theta(e_3)\,\theta(e_4)\right] , \tag{6.4.3}$$

where we define $e_1 = 2a - 2r + t_1 - t_2$, $e_2 = 2r + t_1 - t_2$, $e_3 = 2a - 2r - t_1 + t_2$ and $e_4 = 2r - t_1 + t_2$. This result is

$$\begin{aligned} 16\pi^2 r^2 \Delta\mathcal{W}(t_1,t_2) &= \ln\left[\frac{|4(a-r)^2 - (t_1-t_2)^2|}{|4r^2 - (t_1-t_2)^2|}\right] \\ &+ i\pi\,\mathrm{sgn}(t_1-t_2)\theta\left(r - |t_1-t_2|/2\right)\theta\left(a - r + |t_1-t_2|/2\right) . \end{aligned} \tag{6.4.4}$$

The change in Wightman function is logarithmic divergent when $|t_1 - t_2| = 2r$, which is the time it takes for the field to bounce back from the shell. It is also λ independent due to the λ independence of the mode functions in the future region. The detector response does not diverge, because the logarithmic divergence in eq.(6.4.4) is integrable.

6.5 Summary and discussion

In this chapter, we investigated shell formation in 3+1 dimensions. We modeled the formation of a spherical shell with one parameter self-adjoint operator extension at radius $r = a$. We solved for the mode functions of the Klein-Gordon equation under such boundary condition, and quantize the field. We derived the expressions of the energy density and Unruh-DeWitt detector response. The results share some similarities with the 1+1 and 3+1 dimensional point source model, but also have some major differences.

A common feature is that the energy density in all three models is unbounded. For different models, it seems general that the energy density is divergent along some null surface.

For 1+1 dimensional model, the energy density is divergent just below the line $t = |x| + 1/\lambda$. For 3+1 dimensional point source model, the energy density is divergent not only just above the hypersurface $t = r$, but also at the origin $r = 0_+$ and at time infinity $t \to \infty$. For 3+1 dimensional shell model, the energy density is divergent just below the hypersurface $t = |r - a| + 1/\lambda$ and right inside/outside the shell.

A significant difference is in the Unruh-DeWitt detector response. The 3+1 dimensional shell creation model has finite detector response, due to the lack of a memory term such as C_K in eq.(5.2.16). The 3+1 dimensional point source has divergent detector response when the boundary condition is suddenly turned on, so it is best suited for firewall.

To sum up, the second model in 3+1 dimensions does not support a firewall-like singular structure. Therefore, should firewall really exist, we probably need a more exotic mechanism.

Chapter 7

Conclusions

This thesis is set to achieve the following points.

1. A model that creates energy pulse along some null curve or hypersurface.

   We require null curve, or surface, because reference [15] suggests that a firewall (if exist) should wrap around a black hole horizon. This divergence should relate to the stress-energy tensor of the field or particle detector response. It is desirable to have divergent Unruh-DeWitt detector response.

2. To have a divergent Unruh-DeWitt detector response when crossing the 'firewall', or energy pulse.

   This is set to preserve the black hole complementarity in Chapter 2. We seek divergent detector responses, because it means breaking the entanglement in a quantum state [15].

3. Physically, the system should have finite total energy.

4. The physical process should affect background spacetime.

   We assume fixed background, because it leads to an analytically solvable equation. Some back reactions are included in CGHS model [44].

We prioritize the first two goals, because they capture the essence of firewall and the model is analytically solvable. It should be possible to numerically study firewall with metric back reaction.

We give a summary and comparison of the three models.

1. Creation of Dirichlet boundary condition in $1+1$ dimensional spacetime

- Energy density diverges to positive infinity just below the line $t = |x| + 1/\lambda$, at the points where $h(y) \to 0$.
- Detector response is finite and does not depend on how fast the boundary condition evolves, or does not depend on parameter λ.

2. Creation of pointlike source in $3+1$ dimensional spacetime

   - Energy density diverges to negative infinity just above the hypersurface $t = r$, at the points where $h(y) \to 0$. Energy density also diverges to positive infinity at the space origin $r = 0_+$ and when time $t \to \infty$.
   - Detector response is infinite when the boundary condition is switched abruptly. The divergence comes from memory term C_K, which is unique to the model.

3. Creation of spherical shell in $3+1$ dimensional spacetime

   - Energy density diverges to positive infinity just below the hypersurface $t = |r - a| + 1/\lambda$, at the points where $h(y+A) \to 0$ and $h(w-A) \to 0$. Energy density also diverges to positive infinity on surface $r = a_-$ but diverges to negative infinity on surface $r = a_+$.
   - The detector response is finite, as result of no λ dependence in the 'future' mode function, such as the memory term C_K of eq.(5.2.16).

We call dimensionless function $h(x)$ a **profile function** because it describes how the boundary condition evolves.

We note two general features across the models. First, the energy density (of the energy pulse) diverges where profile function $h(x)$ of eq.(4.2.9), eq.(5.2.5) and eq.(6.2.5) approaches zero. Second, besides the divergence in the energy pulses, vacuum polarization also contributes to the divergence in both of the 3+1 dimensional models. The 1+1 dimensions do not have vacuum polarization thus its only divergence is in the pulse.

Based on the three models discussed above, we conjecture that future models should always pay attention to where the profile function vanishes: $h(x) \to 0$. For higher dimensional models, we also pay attention to where vacuum polarization diverges. Physically, the region where profile function $h(x)$ approaches zero is expected to be where the entanglement is completely cut off.

A future work is to solve the $3+1$ dimensional shell creation model numerically with the general Ansatz eq.(6.2.9). Further study would be to integrate the time-dependent boundary conditions in a model with metric back reactions.

Our thesis discusses the possible mechanisms of a drastic modification to general relativity, namely, a 'firewall' around a black hole's horizon. We considered three different

mechanisms in both 1+1 and 3+1 dimensions, with analytical results. We chose flat spacetime because we can solve the equations analytically and discuss the properties stress-energy tensor and particle detector response. The stress-energy tensor and detector response are indicators of how singular this 'firewall' can be. Our results suggest no good evidence for a drastic modification of general relativity, such as 'firewall', in either 1+1 or 3+1 dimensions.

Appendix A

A.1 Rindler coordinates and Unruh effect

In [23], Birrel and Davis considered a massless scalar field in Minkowski space, whose Wightman function is

$$G(x,x') = \frac{-1}{4\pi^2[(t-t'-i\epsilon)^2 - |\vec{x}-\vec{x'}|^2]}\,. \tag{A.1.1}$$

The small imaginary part is to be interpreted under contour integral

$$\frac{1}{x \mp i\epsilon} = \mathcal{P}(\frac{1}{x}) \pm i\pi\delta(x)\,, \tag{A.1.2}$$

where $\mathcal{P}$ is the principal value. They compared the different responses of an inertial trajectory and an accelerating trajectory [23]. See figure A.1. The inertial detector moves along a straight line passing through the origin, while the accelerating detector moves along a hyperbola $\xi = \text{const}$. We label the four wedges of the spacetime diagram as 'R,F,L,P'. See figure A.1. The trajectory with constant acceleration is restricted within 'R' (right Rindler wedge).

For inertial trajectory $\vec{x} = \vec{x_0} + \vec{v}t$ with $t = (1-v^2)^{-1/2}\tau$, the Wightman function is

$$G(x,x') = \frac{-1}{4\pi^2(\tau-\tau'-i\epsilon)^2}. \tag{A.1.3}$$

The transition probability per unit time is proportional to the integral in eq.(2.2.7) and vanishes in this case. This is because for $E - E_0 > 0$ we have to close the contour in the lower half plane where the integration has no pole.

For an accelerating trajectory with $\vec{x} = (0,0,z), z = (t^2+\xi^2)^{1/2}, t = \xi\sinh(\tau/\xi)$ and

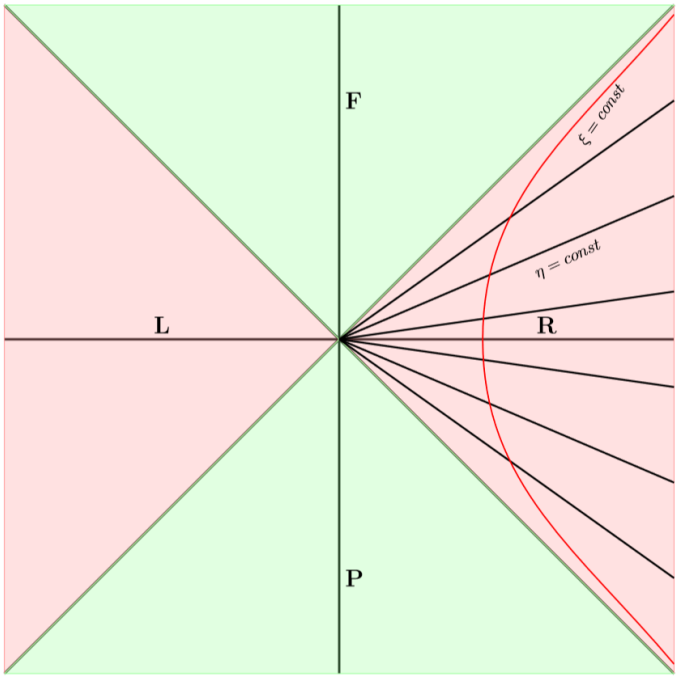

Figure A.1: Spacetime diagram of a Rindler observer. The Horizontal line is z-axis and the verticle line is t-axis. Trajectory $\xi = const$ corresponds to $z = (t^2 + \xi^2)^{1/2}$. A Minkowski observer sees the entire spacetime, but a Rindler observer sees only one of the wedges at the Unruh temperature. As a result, mode functions in wedge 'R' is different from that for the entire space, which leads to the different definitions of the vacuum.

$\xi = \text{const}$, the Wightman function is

$$G(x, x') = \frac{-1}{16\pi^2\xi^2 \sinh^2(\frac{\Delta}{2\xi} - \frac{i\epsilon}{\xi})} \to \frac{-1}{4\pi^2} \sum_{k=-\infty}^{\infty} \frac{1}{(\Delta - 2i\epsilon + 2\pi i\xi k)^2}\,, \tag{A.1.4}$$

where the last part comes from $1/\sin^2 \pi z = \pi^{-2} \sum_k (z-k)^{-2}$ (identity under contour integral). Then we perform a contour integral and get

$$\int_{-\infty}^{\infty} d\Delta\tau e^{-i(E-E_0)\Delta\tau} G(x, x') = \frac{E - E_0}{2\pi} \frac{1}{e^{2\pi(E-E_0)\xi} - 1}\,. \tag{A.1.5}$$

It states that the detector sees the Minkowski vacuum as a thermal state at the Unruh temperature $T_U = 1/2\pi\xi$. This is the so-called Unruh effect [20, 21].

The significance of the Unruh effect is more than the fact that an accelerating observer

sees the Minkowski vacuum as a thermal state at Unruh temperature. We want to emphasize that the Unruh effect states again that the definition of the vacuum is not universal. By the equivalence of acceleration and gravity, observers at different local patches of the spacetime may not agree on the vacuum.

The analogous calculation can be done in curved spacetime [7]. Hawking showed that a static observer at future null infinity sees an ingoing pure state as thermal. This means that the vacuum state near a black hole's horizon is not seen as the vacuum by observers at future null infinity.

A.2 Penrose diagram

A Penrose diagram is a diagram that draws spacetime infinities within a finite range. We include spacetime infinities because the causal structure of a manifold is what we are most interested in gravity thought experiments. Geometry comes in second place comparing to causal structure. We can achieve this by the following theorem from [6].

"Two spacetimes whose metrics differ only by an overall positive factor have the same null geodesics. If there is relationship $g'_{\mu\nu}(x) = e^{f(x)} g_{\mu\nu}(x)$ between two metrics $g'_{\mu\nu}(x)$ and $g_{\mu\nu}(x)$, and $f(x)$ is a real function, then the null geodesics will stay null geodesics, timelike curves will stay timelike and spacelike curves will stay spacelike."

For example, we choose coordinate transformation

$$\begin{aligned} T + R &= \arctan(t + r) \\ T - R &= \arctan(t - r)\,, \end{aligned} \tag{A.2.1}$$

so that

$$\begin{aligned} ds^2 &= dt^2 - dr^2 - r^2 d\varphi d\theta \\ &= \frac{1}{\cos^2(T+R)\cos^2(T-R)} \Big[dT^2 - dR^2 - \Big(\frac{\sin(2R)}{2}\Big)^2 d\varphi d\theta \Big]\,, \end{aligned} \tag{A.2.2}$$

with $R \geq 0\,, |T \pm R| < \pi/2$. If we ignore the overall factor of the metric, the full Minkowski spacetime is plotted as Fig.A.2.

A.3 Monogamy of pure state entanglement

Some definitions:

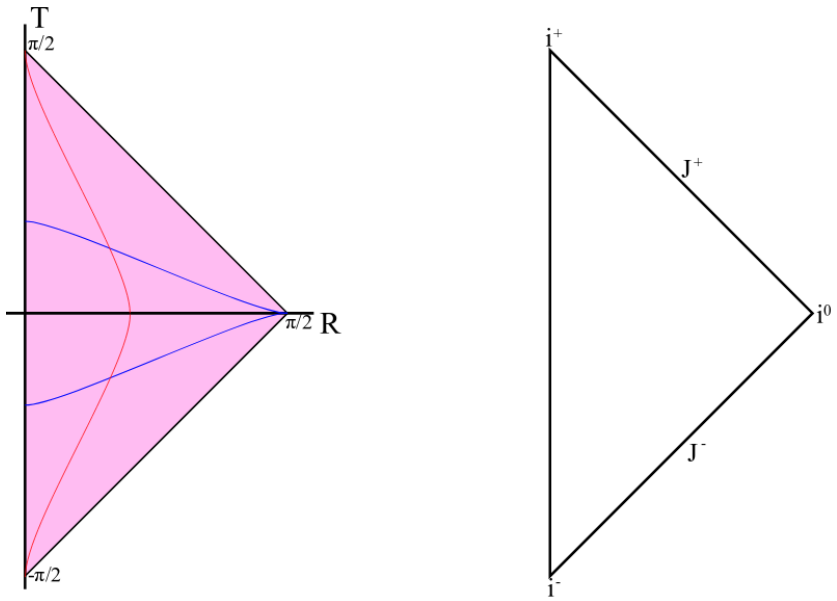

Figure A.2: Penrose diagram of Minkowski spacetime from [6]: $\mathcal{J}^-$ is past null infinity, i^- is past timelike infinity, $\mathcal{J}^+$ is future null infinity, i^+ is future timelike infinity. Each point in the diagram represents a **S**2-sphere that we have suppressed.

For system described by density matrix ρ, it is **pure** if and only if $\rho^2 = \rho$, it is **mixed** when $\rho^2 < \rho$.

A **pure bipartite** state is entangled if it cannot be written as a product state, viz $|AB\rangle \neq |A\rangle \otimes |B\rangle$ [3]. This definition can be generalized to **multipartite** systems as well. A state of a system defined on Hilbert space $H_{ABC} = H_A \otimes H_B \otimes H_C \cdots$ is (fully) **separable** if it has a product form $|\psi_A\rangle \otimes |\psi_B\rangle \otimes |\psi_C\rangle \cdots$, otherwise it is entangled [3].

In terms of density matrices $\rho_A\,, \rho_B \cdots$, a multipartite system on Hilbert space $H_{ABC} = H_A \otimes H_B \otimes H_C \cdots$ is separable when condition $\rho_{ABC\cdots} = \sum_{i=1}^{min\{rank(H_A \cdots)\}} p_i \rho_A^i \otimes \rho_B^i \cdots$ is satisfied [3]. So by definition, as long as the state is non-separable, it is entangled.

Monogamy of pure state entanglement:

This statement follows reference [55]. 'If a pure quantum state of two systems is entangled, then none of the two systems can be entangled with a third system.'

We assume that systems 'a' and 'b' are entangled in a pure state $\rho_{ab}^2 = \rho_{ab}$, such as $\frac{1}{\sqrt{2}}[|0_a 0_b\rangle + |1_a 1_b\rangle]$. When the system 'a, b' is part of a larger system, the reduced density

operator for ‘ab’ must by assumption be pure. However, for the composite system ‘ab’ (or for any of its subsystems ‘a’ or ‘b’) to be entangled with another system ‘c’, the reduced density operator of ‘ab’ $\rho_{ab} = Tr_c[\rho_{abc}]$ must be a mixed state. But this contradicts the assumption that it is pure, therefore no entanglement between ‘ab’ and any other system can exist. This feature is referred to as the monogamy of pure state entanglement

Appendix B

B.1 Orthonormality of the mode function in $1+1$ dimensions

For any valid solution, we need to verify whether it can be ortho-normalized.

When $u \leq 0$ or $u \geq 1/\lambda$, we can easily verify the mode functions being ortho-normalized.

When $0 < u < 1/\lambda$, it is not straightforward how our solution can be ortho-normalized. A verfication thanks to Jorma Louko is presented here. The Klein-Gordon inner product of modes in eq.(4.2.6) is

$$\begin{aligned}
(\phi_k, \phi_{k'}) &= \frac{2i}{8\pi\sqrt{kk'}} \int_0^\infty dx \left[\overline{(e^{-ikv} + E_k(u))} [\partial_t (e^{-ik'v} + E_{k'}(u))] - \overline{\partial_t (e^{-ikv} + E_k(u))} (e^{-ik'v} + E_{k'}(u)) \right] \\
&= \frac{i}{4\pi\sqrt{kk'}} \int_0^\infty dx \left[\overline{(e^{-ikv} + E_k(u))} [\partial_t (e^{-ik'v} + E_{k'}(u))] + \overline{(e^{-ikv} - E_k(u))} [\partial_t (e^{-ik'v} - E_{k'}(u))] \right] \\
&= \frac{i}{2\pi\sqrt{kk'}} \left[\underbrace{\int_0^\infty dx \left[[\partial_t e^{-ik'v}] e^{ikv} + [\partial_t e^{-ik'u}] e^{iku} \right]}_{①} + \underbrace{\int_{t-1/\lambda}^t dx \left[[\partial_t E_{k'}(u)] \overline{E_k(u)} - [\partial_t e^{-ik'u}] e^{iku} \right]}_{②} \right].
\end{aligned} \tag{B.1.1}$$

From the first to the second line, we make use of $\partial_t E_k(u) = -\partial_x E_k(u)$ and $\partial_t e^{-ik'v} = \partial_x e^{-ik'v}$ in the second term in the big square bracket, then integrate by part to get rid of a surface term $(e^{-ik'v} + E_{k'}(u))\overline{(e^{-ikv} - E_k(u))}|_0^\infty$ and switch back to ∂_t. After cancellation of cross terms, we make use the fact that $E_k(u)$ is different from plane wave only in the region $t - 1/\lambda < x < t$ to arrive at the last line.

Integral ① can be easily shown to contribute to delta function $\delta(k - k')$.

Integral ② can be rearranged as (the prime in $R'_k(y)$ being derivative over its argument) an integration over a total derivative.

Be aware that K' is not a derivative, while all the other primes (i.e. $R'_K(y)$, etc) are derivative over the argument of the functions, we can rewrite the integral ②

$$\begin{aligned}&\int_{t-1/\lambda}^{t} dx\bigg([\partial_t E_{k'}(u)]\overline{E_k(u)} - [\partial_t e^{-ik'u}]e^{iku}\bigg)\\ =&\int_0^1 dy\bigg(\Big[R'_{K'}(y)\Big]\overline{R_K(y)} + iK'e^{i(K-K')y}\bigg)\,,\end{aligned} \tag{B.1.2}$$

by switching integral variable from dx to $dy = \lambda du$, and defining $K' := k'/\lambda$, and $K := k/\lambda$.

The integrand of eq.(B.1.2) can be rearranged as:

$$\begin{aligned}&R'_{K'}(y)\overline{R_K(y)} + iK'e^{i(K-K')y}\\ =&-\frac{2}{B(y)}e^{iKy}J'_{K'}(y) - \frac{4B'(y)}{B^3(y)}\overline{J_K(y)}J_{K'}(y) + \frac{4}{B^2(y)}\overline{J_K(y)}J'_{K'}(y)\\ &-\frac{2}{B(y)}\overline{J_K(y)}(e^{-iK'y})' + \frac{2}{B^2(y)}(\overline{J_K(y)})'J_{K'}(y)\,,\end{aligned} \tag{B.1.3}$$

where we have defined

$$J_K(y) := \int_0^y dz B'(z)e^{-Kz}\,, \tag{B.1.4}$$

and have made use of $J'_k(y) = B'(y)e^{-iKy}$ in the last line.

Further rearrangements give a total derivative

$$\begin{aligned}&2\Big[(\frac{1}{B^2})'\overline{J_K}J_{K'} + \frac{1}{B^2}(\overline{J_K})'J_{K'} + \frac{1}{B^2}\overline{J_K}J'_{K'}\Big] + 2\bigg[\frac{1}{B^2}\overline{J_K}J'_{K'} - \frac{1}{B}e^{iKy}J'_{K'} - \frac{1}{B}(e^{-iK'y})'\overline{J_K}\bigg]\\ =&2\bigg(\frac{1}{B^2}\overline{J_K}J_{K'} - e^{-iK'y}\frac{\overline{J_K}}{B}\bigg)'\,,\end{aligned} \tag{B.1.5}$$

where we omit the argument y from $B(y)\,, J_k(y)$ and $J_{K'}(y)$. It should vanish upon integration.

B.2 Mode function regularity across $t = |x| + 1/\lambda$

B.2.1 Smoothness of $1/B(y)$

Before going to the next section, it can be shown from eq.(4.2.8) that for $0 \leq y \leq 1$

$$B(y) = \exp\Big[\int_0^y \frac{dz}{g(z)}\Big] \tag{B.2.1}$$

with $g(y) := \tan h(y)$ where $h(y)$ is smooth on its entire domain, therefore $B(y)|_{y\to 1_-} \to \infty$.

To prove the smoothness of our solution, we need to prove: $R_K(y)$ is smooth at both $y = 0$ and $y = 1$. It is straightforward that $R_K(y)$ is smooth at $y = 0$ by using $B(0) = 1\,, B^{(n)}(0) = 0$, so our focus is on proving the smoothness at $y = 1$.

From the expression of $B(y)$ and the property of function $h(y)$, it can be proven rigorously that $1/B(y)$ and all of its derivatives are zero when $y \to 1_-$.

The derivatives can be written as

$$\frac{d^n}{dy^n}\Big(\frac{1}{B(y)}\Big) = \frac{(-1)^n P_n(y)}{B(y)[g(y)]^n} \tag{B.2.2a}$$

$$P_0(y) = 1\,, P_n(y) = -P'_{n-1}(y)g(y) + P_{n-1}(y)[1 + (n-1)g'(y)]\,, \tag{B.2.2b}$$

where $P_n(y)$ are polynomials of $g(y)$ and its derivatives, and $P_n(y)\Big|_{y\to 1_-} \to 1$. Since $P_n(y)$ are bounded as $y \to 1_-$, it suffices to show that $\Big[1/B(y)[g(y)]^n\Big]\Big|_{y\to 1_-} \to 0$ for $n \in \mathbb{N}$.

We have

$$\ln\Big[\frac{1}{B(y)g^n(y)}\Big] = -\Big[\int_0^y \frac{dz}{g(z)}\Big]\Big[1 + \frac{n\ln(g(y))}{\int_0^y \frac{dz}{g(z)}}\Big]\,, \tag{B.2.3}$$

the first square bracket goes to infinity as $y \to 1_-$, the second square bracket tend to 1 by L'Hopital. Therefore $\ln\Big[1/B(y)[g(y)]^n\Big] \to -\infty$ as $y \to 1_-$, and the derivatives of $1/B(y)$ vanish as $y \to 1_-$. This result can also be understood by the observation that exponential increases faster than polynomials.

B.2.2 Differentiability of $R_K(y)$

From the smoothness of $1/B(y)$, to prove the smoothness of the mode function is to prove the smoothness of the third term in eq.(4.2.12):

$$\lim_{y\to 1_-} \frac{d^n}{dy^n}\Big[\frac{2iK}{B(y)}\int_0^y dz B(z)e^{-iKz}\Big] = 0\,. \tag{B.2.4}$$

In order to do so, we define

$$\mathcal{J}_K(z) := \int_0^y dz B(z)e^{-iKz} \tag{B.2.5}$$

$$\mathcal{F}_K(y) := \frac{\mathcal{J}_K(y)}{B(y)}\,. \tag{B.2.6}$$

I. For $n = 1$, with the help of eq.(B.2.2a), we have

$$\lim_{y\to 1_-} \frac{d}{dy}\Big[\frac{\mathcal{J}_K(y)}{B(y)}\Big] \xrightarrow{l'Hopital} \lim_{y\to 1_-} \frac{[g'(y) - iKg(y)]e^{-iKy}}{1+g'(y)} = 0\,. \tag{B.2.7}$$

II. For general n, we outline the steps below.

(a) Calculate n derivatives of $\mathcal{F}_K(y)$ using equation $B(y) = B'(y)g(y)$ after taking each derivative to remove factors of $B'(y)$. The result is an expression for $\mathcal{F}_K^{(n)}(y)$ that does not contain any derivatives of $B(y)$.

(b) Define $\mathrm{den}(y) = B(y)\big(g(y)\big)^n$ and $\mathrm{num}(y) = \mathcal{F}_K^{(n)}(y)\,\mathrm{den}(y)$.

(c) In preparation for using l'Hôpital n times, calculate $\mathrm{num}^{(n)}(y)$ and $\mathrm{den}^{(n)}(y)$, again using $B(y) = B'(y)g(y)$ after taking each derivative.

(d) Define $\mathbf{num}^{(n)}(y) = \mathrm{num}^{(n)}(y)/B(y)$ and $\mathbf{den}^{(n)}(y) = \mathrm{den}^{(n)}(y)/B(y)$ and replace all remaining factors of $\mathcal{J}_K(y)$ by $\mathcal{F}_K(y)\,B(y)$. The limit of the n-th derivative of $\mathcal{F}(y)$ as $y \to 1_-$ now has the form

$$\lim_{y\to 1_-} \mathcal{F}^{(n)}(y) = \lim_{y\to 1_-} \frac{\mathbf{num}^{(n)}(y)}{\mathbf{den}^{(n)}(y)}\,. \tag{B.2.8}$$

This procedure can be verified up to any order n and the quantities $\mathbf{num}^{(n)}(y)$ and $\mathbf{den}^{(n)}(y)$ have the form

$$\mathbf{num}^{(n)}(y) = P(y)\,, \quad \mathbf{den}^{(n)}(y) = 1 + Q(y)$$

where $P(y)$ and $Q(y)$ are polynomials of $g(y)$ and its derivatives, $\mathcal{F}(y)$, and factors e^{-iKy}, and each term contains at least one power of $\mathcal{F}(y)$ or $g^{(j)}(y)$ $j \in (0, n)$. This means that both $P(y)$ and $Q(y)$ go to 0 as $y \to 1_-$. We therefore have from (B.2.8) that $\mathcal{F}(y)$ is C^∞ at $y = 1$. The authors of [18] have verified this up to $n = 26$ using computer algebra. They stopped the calculation at $n = 26$ because of limitations of computing time and memory, but there is no reason to believe this will not hold for a general n. If the proof extends to $n \in \mathbb{N}$, we would have that $R_K(y)$ is smooth at $y = 1$.

We can also reach the same conclusion intuitively by

$$\begin{aligned} &\lim_{y\to 1_-} \frac{1}{B(y)} \int_0^y dz B(z) e^{-iKz} \\ &\xrightarrow{l'Hopital} e^{-iKy} \tan(h(y)) \sim e^{-iKy} h(y)\,, \end{aligned} \tag{B.2.9}$$

where the expression and all of its derivatives approach zero as $y \to 1_-$. We note that $R_K(y)$ being smooth across $y = 1$ is directly related to function $h(y)$ being smooth.

B.3 Expansion of $E_k(u)$ in $1+1$ dimensions

As an example, we expand $|E_k'(u)|^2$ as a series.

For $k \to \infty$, we integrate by parts by taking anti-derivatives of $e^{-ikz/\lambda}$. We have

$$E_k(u) = e^{-iku} - \frac{2B'(\lambda u)}{B(\lambda u)} \frac{i\lambda}{k} \left(e^{-iku} - \frac{1}{B'(\lambda u)} \int_0^{\lambda u} B''(z) e^{-i\frac{k}{\lambda}z} dz \right), \tag{B.3.1}$$

and

$$E_k'(u) = -ike^{-iku} - \frac{2B'(\lambda u)}{B(\lambda u)} \lambda e^{-iku} + 2i\lambda^2 e^{-iku} \Big(\frac{B'(\lambda u)}{B(\lambda u)} \Big)^2 \frac{1}{k} + O(1/k^2)\,. \tag{B.3.2}$$

When calculating $|E_k'|^2$, terms of order $O(k)$, $O(1)$ and $O(1/k)$ all cancel out because they are pure imaginary. We derive

$$|E_k'(u)|^2 = k^2 + O(k^{-2})\,. \tag{B.3.3}$$

Similarly for $k \to 0$, we integrate by parts and get

$$E_k(u) = 1 - iku - \frac{2}{B(\lambda u)} \int_0^{\lambda u} B'(z) dz + i\frac{k}{\lambda} \frac{2}{B(\lambda u)} \int_0^{\lambda u} B'(z) z dz + O(k^2) \tag{B.3.4}$$

and

$$E'_k(u) = -ik - \frac{2\lambda B'(\lambda u)}{B^2(\lambda u)} + \frac{2ik\lambda u B'(\lambda u)}{B(\lambda u)} - \frac{2ikB'(\lambda u)}{B^2(\lambda u)} \int_0^{\lambda u} B'(z) z dz + O(k^2)\,. \quad \text{(B.3.5)}$$

We derive $|E'_k(u)|^2 = 4\lambda^2 |\frac{B'(\lambda u)}{B^2(\lambda u)}|^2 + O(k^2)$.

B.4 Divergence of the $\langle T_{00} \rangle$ in 1+1 dimensions

In this section, we want to prove that even when the evolution is smooth, the stress-energy tensor is still divergent along the null lines $t = |x| + 1/\lambda$.

We start with expressions on the positive axis

$$\begin{aligned} T_{00} &= \int_\mu^\infty \frac{dk}{8\pi k} [|E'_k(u)|^2 - k^2] \\ &= \frac{\lambda^2}{8\pi} \int_{\mu/\lambda}^\infty \frac{dK}{K} [|R'_K(y)|^2 - K^2]\,, \end{aligned} \quad \text{(B.4.1)}$$

where $y = \lambda u$, $K = k/\lambda$ and $R'_K(y)$ means taking derivative over the argument.

We split the integral $\int_{\mu/\lambda}^\infty$ into $\int_{\mu/\lambda}^1$ and $\int_1^\infty$, and consider the corresponding two expressions separately. Namely, we define

$$F_+(y) = \frac{\lambda^2}{8\pi} \int_1^\infty \frac{dK}{K} [|R'_K(y)|^2 - K^2]\,, \quad \text{(B.4.2)}$$

and

$$F_-(y) = \frac{\lambda^2}{8\pi} \int_{\mu/\lambda}^1 \frac{dK}{K} [|R'_K(y)|^2 - K^2]\,. \quad \text{(B.4.3)}$$

B.4.1 Proof of $F_-(y) \xrightarrow{y\to 1} 0$

Using expression

$$R_K(y) = -e^{-iKy} + \frac{2}{B(y)} - \frac{2iK}{B(y)} \int_0^y dz B(z) e^{-iKz}$$

and its derivative, we rewrite the integrand of $F_-(y)$ as

$$\begin{aligned}\frac{1}{K}\Big(|R'_K(y)|^2 - K^2\Big) = &\frac{4}{KB^2(y)g^2(y)} + \frac{4K|\mathcal{F}_K(y)|^2}{g^2(y)} + \frac{4K\sin(Ky)}{B(y)g(y)} \\ &- \frac{2K[e^{iKy}\mathcal{F}_K(y) + c.c]}{g(y)} - \frac{4[i\mathcal{F}_K(y) + c.c]}{B(y)g^2(y)}\,,\end{aligned} \tag{B.4.4}$$

where $\mathcal{F}_K(y)$ is defined in equation (B.2.6).

The first and third term in eq.(B.4.4) vanish after finishing the K integral, taking $y \to 1$ and using the results in Appendix B.2.1. The second, the fourth and the last term also vanish, by first finishing the K integral and then using L'Hopital as $y \to 1$.

EXAMPLE: The second last term can be written as

$$-\frac{2K[e^{iKy}\mathcal{F}_K(y) + c.c]}{g(y)} = -\frac{4}{B(y)g(y)}\int_0^y dz B(z) K\cos K(y-z)\,. \tag{B.4.5}$$

We find out that it vanishes when $y \to 1$ by first finishing the K integral and then using l'Hopital .

B.4.2 Proof of $F_+(y) \xrightarrow{y\to 1} +\infty$

Notice that in $F_+(y)$, the K integral's upper bound is infinity. To finish the K integral, we need terms with enough powers of K in the denominators. After finishing the K integral, we analyze the behavior of each term separately.

We use an alternative expression of $R_K(y)$

$$R_K(y) = e^{-iKy} - \frac{2ie^{-iKy}}{Kg(y)} + \frac{2i}{KB(y)}\int_0^y dz e^{-iKz}B''(z) \tag{B.4.6}$$

to rearrange the integrand of $F_+(y)$ to the following expression

$$\begin{aligned}\frac{1}{K}\Big(|R'_K(y)|^2 - K^2\Big) = &\frac{4}{K^3g^4(y)} + \frac{4|V_K(y)|^2}{K^3g^2(y)} - \frac{4[e^{iKy}V_K(y) + c.c]}{K^3g^3(y)} \\ &+ \frac{4[ie^{iKy}V_K(y) + c.c]}{K^2g^2(y)} - \frac{2[ie^{iKy}W_K(y) + c.c]}{K^2g(y)}\,,\end{aligned} \tag{B.4.7}$$

where

$$V_K(y) = \frac{1}{B(y)}\int_0^y dz e^{-iKz}B''(z) \tag{B.4.8}$$

and

$$W_K(y) = \frac{1}{B(y)} \int_0^y dz e^{-iKz} B'''(z)\,. \tag{B.4.9}$$

First we need to finish the K integral. This step requires the use of Exponential Integral or Cosine Integral. Then we integrate by parts in z to remove all of the derivatives on $B(z)$, by which we mean to integrate by parts until $B''(z)$ and $B'''(z)$ in $V_K(y)$ and $W_K(y)$ are gone. This procedure will create a lot of terms, but each term is relatively easy to analyze and many cancel out.

We drop terms that approach constant as $y \to 1$ (for instance: term $\frac{\mathrm{Ci}(y)}{B(y)}|_{y\to 1} \to 0$), the results are listed below.

I. The first term of eq.(B.4.7) is $\frac{2}{g^4(y)}$.

II. The second term of eq.(B.4.7) is

$$\begin{aligned} &\int_1^\infty dK \frac{4|V_K(y)|^2}{K^3 g^2(y)} \\ \xrightarrow{y\to 1_-} &\frac{2}{g^4(y)} + \frac{8}{B^2(y) g^2(y)} \int_0^y dw B''(w) \int_0^w dz B(z)\,\mathrm{Ci}(w-z)\,, \end{aligned} \tag{B.4.10}$$

where we have integrated by part in the second $\int dz$ integral but have kept $\int dw B''(w)$. Function $\mathrm{Ci}(y)$ is the Cosine Integral.

We note that this term is formidable due to the double integral in $|V_K(y)|^2$. We change the integral limits from $\int_0^y dw \int_0^y dz$ to $\int_0^y dw \int_0^w dz$ and integrate the second integral $\int_0^w dz$ by part to get rid of the derivatives on $B''(z)$.

III. The third term of eq.(B.4.7) is

$$\begin{aligned} &-\frac{4[e^{iKy} V_K(y) + c.c]}{K^3 g^3(y)} \\ \xrightarrow{y\to 1_-} &-\frac{4}{g^3(y)} \left[\frac{1}{g(y)} + \frac{2}{B(y)} \int_0^y dz B(z)\,\mathrm{Ci}(y-z) \right]. \end{aligned} \tag{B.4.11}$$

IV. The fourth term of eq.(B.4.7) is

$$\begin{aligned} &\int_1^\infty dK \frac{4[ie^{iKy} V_K(y) + c.c]}{K^2 g^2(y)} \\ \xrightarrow{y\to 1_-} &\frac{4}{g^2(y)} \left[2\,\mathrm{Ci}(y) - \frac{2}{B(y)} \int_0^y dt \frac{B(y) - B(y-t)}{t} \cos t \right]. \end{aligned} \tag{B.4.12}$$

V. The last term of eq.(B.4.7).

We notice that this term differs from the second last term only by the coefficient and the triple derivatives on $B'''(z)$. We are confident that its form is similar to the fourth term above,

$$\begin{aligned} &-\int_1^\infty dK \frac{2[ie^{iKy}W_K(y)+c.c]}{K^2 g(y)} \\ \xrightarrow{y\to 1_-} &-\frac{2}{g(y)}\Big[\frac{2\,\mathrm{Ci}(y)}{g(y)} - \frac{2}{B(y)}\int_0^y dt \frac{B'(y)-B'(y-t)}{t}\cos t\Big]\,. \end{aligned} \tag{B.4.13}$$

Collecting all the terms, we find out

$$\begin{aligned} F_+(y) \xrightarrow{y\to 1_-} &\frac{4\,\mathrm{Ci}(y)}{g^2(y)} - \frac{8}{B(y)g^2(y)}\int_0^y dt \frac{B(y)-B(y-t)}{t}\cos t \\ &+ \frac{4}{B(y)g(y)}\int_0^y dt \frac{B'(y)-B'(y-t)}{t}\cos t - \frac{8}{B(y)g^3(y)}\int_0^y dz B(z)\,\mathrm{Ci}(y-z) \\ &+ \frac{8}{B^2(y)g^2(y)}\int_0^y dw B''(w)\int_0^w dz B(z)\,\mathrm{Ci}(w-z)\,. \end{aligned} \tag{B.4.14}$$

To further analyze the double integral, we switch to new variable $t = w - z$ and integrate by parts to reduce the derivatives on $B''(w)$. After we discard the terms that vanish as $y \to 1_-$, the double integral becomes

$$\begin{aligned} &\frac{8}{B^2(y)g^2(y)}\int_0^y dw B''(w)\Big[\int_0^w dt B(w-t)\,\mathrm{Ci}(t)\Big] \\ \to &\frac{8}{B(y)g^3(y)}\int_0^y dt B(z)\,\mathrm{Ci}(y-z) - \frac{4\,\mathrm{Ci}(y)}{g^2(y)} + \frac{4}{B^2(y)g^2(y)}\int_0^y dw \frac{B^2(w)-1}{w}\cos(w) \\ &+ \frac{8}{B^2(y)g^2(y)}\int_0^y dw B'(w)\int_0^w dt[B(w)-B(w-t)]\frac{\cos(t)}{t}\,, \end{aligned} \tag{B.4.15}$$

where the last term in eq.(B.4.15) can be further integrated by parts as

$$\begin{aligned}
&\frac{4}{B(y)g^2(y)}\int_0^y dt[B(y)-B(y-t)]\frac{\cos(t)}{t}\\
&+\frac{4}{B^2(y)g^2(y)}\int_0^y dwB'(w)\int_0^w dt[B(w)-B(w-t)]\frac{\cos(t)}{t}\\
&-\frac{4}{B^2(y)g^2(y)}\int_0^y dw\frac{B^2(w)-B(w)}{w}\cos(w)\\
&-\frac{4}{B^2(y)g^2(y)}\int_0^y dwB(w)\int_0^w dt[B'(w)-B'(w-t)]\frac{\cos(t)}{t}\,.
\end{aligned}\tag{B.4.16}$$

After cancellation and discarding vanishing terms using l'Hôpital, our terms become

$$\begin{aligned}
F_+(y)\xrightarrow{y\to 1_-}&-\frac{4}{B^2(y)(y)}\int_0^y dt\frac{B'(y)B(y)-B'(y)B(y-t)}{t}\cos t\\
&+\frac{4}{B^2(y)g(y)}\int_0^y dt\frac{B'(y)B(y)-B(y)B'(y-t)}{t}\cos t\\
&\frac{4}{B^2(y)g^2(y)}\int_0^y dw\int_0^w dt[B(w)B'(w-t)-B'(w)B(w-t)]\frac{\cos(t)}{t}\\
=&\frac{4}{B^2(y)g^2(y)}\Big[-B(y)J(y)+\int_0^y dwB'(w)J(w)\Big]\,,
\end{aligned}\tag{B.4.17}$$

where

$$J(w)=\int_0^w dtB'(w-t)[g(w)-g(w-t)]\frac{\cos(t)}{t}\,.\tag{B.4.18}$$

Taking L'Hopital of the final form of $F_+(y)$, we have

$$F_+(y)\xrightarrow{y\to 1_-}-\frac{J'(y)}{B(y)g(y)}\tag{B.4.19}$$

with

$$\begin{aligned}
J'(y)=&-\frac{\cos y}{y}+\int_0^\epsilon dt\cos(t)\Big[B''(y-t)\frac{g(y)-g(y-t)}{t}+B'(y-t)\frac{g'(y)-g'(y-t)}{t}\Big]\\
&+\int_\epsilon^y dt\cos(t)\frac{B'(y-t)}{g(y-t)}\Big[\frac{g(y)-g(y-t)}{t}+\frac{g'(y)g(y-t)-g(y)g'(y-t)}{t}\Big]\,.
\end{aligned}\tag{B.4.20}$$

By the assumptions of Appendix B.5, there are

$$\begin{aligned}
\text{For} \quad 0 \le t \le \epsilon : \; & \frac{g(y)-g(y-\epsilon)}{\epsilon} \le \frac{g(y)-g(y-t)}{t} \le g'(y) < 0 \\
& g''(y) \le \frac{g'(y)-g'(y-t)}{t} \le \frac{g'(y)-g'(y-\epsilon)}{\epsilon} \\
\text{For} \quad t \ge \epsilon : \; & \frac{g(y)-g(y-t)}{t} \le \frac{g(y)-g(y-\epsilon)}{\epsilon} < 0 \\
& \frac{g'(y)-g'(y-\epsilon)}{\epsilon} \le \frac{g'(y)-g'(y-t)}{t}
\end{aligned} \tag{B.4.21}$$

and $g'(y)/g(y) \xrightarrow{y \to 1_-} -\infty$. We find out $F_+(y) \to +\infty$ as $y \to 1_-$.

B.5 Conditions on $g(y)$

We introduce the technical assumption that $g'''(y) < 0$ for $0 < y < 1$. It follows that there are $g''(y) > 0$ and $g'(y) < 0$ for $0 < y < 1$ (this means that $h(y)$ must be monotonically decreasing for $0 < y < 1$). For $0 < z \le y < 1$, they imply

$$g'(z) \le \frac{g(y)-g(z)}{y-z} \le g'(y) < 0\,, \tag{B.5.1}$$

$$0 < g''(y) \le \frac{g'(y)-g'(z)}{y-z} \le g''(z)\,, \tag{B.5.2}$$

where the quotients are understood at $z = y$ in the limiting sense. Equation (B.5.1) can be verified by writing the numerator as the integral of g' and using the monotonicity of g', and eq.(B.5.2) can be verified similarly by writing the numerator as the integral of g''. We will derive two more results on two integrals in Appendix D.5 which are used in Appendix D.3.2 and D.3.3.

B.5.1 Implications

For $0 < y < 1$, using $\lim_{y \to 1_-} g(y) = 0$ and the monotonicity of g', we have

$$g(y) = -\int_y^1 g'(z)dz \le -g'(y)\int_y^1 dz = -(1-y)g'(y)\,. \tag{B.5.3}$$

Hence $g'(y)/g(y) \leq -1/(1-y)$, it implies

$$\lim_{y\to 1_-} \frac{g'(y)}{g(y)} \to -\infty\,. \tag{B.5.4}$$

This conclusion can be generalized. In fact, we can prove $g''(y)/g(y) \xrightarrow{y\to 1_-} +\infty$.

PROOF: We start with

$$g'(y) = -\int_y^1 g''(z)dz \geq -g''(y)\int_y^1 dz = -g''(y)(1-y) \tag{B.5.5}$$

which gives

$$g(y) \leq -(1-y)g'(y) \leq (1-y)^2 g''(y) \to \frac{g''(y)}{g(y)} \geq \frac{1}{(1-y)^2}\,. \tag{B.5.6}$$

If assuming $g^{(2k+1)}(y) < 0$ with $n \leq 2k+1$, we see the general pattern is

$$(-1)^n \frac{g^{(n)}(y)}{g(y)} \geq \frac{1}{(1-y)^n} \tag{B.5.7}$$

$$\Rightarrow \qquad \lim_{y\to 1_-} \frac{g^{(n)}(y)}{g(y)} \to (-1)^n \infty\,. \tag{B.5.8}$$

Appendix C

C.1 Mode function regularity across $r = t$

In this appendix we show that the function $B(y)$ of (5.2.14) is smooth at $y = 0$ and the function $R_K(y)$ of (5.2.17) is C^{25} at $y = 0$. This shows that the mode functions are C^{25} across $r = t$.

C.1.1 Smoothness of $B(y)$

We show that the function $B(y)$ of eq.(5.2.14) is smooth at $y = 0$.

From eq.(5.2.14) it is immediate that $B(y) \to 0$ as $y \to 0_+$. We show below in Proposition C.1.1 that $B^{(n)}(y) \to 0$ as $y \to 0_+$ for $n \in \mathbb{N} = \{1, 2, \ldots\}$. It follows by L'Hôpital and induction in n that all derivatives of $B(y)$ at $y = 0$ exist and vanish.

Proposition C.1.1. *For $n \in \mathbb{N}$, $B^{(n)}(y) \to 0$ as $y \to 0_+$.*

Proof. See [18]. Let $0 < y < 1$, and write $g(y) := \tan\big(h(y)\big)$, where h is defined in Section 5.2.1. Note that $g(y) > 0$, $g(y)$ and all its derivatives approach 0 as $y \to 0_+$, and from (5.2.14) we have

$$B(y) = \exp\left(-\int_y^1 \frac{dz}{g(z)}\right), \tag{C.1.1}$$

$$B'(y) = B(y)/g(y)\,. \tag{C.1.2}$$

For $n \in \mathbb{N}$, induction gives

$$B^{(n)}(y) = P_n(y) f_n(y)\,, \tag{C.1.3a}$$

$$f_n(y) = \frac{B(y)}{\big(g(y)\big)^n}\,, \tag{C.1.3b}$$

where each P_n is a polynomial in g and its derivatives. Since each P_n is bounded as $y \to 0_+$, it suffices to show that $f_n(y) \to 0$ as $y \to 0_+$ for $n \in \mathbb{N}$.

From (C.1.3b) we have

$$\ln\big(f_n(y)\big) = -\left(\int_y^1 \frac{dz}{g(z)}\right)\left(1 + \frac{n\ln\big(g(y)\big)}{\displaystyle\int_y^1 \frac{dz}{g(z)}}\right) . \tag{C.1.4}$$

As $y \to 0_+$, the first parentheses in (C.1.4) tend to ∞, while the second parentheses tend to 1 by L'Hôpital. Hence $\ln\big(f_n(y)\big) \to -\infty$ as $y \to 0_+$, by which $f_n(y) \to 0$ as $y \to 0_+$. □

C.1.2 Differentiability of $R_K(y)$

We shall show that the function $R_K(y)$ as in eq.(5.2.17) is C^{25} at $y = 0$.

We write equation (5.2.17) as

$$R_K(y) = \begin{cases} -e^{-iKy} & \text{for } y \le 0 \,, \\ -e^{-iKy} - 2iK\mathcal{F}_K(y) & \text{for } 0 < y < \infty \,, \end{cases} \tag{C.1.5}$$

where $K > 0$ and $\mathcal{F}_K$ is defined the same as in eq.(B.2.6)

$$\mathcal{F}_K(y) = \mathcal{J}_K(y)/B(y)\,, \tag{C.1.6a}$$

$$\mathcal{J}_K(y) = \int_0^y B(z)\, e^{-iKz}\, dz\,. \tag{C.1.6b}$$

We show below in Proposition C.1.3 that $\mathcal{F}_K^{(n)}(y) \to 0$ as $y \to 0_+$ for $n = 0, 1, 2, \ldots, 25$. This and (C.1.5) show that $R_K(y)$ is C^{25} at $y = 0$. For the purposes of Appendix C.2, we formulate Proposition C.1.3 for $\mathcal{F}_K$ that is defined by (C.1.6) not just for $K > 0$ but for $K \in \mathbb{R}$.

Lemma C.1.2. *For $K \in \mathbb{R}$, $0 < y < 1$ and $n \in \{1, 2, \ldots, 25\}$, we have*

$$\mathcal{F}_K^{(n)}(y) = \frac{h_{K,n}(y)}{B(y)\big(g(y)\big)^n}\,, \tag{C.1.7}$$

where g was defined above (C.1.1) *and $h_{K,n}$ satisfies*

$$h_{K,n}^{(k)}(y) = r_{K,n,k}(y)B(y) + s_{K,n,k}(y)\mathcal{J}_K(y) \quad \textit{for} \quad 0 \le k \le n\,, \tag{C.1.8}$$

where each $r_{K,n,k}$ and $s_{K,n,k}$ is a polynomial in g, its derivatives and e^{-iKy}, and $r_{K,n,n}(y) \to 0$ as $y \to 0_+$.

Proof. Starting from eq.(C.1.6) and using repeatedly eq.(C.1.2) and the identity

$$\mathcal{J}_K'(y) = e^{-iKy}\, B(y)\,, \tag{C.1.9}$$

we have verified the claim case by case for each n and k, with the help of algebraic computing [18]. □

Proposition C.1.3. *For $K \in \mathbb{R}$ and $n \in \{0, 1, 2, \ldots, 25\}$, $\mathcal{F}_K^{(n)}(y) \to 0$ as $y \to 0_+$.*

Proof. Consider $\mathcal{F}_K$. We use in (C.1.6a) L'Hôpital with (C.1.2) and (C.1.9), obtaining $\lim_{y\to 0_+} \mathcal{F}(y) = \lim_{y\to 0_+} \mathcal{J}'(y)/B'(y) = \lim_{y\to 0_+} e^{-iKy}\, g(y) = 0$.

Consider then the derivatives of S_K. From (C.1.2) we have

$$\frac{d}{dy}\big[B(y)\big(g(y)\big)^n\big] = B(y)\big(g(y)\big)^{n-1}\big(1 + ng'(y)\big)\,. \tag{C.1.10}$$

By Lemma C.1.2, we may hence evaluate $\lim_{y\to 0_+} \mathcal{F}_K^{(n)}(y)$ for $n \geq 1$ by applying L'Hôpital to (C.1.7) n times, using after the nth differentiation $\lim_{y\to 0_+} \mathcal{J}_K(y)/B(y) = \lim_{y\to 0_+} \mathcal{F}_K(y) = 0$. □

We stopped Lemma C.1.2 at $n = 25$ because of computing time limitations in the case-by-case proof [18]. If Lemma C.1.2 extends to $n \in \mathbb{N}$, the proof of Proposition C.1.3 generalises to $n \in \mathbb{N}$ and implies smoothness of $R_K(y)$ at $y = 0$.

C.2 $\langle T_{00} \rangle$ at intermediate times in 3+1 dimensions

In this appendix we verify the properties of $\langle T_{00} \rangle$ quoted in Section 5.3.2 in the intermediate time region, $r \leq t \leq r + \lambda^{-1}$.

C.2.1 Preliminaries

For $r < t < r+\lambda^{-1}$, the integrals in eq.(5.3.8) and in the first term of eq.(5.3.7) are convergent because (5.2.15) implies for fixed $y \in (0, 1)$ the small K estimates

$$R_K(y) = -1 + O(K)\,, \tag{C.2.1a}$$

$$|R_K'(y)|^2 = O\big(K^2\big)\,, \tag{C.2.1b}$$

and the large K estimates

$$R_K(y) = e^{-iKy}\left[1 + 2\frac{B'(y)}{B(y)}\frac{1}{iK} + O\big(K^{-2}\big)\right], \tag{C.2.2a}$$

$$|R_K(y)|^2 = 1 + O\big(K^{-2}\big), \tag{C.2.2b}$$

$$|R'_K(y)|^2 = K^2 + O\big(K^{-2}\big). \tag{C.2.2c}$$

For $t = r$, the integrands in eq.(5.3.8) and in the first term of eq.(5.3.7) vanish.

For $t = r+\lambda^{-1}$, the integrand in eq.(5.3.7) vanishes, while eq.(5.3.8) is given by eq.(5.3.10) with $t = r + \lambda^{-1}$, and all the steps from eq.(5.3.10) to eq.(5.3.12) still hold with $t = r + \lambda^{-1}$.

Collecting, we see that $\mathcal{G}_\lambda(t, r)$ of eq.(5.3.8) and the first term of eq.(5.3.7) are well defined everywhere in $r \le t \le r + \lambda^{-1}$.

What remains is to examine the existence and continuity of $\partial_r\mathcal{G}_\lambda(t, r)$, and the continuity of the first term in (5.3.7). We address each in turn.

C.2.2 $\partial_r\mathcal{G}_\lambda(t, r)$

We show first that $\partial_r\mathcal{G}_\lambda(t, r)$ exists and is continuous in r for $0 < r < t$, for each positive t. We then assume that $g'''(y) \ge 0$ for sufficiently small positive y, and show that $\partial_r\mathcal{G}_\lambda(t, r) \to 0$ as $r \to t_-$. This establishes that the second term of (5.3.7) exists and is continuous in r.

We introduce dimensionless variables by $\lambda t = \sigma > 0$ and $\lambda r = \sigma - y$, where $0 < y < \sigma$. The quantity of interest is then $\mathcal{G}_\lambda\big(\sigma/\lambda, (\sigma - y)/\lambda\big) = F_-(y) + F_+(y)$, where

$$F_-(y) = \int_0^1 \frac{dK}{K}\Big[\big|R_K(y)\big|^2 + 2\cos\big(2K(\sigma - y)\big) - 1 + R_K(y)e^{iK(2\sigma-y)} + \overline{R_K(y)}e^{-iK(2\sigma-y)}\Big], \tag{C.2.3a}$$

$$F_+(y) = \int_1^\infty \frac{dK}{K}\Big[\big|R_K(y)\big|^2 + 2\cos\big(2K(\sigma - y)\big) - 1 + R_K(y)e^{iK(2\sigma-y)} + \overline{R_K(y)}e^{-iK(2\sigma-y)}\Big], \tag{C.2.3b}$$

and the notation suppresses the dependence of $F_\pm$ on σ.

In F_-, we use eq.(C.1.5) and derive

$$F_-(y) = 2\int_0^1 dK\Big[i\left(e^{iKy} - e^{iK(2\sigma-y)}\right)S_K(y) - i\left(e^{-iKy} - e^{-iK(2\sigma-y)}\right)\overline{S_K(y)} + 2\big|S_K(y)\big|^2\Big]\,. \tag{C.2.4}$$

Straightforward convergence estimates show that $F_-(y)$ is C^1 for $y > 0$, and estimates using Proposition C.1.3 show that $F'_-(y) \to 0$ as $y \to 0$.

In F_+, we use the identity

$$R_K(y) = e^{-iKy} - \frac{2i}{K}\left[\frac{B'(y)}{B(y)}e^{-iKy} - V_K(y)\right]\,, \tag{C.2.5}$$

where

$$V_K(y) = \frac{1}{B(y)}\int_0^y B''(z)\,e^{-iKz}\,dz\,, \tag{C.2.6}$$

obtained by integrating eq.(5.2.15) by parts. This gives

$$\begin{aligned} F_+(y) = 2\int_1^\infty dK\Bigg\{ &\frac{2}{K^3}\left(\frac{B'(y)}{B(y)}\right)^2 + \frac{2}{K}\cos\big(2K(\sigma-y)\big) + \frac{2}{K^2}\frac{B'(y)}{B(y)}\sin\big(2K(\sigma-y)\big) \\ &+ \left[-\frac{2}{K^3}\frac{B'(y)}{B(y)}e^{iKy} + \frac{i}{K^2}e^{iKy} + \frac{i}{K^2}e^{iK(2\sigma-y)}\right]V_K(y) \\ &+ \left[-\frac{2}{K^3}\frac{B'(y)}{B(y)}e^{-iKy} - \frac{i}{K^2}e^{-iKy} - \frac{i}{K^2}e^{-iK(2\sigma-y)}\right]\overline{V_K(y)} \\ &+ \frac{2}{K^3}\big|V_K(y)\big|^2\Bigg\}\,, \end{aligned} \tag{C.2.7}$$

from which straightforward estimates show that $F_+(y)$ is C^1 for $y > 0$.

To examine $F_+(y)$ and $F'_+(y)$ as $y \to 0$, we evaluate the integral over K in eq.(C.2.7). In the terms that do not involve V_K, the integral over K produces elementary functions and the cosine integral Ci [56]. In the terms that involve V_K, we use eq.(C.2.6), we interchange the integrations as justified by the absolute convergence of the multiple integral, and we evaluate first the integral over K in terms of elementary functions and the exponential integral E_1 [56]. Among the terms that ensue, several have B' or B'' under an integral; however, integration

by parts reduces most of these terms to combinations that involve $S_1(y)$ and $T_1(y)$, where

$$T_K(y) = \frac{1}{B(y)} \int_0^y B(z)\, z\, e^{-iKz}\, dz\,, \tag{C.2.8}$$

and the small y behaviour of these terms and their derivatives can be analysed by Proposition C.1.3 and its generalisations. We find that F_+ decomposes as $F_+(y) = F_{+1}(y) + F_{+2}(y)$, where we omit the lengthy expression for $F_{+1}(y)$ but just note that it satisfies $F_{+1}(y) \to 0$ and $F'_{+1}(y) \to 0$ as $y \to 0$, while the expression for $F_{+2}(y)$ for $y < 1$ reads

$$F_{+2}(y) = \frac{4}{B^2(y)} \int_0^y dz\, B'(z) \int_0^z dt \cos t\, B'(z-t)\, \frac{g(z) - g(z-t)}{t}\,. \tag{C.2.9}$$

To control $F_{+2}(y)$, we introduce the additional technical assumption that $g'''(y) \geq 0$ for sufficiently small positive y. For sufficiently small positive y, an elementary analysis then gives for $t \in [0, y]$ the inequalities

$$\frac{g'(y)}{y} \leq \frac{g'(y) - g'(y-t)}{t} \leq g''(y)\,, \tag{C.2.10a}$$

$$\frac{g(y)}{y} \leq \frac{g(y) - g(y-t)}{t} \leq g'(y)\,, \tag{C.2.10b}$$

understood at $t = 0$ in the limiting sense. From now on we assume $y < 1$ and so small that eq.(C.2.10) hold.

Consider now $F_{+2}(y)$. Applying L'Hôpital in eq.(C.2.9) and using eq.(C.2.10b), we find that $F_{+2}(y) \to 0$ as $y \to 0$.

Consider then $F'_{+2}(y)$. Differentiating eq.(C.2.9) gives

$$F'_{+2}(y) = \frac{4}{g(y)B^2(y)} \Bigg[B(y) \int_0^y dt \cos t\, B'(y-t)\, \frac{g(y) - g(y-t)}{t} - 2 \int_0^y dz\, B'(z) \int_0^z dt \cos t\, B'(z-t)\, \frac{g(z) - g(z-t)}{t} \Bigg]. \tag{C.2.11}$$

For the limit of $F'_{+2}(y)$ as $y \to 0$, L'Hôpital shows that it suffices to consider

$$\frac{2}{g(y)B(y)} \int_0^y dt \cos t \Bigg[-B'(y-t) \frac{g(y)-g(y-t)}{t} + g(y)B''(y-t) \frac{g(y)-g(y-t)}{t} + g(y)B'(y-t) \frac{g'(y)-g'(y-t)}{t} \Bigg]. \tag{C.2.12}$$

The last term of eq.(C.2.12) can be controlled by eq.(C.2.10a). The combination of the first two terms can be controlled by taking y to be so small that $g' < 1$, writing $B' = gB''/(1-g')$, and using eq.(C.2.10b) and the monotonicity of g'. We find that $F'_{+2}(y) \to 0$ as $y \to 0$.

Combining these results shows that $\partial_r \mathcal{G}_\lambda(t,r)$ is continuous in r for $0 < r \leq t$. This establishes that the second term in eq.(5.3.7) exists at each point and is continuous in r.

C.2.3 First term of eq.(5.3.7)

To analyse the first term of eq.(5.3.7), it suffices to consider $\tilde{F}(y) = \tilde{F}_-(y) + \tilde{F}_+(y)$, where $y > 0$ and

$$\tilde{F}_-(y) = \int_0^1 \frac{dK}{K} \left[\left| R'_K(y) \right|^2 - K^2 \right], \tag{C.2.13}$$

$$\tilde{F}_+(y) = \int_1^\infty \frac{dK}{K} \left[\left| R'_K(y) \right|^2 - K^2 \right]. \tag{C.2.14}$$

We show first that $\tilde{F}(y)$ is continuous for $y > 0$. We then assume that $g'''(y) \geq 0$ for sufficiently small positive y, and show that $\tilde{F}(y) \to -\infty$ as $y \to 0$, faster than any negative multiple of $1/g(y)$.

In $\tilde{F}_-$, we use eq.(C.1.5) and proceed as with F_- eq.(C.2.3a). We find that $\tilde{F}_-(y)$ is continuous for $y > 0$ and $\tilde{F}_-(y) \to 0$ as $y \to 0$.

In $\tilde{F}_+$, we start as with F_+ eq.(C.2.3b), finding

$$\tilde{F}_+(y) = 2\int_1^\infty dK \Bigg\{ \frac{2}{K^3}\left(\frac{B'(y)}{B(y)}\right)^4 + \frac{2}{K^3}\left(\frac{B'(y)}{B(y)}\right)^2 \left|V_K(y)\right|^2 - \frac{2}{K^3}\left(\frac{B'(y)}{B(y)}\right)^3 \left[e^{iKy}\, V_K(y) + e^{-iKy}\,\overline{V_K(y)}\right] + \frac{2i}{K^2}\left(\frac{B'(y)}{B(y)}\right)^2 \left[e^{iKy}\, V_K(y) - e^{-iKy}\,\overline{V_K(y)}\right] - \frac{i}{K^2}\frac{B'(y)}{B(y)}\left[e^{iKy}\, W_K(y) - e^{-iKy}\,\overline{W_K(y)}\right] \Bigg\}, \tag{C.2.15}$$

where V_K is given by eq.(C.2.6) and

$$W_K(y) = \frac{1}{B(y)}\int_0^y B'''(z)\, e^{-iKz}\, dz\,. \tag{C.2.16}$$

This shows that $\tilde{F}_+(y)$ is continuous for $y > 1$.

Proceeding as with (C.2.7), and assuming $y < 1$, we find $\tilde{F}_+(y) = \tilde{F}_{+1}(y) + \tilde{F}_{+2}(y)$, where we omit the lengthy expression for $\tilde{F}_{+1}(y)$ but just note that it satisfies $\tilde{F}_{+1}(y) \to 0$ as $y \to 0$, and

$$\tilde{F}_{+2}(y) = \frac{4}{g^2(y)B^2(y)}\left[\int_0^y dz\, B'(z)J(z) \;- B(y)J(y)\right], \tag{C.2.17}$$

where

$$J(y) = \int_0^y dt \cos t\, B'(y-t)\,\frac{g(y) - g(y-t)}{t}\,. \tag{C.2.18}$$

No assumptions about the sign of $g'''(y)$ have been made yet. We now assume that $g'''(y) \geq 0$ for sufficiently small positive y, and we take y to be so small that eq.(C.2.10) hold, $\cos y \geq 1/2$, and $g' \leq 1/2$, the last of which implies $B'' > 0$. Differentiating eq.(C.2.18) and using eq.(C.2.10), we then have $J'(y) \geq \frac{1}{2}B(y)/y$. Using eq.(C.2.17), and noting that the square brackets therein have the derivative $-B(y)J'(y)$, L'Hôpital hence shows that $g(y)\tilde{F}_{+2}(y) \to -\infty$ as $y \to 0$.

Collecting, these observations show that $\tilde{F}(y)$ is continuous for $y > 0$, but $\tilde{F}(y) \to -\infty$ as $y \to 0$, faster than any negative multiple of $1/g(y)$.

C.3 Some useful integrals

In this appendix we collect results about integrals that appear in Section 5.4 and Appendix C.2. We recall that C_K (5.2.16) is smooth in K, it falls off at large K faster than any inverse power of K, and $C_0 = 1$.

Proposition C.3.1. *For $\alpha, \beta > 0$, we have*

$$\int_0^\infty \frac{dK}{K} \left(e^{i\alpha K} - e^{i\beta K}\right) = \ln(\beta/\alpha)\,, \tag{C.3.1a}$$

$$\int_0^\infty \frac{dK}{K} \left(e^{i\alpha K} - e^{-i\beta K}\right) = \ln(\beta/\alpha) + i\pi\,, \tag{C.3.1b}$$

$$\int_0^\infty \frac{dK}{K} \Big[|C_K|^2 - \cos(\alpha K)\Big] = \ln\alpha + k_1\,, \tag{C.3.1c}$$

where the integrals are improper Riemann integrals,

$$k_1 = \gamma + \int_0^1 \frac{dK}{K}\big(|C_K|^2 - 1\big) + \int_1^\infty \frac{dK}{K}\,|C_K|^2 \tag{C.3.2}$$

and γ is Euler's constant.

Proof. In eq.(C.3.1a) and eq.(C.3.1b), we insert a low K cutoff, express the integral of each term in terms of the exponential integral E_1 [56], and use small argument form of E_1 to remove the cutoff.

In eq.(C.3.1c), we break the integral into the subintervals $0 < K < 1$ and $1 < K < \infty$, express the contributions from the subintervals in terms of the cosine integrals Cin and Ci [56], and use the cosine integral identities [56]. Note that k_1 is finite because of the small and large K properties of C_K. □

Proposition C.3.2. *For $\alpha > 0$, let*

$$H(\alpha) := \int_0^\infty \frac{dK}{K}(1 - C_K)\, e^{i\alpha K}\,, \tag{C.3.3}$$

where the integral is an improper Riemann integral. Then

$$H(\alpha) = \begin{cases} -\displaystyle\int_0^1 dz\, \frac{B(\alpha) - B(z)}{\alpha - z} + \big(1 - B(\alpha)\big)\big(\ln(\alpha^{-1} - 1) + i\pi\big) & \text{for } 0 < \alpha < 1; \\ -\displaystyle\int_0^1 dz\, \frac{B(\alpha) - B(z)}{\alpha - z} & \text{for } \alpha \geq 1. \end{cases} \tag{C.3.4}$$

It follows that H is C^∞, $H(\alpha)$ is real for $\alpha \geq 1$, and $H(\alpha)$ for $\alpha > 1$ has the absolutely convergent series representation

$$H(\alpha) = -\sum_{p=0}^{\infty} \frac{1}{\alpha^{p+1}} \int_0^1 dz\, z^p \big(1 - B(z)\big)\,. \tag{C.3.5}$$

Proof. Consider first $\operatorname{Im} H(\alpha)$. Taking the imaginary part of (C.3.3) under the integral, recalling that $\int_0^\infty dK \sin(\alpha K)/K = \pi/2$ (since $\alpha > 0$ by assumption), and introducing a large K cutoff $M > 0$, we have

$$\operatorname{Im} H(\alpha) = \frac{\pi}{2} + \lim_{M\to\infty} I(M, \alpha)\,, \tag{C.3.6}$$

where

$$\begin{aligned} I(M,\alpha) &:= -\int_0^M \frac{dK}{K} \int_0^1 dz\, B'(z) \sin\big((\alpha - z)K\big) \\ &= -\int_0^1 dz\, B'(z) \int_0^M \frac{dK}{K} \sin\big((\alpha - z)K\big) \\ &= -\int_0^1 dz\, B'(z)\, \operatorname{Si}\big((\alpha - z)M\big) \\ &= -\operatorname{Si}\big((\alpha - 1)M\big) - \int_0^1 dz\, B(z)\, \frac{\sin\big((\alpha - z)M\big)}{\alpha - z} \\ &= -\operatorname{Si}\big((\alpha - 1)M\big) - B(\alpha) \int_0^1 dz\, \frac{\sin\big((\alpha - z)M\big)}{\alpha - z} \\ &\quad + \int_0^1 dz\, \frac{B(\alpha) - B(z)}{\alpha - z} \sin\big((\alpha - z)M\big) \\ &= \big(B(\alpha) - 1\big) \operatorname{Si}\big((\alpha - 1)M\big) - B(\alpha) \operatorname{Si}(\alpha M) \\ &\quad + \int_0^1 dz\, \frac{B(\alpha) - B(z)}{\alpha - z} \sin\big((\alpha - z)M\big)\,. \end{aligned} \tag{C.3.7}$$

The first equality in (C.3.7) is a definition, the second equality comes by interchanging the integrals, justified by the absolute convergence of the double integral, and the third equality uses the definition of the sine integral function Si [56]. The fourth equality comes from integration by parts, the fifth equality by decomposing the integrand, and the sixth equality by using again the definition of Si. In the last expression in (C.3.7), the integral term vanishes as $M \to \infty$ by the Riemann-Lebesgue lemma, and since $\mathrm{Si}(x) \to \pm\pi/2$ as $x \to \pm\infty$ [56], the other two terms show that $I(M, \alpha) \to -\pi B(\alpha) + \pi/2$ as $M \to \infty$. From this and (C.3.6) we obtain the imaginary part of (C.3.4).

Consider then $\operatorname{Re} H(\alpha)$. Taking the real part of (C.3.3) under the integral, we introduce both a large K cutoff and a small K cutoff and proceed as above, using now the cosine integrals Cin and Ci [56]. Removing the cutoffs with the help of the cosine integral identities [56] gives the real part of (C.3.4).

The smoothness of H and the reality of $H(\alpha)$ for $\alpha \geq 1$ are immediate from (C.3.4). The series (C.3.5) follows from (C.3.4) by writing $(\alpha - z)^{-1} = \alpha^{-1}\big(1 - (z/\alpha)\big)^{-1}$ and using the geometric series. □

Appendix D

D.1 Lemma

We start with a lemma.

Lemma D.1.1.

(i) For a complex-valued function $f(y,z)$ that is bounded for $y \in [0,1]$ and $z \in [0,1+A]$, we have

$$\lim_{y+A\to 1_-} \frac{1}{B(y+A)} \int_0^{y+A} B(z) f(y,z)\, dz = 0\,. \tag{D.1.1}$$

(ii) If in addition $\partial_y f(y,z)$ is bounded for $y \in [0,1]$ and $z \in [0,1+A]$, we have

$$\lim_{y+A\to 1_-} \partial_y \left(\frac{1}{B(y+A)} \int_0^{y+A} B(z) f(y,z)\, dz \right) = 0\,. \tag{D.1.2}$$

(iii) If in addition $\partial_y^n f(y,z)$ is bounded for $n \in \mathbb{Z}^+$, $y \in [0,1]$ and $z \in [0,1+A]$, we have

$$\lim_{y+A\to 1_-} \partial_y^n \left(\frac{1}{B(y+A)} \int_0^{y+A} B(z) f(y,z)\, dz \right) = 0\,. \tag{D.1.3}$$

Proof.

(i) The boundedness of f means there is a positive constant C such that $|f(y,z)| \le C$. For $0 < y + A < 1$, we then have

$$\left| \frac{1}{B(y+A)} \int_0^{y+A} B(z) f(y,z)\, dz \right| \le \frac{C}{B(y+A)} \int_0^{y+A} B(z)\, dz\,, \tag{D.1.4}$$

using the triangle inequality and the positivity of B. When $y + A \to 1$, the rightmost expression in eq.(D.1.4) goes to zero, using l'Hôpital and eq.(C.1.1).

(ii) For $0 < y + A < 1$, expanding out the derivative in eq.(D.1.2) and using eq.(C.1.1) gives

$$f(y, y+A) - \frac{1}{g(y+A)B(y+A)} \int_0^{y+A} B(z) f(y,z)\, dz + \frac{1}{B(y+A)} \int_0^{y+A} B(z)\, \partial_y f(y,z)\, dz\,. \tag{D.1.5}$$

The last term in eq.(D.1.5) goes to zero when $y + A \to 1$, applying part (i). In the second term in eq.(D.1.5), we observe that $g(y + A)B(y + A) \to \infty$ as $y + A \to 1$, by the property of $1/B$ being smooth. Applying l'Hôpital as $y + A \to 1$ and using eq.(C.1.1) gives two terms, one of which cancels the first term in eq.(D.1.5), while the other gives zero applying part (i).

(iii) Statement (iii) is a generalization of statement (ii).

This lemma can also be understood from the intuitive observation

$$\left| \frac{1}{B(y+A)} \int_0^{y+A} B(z) f(y,z)\, dz \right| \sim \frac{C}{B(y+A)} \int_0^{y+A} B(z) \xrightarrow{y+A \to 1_-} g(y+A)\,, \tag{D.1.6}$$

and the fact that $g^{(n)}(y + A) \to 0$ when $y + A \to 1_-$.

D.2 Differentiability of $R_K(y)$

We introduce the definitions

$$\mathcal{J}_K(y) = \int_0^y B(z)\, e^{-iKz}\, dz \tag{D.2.1}$$

$$\mathcal{F}_K(y) = \mathcal{J}_K(y)/B(y) \tag{D.2.2}$$

$$\mathcal{H}_K(y) = \mathcal{J}_K(y)/\left(g(y)\, B(y)\right)\,. \tag{D.2.3}$$

Using Lemma D.1.1 we have that $\lim_{y\to 1_-} \mathcal{F}_K(y) = 0$, and L'Hôpital gives $\lim_{y\to 1_-} \mathcal{H}_K(y) = e^{-iK}$. We rewrite the mode function in eq.(6.2.15) as

$$R_K(y) = -e^{-iK(2A+y)} - \frac{2i\sin(AK)}{B} - 2K\sin(AK)\mathcal{F}_K(y+A)\,. \tag{D.2.4a}$$

We can show that $R_K(y)$ is smooth at $y + A \to 1_-$ by showing that $\mathcal{F}_K(y)$ is smooth as $y \to 1_-$, exactly the same as was done in Appendix B.2.2.

D.3 $\langle T_{00}\rangle$ in the intermediate region, outside the shell

In this section we study the behaviour of the energy density outside the shell ($r > a$) in the intermediate region ($-A \le y \le 1-A$), which is given in eq.(6.3.3) with the function $\mathcal{G}_{\rm out}$ defined in eq.(6.3.4), and $R_K(y)$ given in the middle line of eq.(6.2.13). We rewrite these expressions as

$$\langle T_{00}\rangle = \frac{\lambda^2}{16\pi^2 r^2}\big[F(y)+\tilde F(y)\big] \tag{D.3.1}$$

$$F(y) = \int_0^\infty \frac{dK}{K}\,\left[|R_K'(y)|^2 - K^2\right] \tag{D.3.2}$$

$$\tilde F(y) = -\frac{1}{w-y}\left[\partial_w - \partial_y - \frac{2}{w-y}\right]\mathcal{G}_{\rm out} \tag{D.3.3}$$

$$\text{with}\qquad \mathcal{G}_{\rm out} = \int_0^\infty \frac{dK}{K}\Big[|e^{-iKw}+R_K(y)|^2 - |e^{-iKw}-e^{-iKy}|^2\Big]\,,$$

where the notation suppresses the dependence of $F(y)$ and $\tilde F(y)$ on w. We comment that the denominators in eq.(D.3.3) are produced by the factor $1/r$ in equation eq.(6.3.3), and the action of the derivative ∂_r on this factor.

D.3.1 Preliminaries

From eq.(6.2.15) we have for fixed $y \in (-A, 1-A)$ at the small K limit estimates

$$R_K(y) = -1 + O(K)\,, \tag{D.3.4}$$

$$|R_K'(y)|^2 = O(K^2)\,, \tag{D.3.5}$$

and at large K limit estimates

$$R_K(y) = -e^{-iKy}\Big[1 + 2\frac{B'}{B}\frac{e^{-iKA}\sin(AK)}{K} + O(K^{-2})\Big]\,, \tag{D.3.6}$$

$$|R_K(y)|^2 = 1 + \frac{2B'}{B}\frac{\sin(2AK)}{K} + O(K^{-2})\,, \tag{D.3.7}$$

$$|R_K'(y)|^2 = K^2 + \frac{2B'}{B}K\sin(2AK) + O(K^{-1})\,. \tag{D.3.8}$$

Using these results it is straightforward to show that the integrals in equations eq.(D.3.2) and eq.(D.3.3) are well defined for $y \in (-A, 1-A)$. The integral over large K has terms of

the form $\int_1^\infty dK \sin(2AK)$ which can be regularized with a factor $e^{-\delta K}$ so that we obtain a finite result in the limit $\delta \to 0$.

At $y = -A$ both integrands vanish. At $y = 1 - A$ the integrand in eq.(D.3.2) vanishes, and a straightforward calculation gives

$$\mathcal{G}_{\rm out}\big|_{y=1-A} = 2\big[\ln(r-a) - \ln r\big] \tag{D.3.9}$$

in agreement with eq.(6.3.7). The conclusion is that equations (D.3.1, D.3.2, D.3.3) agree with eq.(6.3.8) at $y = -A$ and $y = 1 - A$. In the remainder of this appendix we study the continuity of $F(y)$ and $\tilde{F}(y)$ in equations (D.3.2) and (D.3.3) as $y + A \to 1_-$.

D.3.2 The term $F(y)$

We divide the integral in eq.(D.3.2) into two pieces defined as

$$F_-(y) = \int_0^1 \frac{dK}{K}\left[|R'_K|^2 - K^2\right], \tag{D.3.10}$$

$$F_+(y) = \int_1^\infty \frac{dK}{K}\left[|R'_K|^2 - K^2\right]. \tag{D.3.11}$$

To show that $F_-(y)$ is finite, we use the form of $R_K(y)$ in eq.(6.2.15). After differentiating and substituting into (D.3.10),

$$\begin{aligned} F_-^{\rm out}(y) = \int_0^1 dK \Big[& -4if_1 \sin^2(AK)(\mathcal{H}_K - \bar{\mathcal{H}}_K) \\ & +4f_1 \sin(AK)\cos(Ky) + 4K\mathcal{H}_K\bar{\mathcal{H}}_K \sin^2(AK) \\ & -2iK\sin(AK)\left(e^{iKy}\mathcal{H}_K - e^{-iKy}\bar{\mathcal{H}}_K\right) + \frac{4f_2\sin^2(AK)}{KB}\Big] \end{aligned} \tag{D.3.12}$$

where $\mathcal{H}_K$ is defined in Eq.(D.2.3) and the quantities $f_i := f_i(y + A)$ are defined in equation (C.1.3b). It is straightforward to show that $\lim_{y+A\to 1_-} F_-(y)$ exists and is finite.

Now we study the second term $F_+(y)$. Our strategy is as follows:

1. Integrate by parts in z, taking the anti-derivative of the factor $e^{\pm iKz}$, until we have enough powers of $1/K$ so that the K-integral is convergent.

2. Switch the order of the z and K integrals and do the K integral.

3. Integrate by parts again so that derivatives are removed from factors $B(z)$.

4. Analyse the behaviour of the remaining integrals.

The result of step (1) is

$$\begin{aligned} F_+(y) = \quad & \int_1^\infty dK \left[\frac{4V_K \overline{V_K} \sin^2(AK)}{K^3 g^2} - \frac{4\sin^2(AK)\left(V_K e^{iK(A+y)} + \overline{V_K} e^{-iK(A+y)}\right)}{K^3 g^3} \right. \\ & + \frac{4i\sin^2(AK)\left(V_K e^{iK(A+y)} - \overline{V_K} e^{-iK(A+y)}\right)}{K^2 g^2} \\ & + \frac{2i\sin(AK)\left(V_K e^{iKy} - \overline{V_K} e^{-iKy}\right)}{Kg} \\ & \left. + \frac{4\sin^2(AK)}{K^3 g^4} + \frac{2\sin(2AK)}{g} \right], \end{aligned} \tag{D.3.13}$$

where we have defined

$$V_K = \frac{1}{B} \int_0^{y+A} dz\, B''(z) e^{-iKz}\,. \tag{D.3.14}$$

The K integral in the 6th term of eq.(D.3.13) can be regulated with a factor $e^{-\delta K}$ so that we obtain a finite result in the limit $\delta \to 0$. We rewrite the first term in eq.(D.3.13) by substituting eq.(D.3.14) and using the following property

$$\begin{aligned} & \int_0^{y+A} dx \int_0^{y+A} dz\, \mathrm{fcn}(z,x) = \left[\int_0^{y+A} dx \int_0^x dz + \int_0^{y+A} dz \int_0^z dx \right] \mathrm{fcn}(z,x) \\ & = 2\int_0^{y+A} dx \int_0^x dz\, \mathrm{Re}\,\mathrm{fcn}(z,x)\,, \end{aligned} \tag{D.3.15}$$

where $\mathrm{fcn}(z,x)$ is any complex function that satisfies $\mathrm{fcn}(z,x) = \overline{\mathrm{fcn}(x,z)}$ for real x and z.

Potential singularities in the x and z integrations will be controlled by adding the regulator $-\epsilon$ to the upper limit. This justifies interchanging the order of integration. We will show that the ϵ regulator cancels when all terms are combined. We begin by performing the K integrations, and then rearranging the resulting integrand by doing several integrations by parts and identifing combinations of terms that cancel exactly.

Switching the order of integration, the K integrals can be done using integration by parts and Exponential Integral, for example:

$$\int_1^\infty \frac{dK}{K^3}\left(e^{iK\alpha} + e^{-iK\alpha}\right) = \cos(\alpha) - \alpha\sin(\alpha) + \alpha^2 \mathrm{Ci}(\alpha) \tag{D.3.16}$$

where $\alpha > 0$ and Ci and Si are the cosine and sine integrals.

We introduce the parameters $\alpha := A + y - z$, $\beta := A - y + z$, $\gamma := 3A + y - z$, which will be used in 2nd, 3rd and 4th terms of (D.3.13) for which we have $z \in (0, y + A)$; and $\rho := 2A - x + z$, $\sigma := 2A + x - z$ and $\tau := x - z$ for the 1st term of (D.3.13) where $x \in (0, y + A)$ and $z \in (0, x)$. Using our original assumption $A > 1$ these parameters are all positive over the full range of the corresponding integrals. Doing the K integrals we obtain:

$$F_+(y) = \lim_{\epsilon \to 0} \left[T_1 + T_2 + T_3 + T_4 + T_5 \right] \tag{D.3.17}$$

$$\begin{aligned} T_1 = & \frac{2}{B^2 g^2} \int_\epsilon^{y+A} dx\, B''(x) \int_0^{x-\epsilon} dz\; B''(z)\, h_1(\tau) \\ & - \frac{1}{B^2 g^2} \int_0^{y+A} dx\, B''(x) \int_0^{x} dz\; B''(z)\, (h_1(\rho) + h_1(\sigma)) \end{aligned} \tag{D.3.18}$$

$$T_2 = -\frac{2}{Bg^3} \int_0^{y+A-\epsilon} dz\, B''(z) h_1(\alpha) + \frac{1}{Bg^3} \int_0^{y+A} dz\, B''(z)\, (h_1(\beta) + h_1(\gamma)) \tag{D.3.19}$$

$$T_3 = \frac{4}{Bg^2} \int_0^{y+A-\epsilon} dz\, B''(z) h_2(\alpha) + \frac{2}{Bg^2} \int_0^{y+A} dz\, B''(z)\, (h_2(\beta) - h_2(\gamma)) \tag{D.3.20}$$

$$T_4 = -\frac{2}{Bg} \int_0^{y+A-\epsilon} dz\, B''(z)\, \mathrm{Ci}(\alpha) + \frac{2}{Bg} \int_0^{y+A} dz\, B''(z)\, \mathrm{Ci}(\beta) \tag{D.3.21}$$

$$T_5 = \frac{2}{g^4} \left(A(\sin(2A) - 2A\mathrm{Ci}(2A)) + \sin^2(A) \right) , \tag{D.3.22}$$

where we have defined

$$\begin{aligned} h_1(\alpha) &= -\alpha \sin(\alpha) + \cos(\alpha) + \alpha^2 \mathrm{Ci}(\alpha) \\ h_2(\alpha) &= \alpha \mathrm{Ci}(\alpha) - \sin(\alpha)\,. \end{aligned} \tag{D.3.23}$$

Equations (D.3.17 - D.3.22) give the result of the second step of our strategy.

We rewrite the result above for T_1 by integrating by parts in x, which produces two surface terms that exactly cancel T_2 and T_5. The remaining double integral can be rewritten by integrating by parts in z, and we are left with the double integral

$$\begin{aligned} I_{\mathrm{doub}} &= -\frac{4}{B^2 g^2} \int_\epsilon^{y+A} dx\, B'(x) \int_0^{x-\epsilon} dz\, B'(z)\;\; \mathrm{Ci}(\tau) \\ &+ \frac{2}{B^2 g^2} \int_0^{y+A} dx\, B'(x) \int_0^{x} dz\, B'(z) \left[\mathrm{Ci}(\rho) + \mathrm{Ci}(\sigma) \right] . \end{aligned} \tag{D.3.24}$$

Combining the surviving terms we arrive at

$$F_+(y) = \lim_{\epsilon\to 0}\left[\tilde{T}_3 + T_4 + I_{\text{doub}}\right], \tag{D.3.25}$$

where $\tilde{T}_3$ is T_3 through integrating by parts in z.

We show below that $\lim_{y+A\to 1_-}[gF_+(y)] \to \infty$ and therefore $\lim_{y+A\to 1_-} F_+(y) \to \infty$.

We consider the integrals that do not contain factors $\text{Ci}(\alpha)$ or $\text{Ci}(\tau)$. These terms and their derivatives are all bounded within the range of integration and we can easily use Lemma D.1.1 on them. We therefore call their sum I_{easy}. Using l'Hôpital's and integrating by parts to remove all derivatives on B, Lemma D.1.1 gives us $\lim_{y+A\to 1_-} I_{\text{easy}} = -\frac{\cos(2A)}{A}$. The remaining terms can be written

$$I_{\text{hard}} = I_1 + I_2 + I_3 \tag{D.3.26}$$

$$I_1 = \frac{2}{Bg}\int_0^{y+A} dz\,\text{Ci}(\alpha)\left(B'(z) - gB''(z)\right) \tag{D.3.27}$$

$$I_2 = \frac{2}{Bg}\int_0^{y+A} dz\,B'(z)\text{Ci}(\alpha) \tag{D.3.28}$$

$$I_3 = -\frac{4}{B^2 g}\int_0^{y+A} dx\int_0^x dz\,B'(x)B'(z)\text{Ci}(\tau)\,, \tag{D.3.29}$$

where the integrands are divergent at some of the integral limits.

First, we rewrite I_1 by integrating by parts and using l'Hôpital, which gives

$$\begin{aligned}\lim_{y+A\to 1_-} I_1 = \lim_{y+A\to 1_-}\Big[&-\frac{g'}{g} - \frac{g'}{B}\int_0^{y+A}\frac{dz}{\alpha}\cos(\alpha)B'(z)\\ &+\frac{1}{Bg}\int_0^{y+A}\frac{dz}{\alpha^2}B'(z)(g-g(z))(g(\alpha\sin(\alpha)+\cos(\alpha)) - \alpha\cos(\alpha))\Big]\,.\end{aligned} \tag{D.3.30}$$

Next, we rewrite the sum $I_2 + I_3$ as

$$I_{23} = I_2 + I_3 + \hat{I} - \hat{I}_{\text{alt}} \tag{D.3.31}$$

$$= \frac{2}{B^2 g}\int_0^{y+A} dx\int_0^x dz\,\text{Ci}(x-z)\big(B(x)B''(z) - B'(x)B'(z)\big)\,, \tag{D.3.32}$$

with double integral $\hat{I}$ and $\hat{I}_{\rm alt}$. We note that

$$\hat{I} = \frac{2}{B^2 g}\int_0^{y+A} dx \int_0^x dz\, B'(x)B'(z)\mathrm{Ci}(x-z) \tag{D.3.33}$$

and that $\hat{I}_{\rm alt}$ is the alternate expression of $\hat{I}$ when integration by part in x.

Applying l'Hôpital and integrating the result by parts, we get

$$\lim_{y+A\to 1_-} I_{23} = \lim_{y+A\to 1_-} \frac{1}{Bg}\int_0^{y+A} dz\, \cos(\alpha)B'(z)\frac{g-g(z)}{\alpha}\,. \tag{D.3.34}$$

Combining (D.3.30) and (D.3.34), we obtain

$$\begin{aligned}\lim_{y+A\to 1_-} I_{\rm hard} = \lim_{y+A\to 1_-} \Bigg[&-\frac{g'}{g} + \frac{1}{B}\int_0^{y+A} dz\, \frac{\sin(\alpha)}{\alpha}B'(z)(g-g(z)) \\ &+ \frac{1}{B}\int_0^{y+A} dz\, \frac{\cos(\alpha)}{\alpha}B'(z)\Big[\frac{g-g(z)}{\alpha} - g'\Big]\Bigg]\,.\end{aligned} \tag{D.3.35}$$

The two integrals in are denoted $\mathcal{C}(y)$ and $\mathcal{D}(y)$ in Appendix D.5 (equations (D.5.1) and (D.5.14)), where we show $\lim_{y+A\to 1_-}\mathcal{C}(y)\to 0$ and $\lim_{y+A\to 1_-}\mathcal{D}(y)\to 0$. Because Appendix B.5.1 shows $\lim_{y+A\to 1_-} g'/g \to -\infty$, the final result is therefore

$$\lim_{y+A\to 1_-} gF_+(y) \to \infty\,. \tag{D.3.36}$$

D.3.3 The term $\tilde{F}(y)$

The integral in (D.3.3) can be divided into two pieces

$$\mathcal{G}^-_{\rm out} = \int_0^1 \frac{dK}{K}\Big[|e^{-iKw}+R_K(y)|^2 - |e^{-iKw}-e^{-iKy}|^2\Big]\,, \tag{D.3.37}$$

$$\mathcal{G}^+_{\rm out} = \int_1^\infty \frac{dK}{K}\Big[|e^{-iKw}+R_K(y)|^2 - |e^{-iKw}-e^{-iKy}|^2\Big]\,. \tag{D.3.38}$$

We will use two different forms for $R_K(y)$: in $\mathcal{G}^-_{\rm out}$ we use eq.(6.2.15), and in $\mathcal{G}^+_{\rm out}$ we use eq.(6.2.13).

First we look at eq.(D.3.37). We define the factors

$$
\begin{aligned}
l_1(z) &= \frac{\cos(z)-1}{z}\,, \\
l_2(z) &= \frac{\cos(z)-1}{z^2} + \frac{\sin(z)}{z}\,, \\
l_3(w,y,z) &= \big[l_1(\alpha) - l_1(\gamma) + l_1(\xi) - l_1(\chi)\big]\,, \\
l_4(z) &= \big[l_1(\mu) - l_1(\nu) + 2l_1(z)\big]\,, \\
l_5(z,x) &= \big[l_2(\rho) + l_2(\sigma) - 2l_2(\tau)\big]\,,
\end{aligned}
\tag{D.3.39}
$$

where, in addition to the definitions above equation (D.3.17), we use $\mu := 2A-z$, $\nu := 2A+z$, $\xi := A+w-z$ and $\chi := w-z-A$. It is straightforward to show that the parameters μ, ν, ξ, and χ are all positive for $A > 1$, $z \in (0, y+A)$ and $y \in (-A, 1-A)$. We also note that $l_1(z)$ and $l_2(z)$ and their derivatives are bounded on $z \in (0, y+A)$. Using this notation and repeatedly using Lemma D.1.1, the result after doing the K integral can be expressed in the compact form

$$
\begin{aligned}
\mathcal{G}^-_{\rm out} &= 2\ln\left(\frac{w-y-2A}{w-y}\right) - 2{\rm Ci}(w-y-2A) + 2{\rm Ci}(w-y) \\
&+ \frac{2}{B}\int_0^{y+A} dz\; B(z)\; l_3(w,y,z) + \frac{2}{B^2}\int_0^{y+A} dz\; B(z)\; l_4(z) \\
&- \frac{1}{B^2}\int_0^{y+A} dz\; B(z) \int_0^{z} dx\; B(x)\; l_5(z,x) \\
&+ \frac{4}{B^2}\int_0^1 \frac{dK}{K}\sin^2(AK) + \frac{2}{B}\int_0^1 \frac{dK}{K}\int_0^{y+A} dz\,(\cos(K(w-A)) \\
&\qquad\qquad - \cos(K(A+w)) - \cos(K(A+y)) + \cos(K(3A+y)))\,.
\end{aligned}
\tag{D.3.40}
$$

The last two lines of equation (D.3.40) are zero in the limit $y + A \to 1_-$. The factors $l_3(w,y,z)$ and $l_4(z)$, and their derivatives are bounded over the range of the integral, and therefore taking the limit $y + A \to 1_-$ we find that the single integrals containing these factors are zero by Lemma D.1.1. It is easy to show that the double integral is zero using l'Hôpital's rule and then applying Lemma D.1.1. The final result is then

$$
\lim_{y+A\to 1_-} \mathcal{G}^-_{\rm out} = \lim_{y+A\to 1_-} \left[2\ln\left(\frac{w-y-2A}{w-y}\right) - 2{\rm Ci}(w-y-2A) + 2{\rm Ci}(w-y)\right]\,.
\tag{D.3.41}
$$

Now we consider $\mathcal{G}^{+}_{\rm out}$. Interchanging the order of integration and performing the K integrals we obtain

$$\begin{aligned}\mathcal{G}^{+}_{\rm out} &= \frac{2}{B}\int_0^{y+A-\epsilon} dz\, B'(z)\mathrm{Ci}(\alpha) + \frac{2}{B}\int_0^{y+A} dz\, B'(z)(\mathrm{Ci}(\chi)-\mathrm{Ci}(\beta)-\mathrm{Ci}(\xi)) \\ &- \frac{4}{B^2}\int_\epsilon^{y+A} dx\, B'(x)\int_0^{x-\epsilon} dz\, B'(z)\mathrm{Ci}(\tau) \\ &+ \frac{2}{B^2}\int_0^{y+A} dx\, B'(x)\int_0^{x} dz\, B'(z)(\mathrm{Ci}(\rho)+\mathrm{Ci}(\sigma))\,.\end{aligned} \tag{D.3.42}$$

The double integral containing $\rho\,,\sigma$ in (D.3.42) can be shown to render a finite result, by repeatedly using l'Hôpital and Lemma D.1.1. We rewrite the double integral containing τ in two different ways. If we integrate by parts in x, and then integrate by parts in z. The result is

$$\frac{1}{2}I^{\text{version 1}}_{\text{line 2}} = \frac{1}{B^2}\left(B^2-1\right)(\mathrm{Ci}(\epsilon)-\mathrm{Ci}(2A)) \tag{D.3.43}$$

$$- \frac{2}{B}\int_0^{y+A-\epsilon} dz\, B'(z)\mathrm{Ci}(\alpha) \tag{D.3.44}$$

$$+ \frac{2}{B^2}\int_\epsilon^{y+A} dx\, B(x)\int_0^{x-\epsilon} dz\, B'(z)\,\frac{\cos(\tau)}{\tau}\,. \tag{D.3.45}$$

If we start with an integration by parts in z we obtain

$$\frac{1}{2}I^{\text{version 2}}_{\text{line 2}} = -\frac{1}{B^2}\left(B^2-1\right)(\mathrm{Ci}(\epsilon)-\mathrm{Ci}(2A)) \tag{D.3.46}$$

$$+ \frac{2}{B^2}\int_0^{y+A-\epsilon} dz\, B'(\alpha)\mathrm{Ci}(\alpha) \tag{D.3.47}$$

$$- \frac{2}{B^2}\int_\epsilon^{y+A} dx\, B'(x)\int_0^{x-\epsilon} dz\, B(z)\,\frac{\cos(\tau)}{\tau}\,. \tag{D.3.48}$$

Combining these expressions, equation (D.3.42) can be written:

$$\mathcal{G}^{+}_{\rm out} = \lim_{\epsilon\to 0}\left(I_{\text{line 1}} + \frac{1}{2}\left[I^{\text{version 1}}_{\text{line 2}} + I^{\text{version 2}}_{\text{line 2}}\right]\right)\,, \tag{D.3.49}$$

where $I_{\text{line 1}}$ is the first line of eq.(D.3.42).

We substitute and collect terms. The non-integral terms cancel exactly. The single

integrals and their derivatives give vanishing results at limit $y+A \to 1_-$, by first performing a change of variables $z \to y + A - z$ on the term in eq.(D.3.46) that contains $B'(\alpha)$ and integrating by parts in all terms except the one with the factor $\mathrm{Ci}(z)$, then using l'Hôpital and Lemma D.1.1. Therefore only the contribution from the double integral survives.

Combining $\mathcal{G}^-_{\rm out}$ in eq.(D.3.41) and the surviving terms of $\mathcal{G}^+_{\rm out}$ we arrive at

$$\lim_{y+A\to 1_-} \mathcal{G}_{\rm out} = \lim_{y+A\to 1_-} \left[2\ln\left(\frac{w-y-2A}{w-y}\right) + I_{\rm extra} \right] , \tag{D.3.50}$$

where

$$I_{\rm extra} = \frac{2}{B^2}\int_0^{y+A} dx\, B'(x) \int_0^x dz\, B'(z)\cos(x-z)\,\frac{g(x)-g(z)}{x-z}\,. \tag{D.3.51}$$

Using l'Hôpital in (D.3.51), we then find $\lim_{y+A\to 1_-} I_{\rm extra} = \lim_{y+A\to 1_-} \mathcal{C}(y) = 0$, where $\mathcal{C}(y)$ is given by equation (D.5.1) in Appendix D.5. Therefore (D.3.50) becomes

$$\lim_{y+A\to 1_-} \mathcal{G}_{\rm out} = \lim_{y+A\to 1_-} \left[2\ln\left(\frac{w-y-2A}{w-y}\right) \right] , \tag{D.3.52}$$

in agreement with eq.(6.3.7).

D.4 $\langle T_{00}\rangle$ in the intermediate region, inside the shell

In this section we look at the energy density in the region $r < a$, before time $t = a$. We finish the proof of section 6.3.2.

1) F_-:

The result in the outside region is equation (D.3.12).

Doing the same calculation in the inside region we obtain

$$\begin{aligned} F^{\rm in}_-(y,w) = \quad & \int_0^1 dK \Big[-4if_1(w-A)\sin^2(AK)(\mathcal{H}_K(w-A) - \bar{\mathcal{H}}_K(w-A)) \\ & -4f_1(w-A)\sin(AK)\cos(Kw) + 4K\mathcal{H}_K(w-A)\bar{\mathcal{H}}_K(w-A)\sin^2(AK) \\ & +2iK\sin(AK)\left(e^{iKw}\mathcal{H}(w-A) - e^{-iKw}\bar{\mathcal{H}}_K(w-A)\right) + \frac{4f_2(w-A)\sin^2(AK)}{KB(w-A)}\Big] . \end{aligned} \tag{D.4.1}$$

We transform the inside result using $(y,w,A) \to (w,y,-A)$ and find

$$F^{\rm in}_-(y,w)\big|_{A\to -A} - F^{\rm out}_-(y,w) = 0\,. \tag{D.4.2}$$

2) F_+

The outside expression is equations (D.3.17 - D.3.22).

The corresponding expression on the inside can be found by defining the exponents

$$\hat{\alpha} = -A + w - z\,, \hat{\gamma} = A + w - z\,, \hat{\beta} = 3A - w + z\,, \hat{\sigma} = 2A + x - z\,, \hat{\rho} = 2A - x + z\,, \tag{D.4.3}$$

which are all positive throughout the inside region. We transform the inside result using $(y, w, A) \to (w, y, -A)$ and find

$$\begin{aligned} &F_+^{\rm in}(w,y)\big|_{A\to -A} - F_+^{\rm out}(y,w) \\ &= -\frac{4i\pi A^2}{g(A+y)^4} + \frac{2i\pi}{Bg}\int_0^{y+A} dz\, B''(z)\left[\frac{(\beta^2+\gamma^2)}{2g^2} + \frac{(\beta-\gamma)}{g} + 1\right]. \end{aligned} \tag{D.4.4}$$

3) $\mathcal{G}^-$

The outside result is equation (D.3.40). We calculate the corresponding inside expression and perform the transformation $(y, w, A) \to (w, y, -A)$. Subtracting the outside expression from the inside expression, we obtain

$$\mathcal{G}^-_{\rm in}(w,y)|_{A\to -A} - \mathcal{G}^-_{\rm out}(y,w) = 0\,. \tag{D.4.5}$$

4) $\mathcal{G}^+$

The outside result is equation (D.3.42). We calculate the corresponding inside expression using the exponents in eq.(D.4.3) and the additional definitions $\hat{\chi} = A+y-z$, $\hat{\eta} = A-y+z$. Performing the transformation $(y, w, A) \to (w, y, -A)$ and subtracting the original result we obtain

$$\mathcal{G}^+_{\rm in}(w,y)\big|_{A\to -A} - \mathcal{G}^+_{\rm out}(y,w) = \frac{4i\pi}{B}\int_0^{y+A} dz\, B'(z) - \frac{4i\pi}{B^2}\int_0^{y+A} dx\, B'(x)\int_0^x dz\, B'(z)\,. \tag{D.4.6}$$

From equations (D.4.2, D.4.4, D.4.5, D.4.6), the energy density inside the shell is obtained from the outside results by performing the transformation $(y, w, A) \to (w, y, -A)$ and dropping any imaginary parts that are produced.

D.5 Some useful integrals

In this section, we switch the variable y in Appendix B.5 to $y + A$, so all the conclusions therein still hold.

D.5.1 $\mathcal{C}(y)$

For $0 < y + A < 1$, we define

$$\mathcal{C}(y) = \frac{1}{B(y+A)} \int_0^{y+A} dz \cos(y + A - z) B'(z) \, \frac{g(y+A) - g(z)}{y + A - z} \,. \tag{D.5.1}$$

The cosine function in the integrand remains bounded for the whole range $z \in (0, y + A)$, so we focus on the factor $B'(z) \, \frac{g(y+A)-g(z)}{y+A-z}$. We notice that this factor is bounded when $z \in (0, \kappa)$, where κ is any number smaller than $y + A$. When $y + A \to 1_-$, the only divergent contribution of the integrand thus comes from around $z = y + A$. So we reason that we can approximate the integral in eq.(D.5.1) with the following integrals

$$\mathcal{C}(y) \sim \frac{1}{B(y+A)} \int_0^{\kappa} dz \cos(y + A - z) B'(z) \, \frac{g(y+A) - g(z)}{y + A - z} \tag{D.5.2}$$

$$+ \frac{1}{B(y+A)} \int_{\kappa}^{y+A} dz B'(z) \, g'(z) \,. \tag{D.5.3}$$

The first integral obviously has a finite contribution when $y + A \to 1_-$, while the second integral can be treated with l'Hôpital. The result is $\mathcal{C}(y) \to 0$ as $y + A \to 1_-$

A rigorous proof is given below.

We want to investigate the divergence properties of

$$\mathcal{C}(y) = \frac{1}{B(y+A)} \int_0^{y+A} dz \cos(y + A - z) B'(z) \, \frac{g(y+A) - g(z)}{y + A - z} \,. \tag{D.5.4}$$

We define

$$\mathcal{C}_2(y) = \frac{1}{B(y+A)} \int_0^{y+A} dz B'(z)\, \frac{g(y+A)-g(z)}{y+A-z} \tag{D.5.5}$$

$$\mathcal{C}_-(y) = \frac{1}{B(y+A)} \int_0^{\kappa} dz \left[\frac{g(y+A)B'(z)}{y+A-z} - \frac{B(z)}{y+A-z} \right] \tag{D.5.6}$$

$$\mathcal{C}_+(y) = \frac{1}{B(y+A)} \int_\kappa^{y+A} dz B'(z)\, \frac{g(y+A)-g(z)}{y+A-z} \tag{D.5.7}$$

$$\tilde{\mathcal{C}}_-(y) = -\frac{1}{B(y+A)} \int_0^{\kappa} dz \frac{B(z)}{y+A-z} \tag{D.5.8}$$

$$\tilde{\mathcal{C}}_+(y) = \frac{1}{B(y+A)} \int_\kappa^{y+A} dz B'(z) g'(z)\,, \tag{D.5.9}$$

where there is $\mathcal{C}_2(y) = \mathcal{C}_-(y) + \mathcal{C}_+(y)$ and we have introduced constant κ and assumed $0 < \kappa < y + A < 1$.

Using $0 < \cos(y + A - z) \leq 1\,, B'(z) > 0\,, g'(z) < 0$ for $z \in (0, y + A)$ and eq.(B.5.1), there are

$$\mathcal{C}_2(y) < \mathcal{C}(y) < 0 \tag{D.5.10}$$

$$\tilde{\mathcal{C}}_-(y) < \mathcal{C}_-(y) \tag{D.5.11}$$

$$\tilde{\mathcal{C}}_+(y) \leq \mathcal{C}_+(y)\,, \tag{D.5.12}$$

therefore

$$\tilde{\mathcal{C}}_-(y) + \tilde{\mathcal{C}}_+(y) < \mathcal{C}_2(y) < \mathcal{C}(y) < 0\,. \tag{D.5.13}$$

As $y + A \to 1_-$, $\tilde{\mathcal{C}}_-(y)$ goes to zero, while $\tilde{\mathcal{C}}_+(y)$ can be evaluated by l'Hôpital with the result $\lim_{y+A\to 1_-} \tilde{\mathcal{C}}_+(y) = 0$. It then follows that $\lim_{y+A\to 1_-} \mathcal{C}(y) = 0$.

D.5.2 $\mathcal{D}(y)$

We want to investigate the divergence properties of the following expression

$$\mathcal{D}(y) = \frac{1}{B} \int_0^{y+A} dz\, \frac{\cos(y+A-z)B'(z)}{y+A-z} \left[\frac{g(A+y)-g(z)}{y+A-z} - g'(A+y) \right], \tag{D.5.14}$$

where $0 < y + A < 1$. We define

$$\mathcal{D}_+(y) = \frac{1}{B}\int_\kappa^{y+A} dz\, B'(z)\frac{\cos(\alpha)}{\alpha}\left[\frac{g(A+y)-g(z)}{\alpha} - g'(A+y)\right] \tag{D.5.15}$$

$$\begin{aligned}\mathcal{D}_-(y) &= -\frac{1}{B}\int_0^\kappa dz\,\frac{B(z)}{\alpha}\left[\sin(\alpha)+\frac{\cos(\alpha)}{\alpha}\right] \\ &\quad +\frac{1}{B}\int_0^\kappa dz\,\frac{B'(z)}{\alpha}\left[g\big[\sin(\alpha)+\frac{\cos(\alpha)}{\alpha}\big] - g'\cos(\alpha)\right]\end{aligned} \tag{D.5.16}$$

$$\tilde{\mathcal{D}}_+(y) = \frac{1}{B}\int_\kappa^{y+A} dz\,\frac{B'(z)}{\alpha}\left[\frac{g(A+y)-g(z)}{\alpha} - g'(A+y)\right] \tag{D.5.17}$$

$$\tilde{\mathcal{D}}_-(y) = -\frac{1}{B}\int_0^\kappa dz\,\frac{B(z)}{\alpha}\left[\sin(\alpha)+\frac{\cos(\alpha)}{\alpha}\right] \tag{D.5.18}$$

$$\mathcal{D}_3(y) = \frac{1}{B}\int_\kappa^{y+A} dz\,\frac{B'(z)}{\alpha}\big(g'(z)-g'(y+A)\big) \tag{D.5.19}$$

$$\mathcal{D}_4(y) = -\frac{1}{B}\int_\kappa^{y+A} dz\, B'(z)g''(z)\,, \tag{D.5.20}$$

with $\alpha = y + A - z$, $\mathcal{D}(y) = \mathcal{D}_-(y) + \mathcal{D}_+(y)$, $\mathcal{D}_2(y) := \tilde{\mathcal{D}}_+(y) + \tilde{\mathcal{D}}_-(y)$ and constant κ satisfying $0 < \kappa < y + A < 1$.

For $0 < z < y + A$, $B'(z)$, α, $\cos(\alpha)$ and $\sin(\alpha)$ are positive. In addition, the quantity inside the square bracket in equation (D.5.17) is negative for $0 < z \le y + A$, as can be seen from and eq.(B.5.1) and eq.(B.5.2) . Using the same information, and that $g'(z)$ is negative for $0 < z < y + A$, we see that the contribution from the second integral in (D.5.16) is positive.

Combining we write

$$\tilde{\mathcal{D}}_+(y) < \mathcal{D}_+(y) < 0 \tag{D.5.21}$$

$$\tilde{\mathcal{D}}_-(y) < \mathcal{D}_-(y) \tag{D.5.22}$$

$$\mathcal{D}_2(y) < \mathcal{D}(y) < 0 \tag{D.5.23}$$

$$\mathcal{D}_4(y) \le \mathcal{D}_3(y) \le \mathcal{D}_2(y)\,. \tag{D.5.24}$$

Combining these results gives

$$\lim_{y+A\to 1_-}\mathcal{D}_4(y) \le \lim_{y+A\to 1_-}\mathcal{D}_3(y) \le \lim_{y+A\to 1_-}\mathcal{D}_2(y) < \lim_{y+A\to 1_-}\mathcal{D}(y) < 0\,. \tag{D.5.25}$$

L'Hôpital gives $\lim_{y+A\to -_-}\mathcal{D}_4(y) \to 0$ and therefore $\lim_{y+A\to 1_-}\mathcal{D}(y) \to 0$.

Appendix E

E.1 Conservation of the $U(1)$ charge

A Klein-Gordon inner product does not produce a real probability but a $U(1)$ charge instead. In this section we discuss the change in this charge as an analogous discussion of the probability. We find out the change of $U(1)$ charge is given by

$$\begin{aligned}
&\frac{d}{dt}\int_0^\infty r^2 dr d\Omega[\overline{\phi}\partial_t\phi - \overline{\partial_t\phi}\phi] \\
=&\int_0^\infty dr r^2 dr d\Omega[\overline{\phi}\partial_t^2\phi - \overline{\partial_t^2\phi}\phi] \\
=&\int_0^\infty dr r^2 dr d\Omega[\overline{\phi}\nabla^2\phi - \overline{\nabla^2\phi}\phi] \\
=&[\overline{f}f' - \overline{f}'f]\Big|_{boundary},
\end{aligned} \tag{E.1.1}$$

where $\phi = f/\sqrt{4\pi}r$ and prime means ∂_r. We can easily prove that the total charge is conserved.

For the 3+1 dimensional spherical shell formation, the time change of $U(1)$ charge in $r > a$ region is

$$\begin{aligned}
&\frac{d}{dt}\int_{a_+}^\infty r^2 dr d\Omega[\overline{\phi}\partial_t\phi - \overline{\partial_t\phi}\phi] \\
=&-[\overline{f(t,a_+)}f'(t,a_+) - \overline{f'(t,a_+)}f(t,a_+)]\,.
\end{aligned} \tag{E.1.2}$$

We want to see whether the $U(1)$ charge is conserved in the outside region $r > a$ for time $t > 1/\lambda$, meaning we want to see if the charge is conserved outside (or inside) the shell after the shell is completely formed. To do so, we need to substitute the solution into the above formula. It turns out that if we substitute $f_k(t, a_+) \sim e^{-ikv} - e^{-ik(u+2a)}$ for $t > 1/\lambda$, the

charge outside the shell is conserved.

E.2 Instability of the wavefunction

We mentioned that the reason we choose $h(y) \in (0, \pi/2)$ is because otherwise there is tachyonic instability. Mathematically, we have $B(0) = 1\,, B(1) = 0$ for $h(y) \in (\pi/2, \pi)$, therefore the mode functions $R_K(y) \to \infty$ when $y \to 1$. The wave functions either diverge or are no longer continuous. The probability is not defined.

I. In 1+1 dimensions, if function $h(y)$ satisfies $h(0) = \pi/2\,, h(1) = \pi$ while being smooth on $y \in (0, 1)$, we can derive $B(0) = 1\,, B(1) = 0$. We can then prove $R_K(y) \to \infty$ when $y \to 1_-$, where $R_K(y)$ is defined as

$$R_K(y) = e^{-iKy} - \frac{2}{B(y)} \int_0^y B'(z) e^{-iKz} dz\,. \tag{E.2.1}$$

II. For 3+1 dimensional pointlike source, if function $h(y)$ satisfies $h(0) = \pi\,, h(1) = \pi/2$ while being smooth on $y \in (0, 1)$, we have $B(0) = 1\,, B(1) = 0$. We can then prove $R_K(y) \to \infty$ when $y \to 1_-$, where $R_K(y)$ is defined as

$$R_K(y) = -e^{-iKy} - \frac{2iK}{B(y)} \int_0^y B(z) e^{-iKz} dz\,. \tag{E.2.2}$$

III. For 3+1 dimensional spherical shell model, if function $h(y)$ satisfies $h(0) = \pi/2\,, h(1) = \pi$ while being smooth on $y \in (0, 1)$, we can similarly prove $B(0) = 1\,, B(1) = 0$. Therefore we have $R_K(y) \to \infty$ when $y + A \to 1_-$ for

$$R_K(y) = -e^{-iKy} + \frac{2i \sin(AK)}{B(y + A)} \int_0^{y+A} B'(z) e^{-iKz} dz\,. \tag{E.2.3}$$

.

Bibliography

[1] B. P. Abbott et al. Observation of Gravitational Waves from a Binary Black Hole Merger *Physical Review Letters* **116**, 061102, 2016. doi: 10.1103/PhysRevLett.116.061102.

[2] Sean. Carroll. *spacetime and geometry: an introduction to general relativity*. Pearson Education, 2013.

[3] M. Walter, et al. Multi-partite entanglement. *arXiv preprint* arXiv:1612.02437[quant-ph], 2016. URL: https://arxiv.org/abs/1612.02437.

[4] M. Srednicki. Entropy and Area. *Physical Review Letters* **71**(5): 666, 1993. doi: 10.1103/PhysRevLett.71.666.

[5] D. N. Page. Information in black hole radiation. *Physical Review Letters* **71**: 3743, 1993. doi: 10.1103/PhysRevLett.71.3743.

[6] D. Harlow. Jerusalem Lectures on Black Holes and Quantum Information. *Review of Modern Physics* **88**: 15002, 2016. doi:10.1103/RevModPhys.88.015002.

[7] S. Hawking. Particle creation by black holes. *Communications in Mathematical Physics* **43**(3): 199-220, 1975. doi: 10.1007/BF02345020.

[8] D. Marolf. The Black Hole information problem: past, present, and future. and citations therein. *Reports on Progress in Physics* **80**: 092001, 2017. doi: 10.1088/1361-6633/aa77cc.

[9] S. W. Hawking. Breakdown of Predictability in Gravitational Collapse. *Physical Review D* **14**: 2460, 1976. doi: 10.1103/PhysRevD.14.2460.

[10] Samir D. Mathur. The Information Paradox: A Pedagogical Introduction. *Classical and Quantum Gravity* **26**: 224001, 2009. doi: 10.1088/0264-9381/26/22/224001.

[11] Samir D. Mathur. The Information Paradox and the Infall Problem. *Classical and Quantum Gravity* **28**: 125010, 2011. doi: 10.1088/0264-9381/28/12/125010.

[12] W. G. Unruh, R. M. Wald. Information Loss, and citations therein. *Reports on Progress in Physics* **80**:092002, 2017. doi: 10.1088/1361-6633/aa778e.

[13] D.N. Page. Time Dependence of Hawking Radiation Entropy. *Journal of Cosmology and Astroparticle Physics* **09**: 028, 2013. doi: 10.1088/1475-7516/2013/09/028.

[14] Y. Aharonov, Casher, S. Nussinov. The Unitary Puzzle and Planck Mass Stable Particles. *Physics Letter B* **191**: 51, 1987. doi: 10.1016/0370-2693(87)91320-7.

[15] A. Almheiri, D. Marolf, J. Polchinski and J. Sully. Black Holes: Complementarity or Firewalls? *Journal of High Energy Physics* **1302**: 062, 2013. doi: 10.1007/JHEP02(2013)062.

[16] S. L. Braunstein. Black hole entropy as entropy of entanglement, or it's curtains for the equivalence principle. *arXiv preprint* 0907.1190v1 [quant-ph]; S. L. Braunstein, S. Pirandola and K. Zyczkowski. Better Late than Never: Information Retrieval from Black Holes. *Physical Review Letters* **110**: 101301, 2013. doi: 10.1103/PhysRevLett.110.101301.

[17] Eric G.Brown, Jorma Louko. Smooth and sharp creation of a Dirichlet wall in $1 + 1$ quantum field theory, how singular is the sharp creation limit? *Journal of High Energy Physics*. **1508**, 061, 2015. doi: 10.1007/JHEP08(2015)061.

[18] L. Zhou, et al. Smooth and sharp creation of a pointlike source for a (3+1)-dimensional quantum field. *Physical Review D* **95**: 085007, 2017. doi: 10.1103/PhysRevD.95.085007.

[19] M. Carrington, et al. Smooth and sharp creation of a spherical shell for a (3+1)-dimensional quantum field. *Physical Review D* **98**(2): 024035, 2018. doi: 10.1103/PhysRevD.98.024035.

[20] W. Unruh. Notes on black hole evaporation. *Physical Review D.* **14**(4): 870-892, 1976. doi: 10.1103/PhysRevD.14.870.

[21] L C. B. Crispino, et al. Unruh effect and its applications. *Review of Modern Physics* **80**:787-838, 2008. doi: 10.1103/RevModPhys.80.787.

[22] Leonard. Parker, David. Toms. *Quantum Field Theory in Curved Spacetime-Quantized Fields and Gravity*. Cambridge University Press, 2009.

[23] N. D. Birrell, P. C. W. Davies. *Quantum Fields in Curved Space*. Cambridge University Press, 1982.

[24] L. Parker. Quantized fields and particle creation in expanding universes. 1. *Physical Review* **183**(5): 1057, 1969. doi: 10.1103/PhysRev.183.1057.

[25] G. Moore. Quantum theory of electromagnetic field in a variable-length one-dimensional cavity. *Journal of Mathematical Physics* **11**(9): 2679, 1970. doi: 10.1063/1.1665432.

[26] P. Candelas and D. Deutsch. On the vacuum stress induced by uniform acceleration or supporting the ether. *Proceedings of the Royal Society of London. Series A* **354**: 79, 1977. doi: 10.1098/rspa.1977.0057.

[27] C. M. Wilson, G. Johansson, A. Pourkabirian, M. Simoen, J. R. Johansson, T. Duty, F. Nori and P. Delsing. Observation of the dynamical Casimir effect in a superconducting circuit. *Nature* **479**: 376, 2011. doi: 10.1038/nature10561.

[28] Eric G. Brown, etc. What does it mean for half of an empty cavity to be full? *Physical Review D* **91**(1): 016005, 2015. doi: 10.1103/PhysRevD.91.016005.

[29] Jorma Louko. Unruh-DeWitt detector response across a Rindler firewall is finite. *Journal of High Energy Physics* 1409, 142, 2014. doi:10.1007/JHEP09(2014)142.

[30] L. Susskind, J. Lindesay. *An Introduction To Black Holes, Information And The String Theory Revolution: The Holographic Universe*. World Scientific Publishing; 1 edition, 2004.

[31] *http://www.physics.ucc.ie/apeer/PY4112/Sch.pdf*

[32] Eric. Poisson. *A Relativist's Toolkit: The Mathematics of Black-Hole Mechanics*. Cambridge University Press, 2007.

[33] Jacob D. Bekenstein. Black Holes and Entropy. *Physical Review D* **7**: 2333, 1973. doi: 10.1103/PhysRevD.7.2333.

[34] S. W. Hawking. Black holes and thermodynamics. *Physical Review D* **13**: 191, 1976. doi: 10.1103/PhysRevD.13.191.

[35] L. Susskind. Singularities, Firewalls, and Complementarity. *arXiv preprint 1208.3445 [hep-th]*, 2012. **URL: https://arxiv.org/abs/1208.3445**.

[36] L. Susskind, L. Thorlacius and J. Uglum. The Stretched horizon and black hole complementarity. *Physical Review D* **48**: 3743, 1993. doi: 10.1103/PhysRevD.48.3743.

[37] L. Susskind, L. Thorlacius. Gedanken experiments involving black holes. *Physical Review D* **49**: 966, 1994. doi: 10.1103/PhysRevD.49.966.

[38] B. Czech, J. L. Karczmarek, F. Nogueira and M. Van Raamsdonk. The Gravity Dual of a Density Matrix. *Classical and Quantum Gravity* **29**: 155009, 2012. doi: 10.1088/0264-9381/29/15/155009.

[39] B. Czech, J. L. Karczmarek, F. Nogueira and M. Van Raamsdonk. Rindler Quantum Gravity. *Classical and Quantum Gravity* **29**: 235025 2012. doi: 10.1088/0264-9381/29/23/235025.

[40] C. T. Marco Ho, Daiqin Su, Robert B. Mann, Timothy C. Ralph. Black Hole Field Theory with a Firewall in two spacetime dimensions. *Physical Review D* **94**(8): 081502(R), 2016. doi: 10.1103/PhysRevD.94.081502.

[41] A. Almheiri, D. Marolf, J. Polchinski, D. Stanford and J. Sully. An Apologia for Firewalls. *Journal of High Energy Physics* **1309**: 018, 2013. doi:10.1007/JHEP09(2013)018.

[42] J. Hutchinson and D. Stojkovic. Icezones instead of firewalls: Extended entanglement beyond the event horizon and unitary evaporation of a black hole. *Classical and Quantum Gravity* **33**(13): 135006, 2016. doi: 10.1088/0264-9381/33/13/135006.

[43] L. Susskind. Black Hole Complementarity and the Harlow-Hayden Conjecture. *arXiv preprint 1301.4505 [hep-th]*, 2013. **URL: https://arxiv.org/abs/1301.4505**.

[44] C. G. Callan, et al. Evanescent Black Holes. *Physical Review D* **45**(4): R1005, 1992. doi: 10.1103/PhysRevD.45.R1005.

[45] E. Martín-Martínez and J. Louko. (1+1)D Calculation provides evidence that quantum entanglement survives a firewall. *Physical Review Letters* **115**: 031301 (2015) doi:10.1103/PhysRevLett.115.031301.

[46] W. G. Unruh, *Firewalls — A gravitational perspective*, lecture at RQIN-2014 (Seoul, Korea, July 2014).

[47] T. Harada, S. Kinoshita and U. Miyamoto. Vacuum excitation by sudden appearance and disappearance of a Dirichlet wall in a cavity. *Physical Review D* **94**: 025006, 2016. doi:10.1103/PhysRevD.94.025006

[48] Guy Bonneau, Jacques Faraut, Galliano Valent. Self-adjoint extensions of operators and the teaching of quantum mechanics. *American Journal of Physics*, **69**: 322, 2001. doi: 10.1119/1.1328351.

[49] R. M. Wald, *Quantum field theory in curved spacetime and black hole thermodynamics* University of Chicago Press, Chicago, 1994.

[50] G. Kunstatter, J. Louko and J. Ziprick. Polymer quantization, singularity resolution and the $1/r^2$ potential. *Physical Review A* **79**: 032104, 2009. doi:10.1103/PhysRevA.79.032104

[51] M. Reed and B. Simon, *Methods of Modern Mathematical Physics II: Fourier Analysis, Self-adjointness* Academic, New York, 1975.

[52] J. Blank, P. Exner and M. Havlíček, *Hilbert Space Operators in Quantum Physics*, 2nd edition. Springer, New York, 2008.

[53] R. Wong, *Asymptotic Approximations of Integrals*. Society for Industrial and Applied Mathematics, Philadelphia, 2001.

[54] B. S. DeWitt, *Quantum gravity: the new synthesis*, in *General Relativity: an Einstein centenary survey*, edited by S. W. Hawking and W. Israel. Cambridge University Press, Cambridge, 1979. doi: 10.1088/0031-9112/31/4/029.

[55] M. P. Seevinck. Monogamy of Correlations vs. Monogamy of Entanglement. *Quantum Inf Process* **9**(2): 273, 2010. doi: 10.1007/s11128-009-0161-6.

[56] NIST Digital Library of Mathematical Functions. `http://dlmf.nist.gov/`, Release 1.0.13 of 2016-09-16.

[57] J. D. Bekenstein. Universal upper bound on the entropy to energy ratio for bounded systems. *Physical Review D* **23**(2): 287, 1981. doi: 10.1103/PhysRevD.23.287.